

# Transport in Quantum Dots from the Integrability of the Anderson Model

Robert M. Konik

Department of Physics, University of Virginia  
Charlottesville, VA 22903

Hubert Saleur

Department of Physics, University of Southern California  
Los Angeles, CA 90089-0484

Andreas Ludwig

Department of Physics, University of California  
Santa Barbara, CA 93106

In this work we exploit the integrability of the two-lead Anderson model to compute transport properties of a quantum dot, in and out of equilibrium. Our method combines the properties of integrable scattering together with a Landauer-Buttiker formalism. Although we use integrability, the nature of the problem is such that our results are not generically *exact*, but must only be considered as excellent approximations which nonetheless are valid all the way through crossover regimes.

The key to our approach is to identify the excitations that correspond to scattering states and then to compute their associated scattering amplitudes. We are able to do so both in and out of equilibrium. In equilibrium and at zero temperature, we reproduce the Friedel sum rule for an arbitrary magnetic field. From this we compute exactly the behaviour of the zero temperature linear response conductance as a function of both the gate voltage and the field. We also study transport quantities requiring knowledge of

scattering states away from the Fermi surface. We compute the linear response conductance at finite temperature at the symmetric point of the Anderson model, and reproduce Costi et al.'s numerical renormalization group computation of this quantity. We then explore the out-of-equilibrium conductance for a near-symmetric Anderson model, and arrive at quantitative expressions for the differential conductance, both in and out of a magnetic field. We reproduce the expected splitting of the differential conductance peak into two in a finite magnetic field,  $H$ . We determine the width, height, and position of these peaks. In particular we find for  $H \gg T_k$ , the Kondo temperature, the differential conductance has maxima of  $e^2/h$  occurring for a bias  $V$  close to but smaller than  $H$ . The nature of our construction of scattering states suggests that our results for the differential magneto-conductance are not merely approximate but become exact in the large field limit.

## 1. Introduction

The Kondo effect is a cynosure of modern condensed matter physics. Due to the strongly coupled nature of its IR fixed point, understanding its low energy behaviour has proven a major theoretical challenge. Typically the phenomena refers to the interaction of isolated magnetic impurities in a bulk metal. However in the last several years the experimental study of single magnetic impurities has moved to a new arena, that of quantum dots connected to external leads [1] [2] [3] [4] [5]. In analogy to the traditional realization of the Kondo effect, the leads serve as the bulk metal and the dot as the magnetic impurity. The appearance of the Kondo effect in this new setting has brought a new set of theoretical challenges: how to compute transport quantities that form the main experimental signatures of these systems.

Quantum dots come in at least two forms. Semi-conductor quantum dots [1][2][3][4] are a product of the continuing project of the miniaturization of solid state devices. They are fabricated by confining electrons in a two dimensional electron gas (2DEG) within a GaAs/AlGaAs structure using a combination of metallic gates. The region to which the electrons are confined is small enough that its energy levels may be considered discrete. The dot is connected to source and drain contacts (the two leads). Schematically the quantum dot can be pictured as follows:

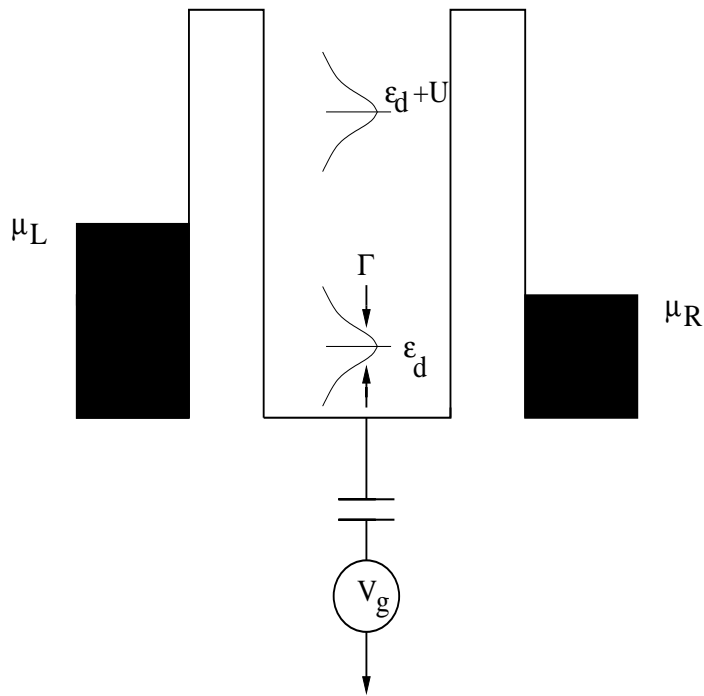


Figure 1: A schematic of the quantum dot.

The source and drain can be held at any relative voltage, thus enabling the study of both linear response and out-of-equilibrium transport quantities. Beyond the gates that serve to confine the electrons of the 2DEG, additional gates can be deposited on the GaAs/AlGaAs heterostructure. Such gates capacitively couple to the quantum dot through a gate voltage,  $V_g$ , thus allowing the chemical potential of the dot to be adjusted. This has two important consequences. By adjusting the gate voltage, one can tune the number of electrons in the confined region to be odd so that there is a single unpaired electron. The presence of an unpaired electron allows the appearance of Kondo-like physics. Moreover by tuning  $V_g$ , the unpaired electron's chemical potential can be adjusted thus controlling the scale,  $T_k$ , where Kondo physics sets in. Such systems are thus said to possess a “tunable” Kondo effect [2].

Quantum dots may also be fabricated from metallic carbon nanotubes [5]. By depositing metallic leads on top of a small section of a carbon nanotube, an effective quantum dot is made. Like their semiconductor counterparts, these dots are tunable: gates may be added to the semiconductor substrate upon which the nanotube/leads lay. Semiconductor dots typically carry 10-100 electrons. Nanotube dots, in contrast, have many thousands of electrons and yet still exhibit Kondo-like physics.

The transport quantities that lie at the focus of the experimental study of a tunable Kondo effect in quantum dots have been measured under a variety of conditions. Conductances of the lead-dot system have been determined both in and out of equilibrium and both in and out of the presence of a magnetic field. Remarkably this wide variety of experimental phenomena is thought to be described by a conceptually simple theory: the Anderson model.

The Anderson model is fashioned from a chain of non-interacting spinful fermions (the leads) connected via hopping to a single site impurity on which alone Coulomb repulsion is present. On a lattice, the Hamiltonian reads (with no bias and  $H=0$ ):

$$\begin{aligned}
 H = & \sum_{i\alpha} -t(c_{i,\alpha}^\dagger c_{i+1,\alpha} + \text{h.c.}) + U n_{d\uparrow} n_{d\downarrow} \\
 & + \sum_{\alpha} (V_1(c_{-1,\alpha}^\dagger d_{\alpha} + \text{h.c.}) + V_2(c_{1,\alpha}^\dagger d_{\alpha} + \text{h.c.})) + \varepsilon_d(n_{d\uparrow} + n_{d\downarrow}).
 \end{aligned}
 \tag{1.1}$$

Here  $c_{\alpha}^\dagger/c_{\alpha}$  are the lead electron creation/destruction operators,  $d^\dagger/d$  the dot electron creation/destruction operators, and  $n_d = d^\dagger d$ . The dot is considered to reside at  $x = 0$ . The index  $\alpha$  indicates spin species. The interaction on the dot is present in the term

$Un_{d\uparrow}n_{d\downarrow}$ . Although deceptively simple, the presence of a non-zero  $U$  makes the problem many-body with all of its manifold complications.

$U$  is pictured in Figure 1 and represents the charging energy incurred when an electron is added to the dot. Roughly it can be estimated as

$$U = \frac{e^2}{2C} + \Delta\varepsilon, \quad (1.2)$$

where  $C$  is the capacitance of the dot and  $\Delta\varepsilon$  is the dot's energy level spacing. For the experiments at hand,  $U \sim 1\text{meV}$ . The counterpart of the gate voltage,  $V_g$ , in the above Hamiltonian is  $\varepsilon_d$ , the parameter that controls the chemical potential of the electrons on the dot. By adjusting  $\varepsilon_d$ , the number of electrons on the model dot can be varied from zero to two. (Although there may be a large number of electrons on the actual dot, the concern here both theoretically and experimentally is of electrons in the highest occupied energy level.) The final pair of parameters,  $V_{1,2}$ , measure the height of the tunnel barriers between the leads and the dot. In general, they differ between the two leads. The quantity,  $\Gamma$ , (see Figure 1) measuring the width of the level resonance that arises through the interaction of the leads and the dot is given in terms of the tunnel barrier heights to be  $\Gamma = (V_1^2 + V_2^2)/2$ . Typically  $\Gamma/U \ll 1$  in the experiments of concern [1][2][3][4].

Although the above described experimental results have come relatively recently, the theoretical study of transport through impurities is much older. Appelbaum and Anderson both studied conductance anomalies present in tunnel junctions due to the presence of magnetic impurities [6]. However their efforts were perturbative in nature and did not describe the strong coupling nature of the Kondo effect. More recently, Ng and Lee [7], studied the linear response conductance both in and out of a magnetic field using the Friedel sum rule. The Friedel sum rule relates the scattering phase of the electrons at the Fermi surface to the average number of electrons sitting on the dot. However the Friedel sum rule is useful only in determining the linear response conductance, a consequence of the rapid variation in the scattering phase as one moves away from the Fermi surface. In contrast to the linear response conductance where the Friedel sum rule is an exact relationship, the techniques used to determine out-of-equilibrium transport are limiting in nature. In one approach, a non-crossing approximation (NCA) [8] [9] was employed. The NCA approach has drawbacks. In order to implement the associated use of slave bosons, one must take  $U = \infty$ . Moreover, NCA is in some sense a large  $N$  approximation where  $N$  is the number of spin degrees of freedom of the impurity (in this case  $N=2$ ). It is known to

be remarkably accurate in computing thermodynamics. However it is less accurate when it comes to transport quantities ( $\sim 15\%$  errors [9]) due to its less accurate prediction of behaviour right at the Fermi surface. And as such these difficulties render it unusable in non-zero magnetic fields [9]. In another approach to computing non-equilibrium properties, a clever combination of the analysis of the equations of motion with perturbation theory was employed to study the differential magneto-conductance [10]. However the truncation of the equations of motion necessary to perform the analysis in this work is in some sense an uncontrolled approximation. The authors of [10] indicate that their methodology underestimates the magnitude of the differential conductance. Another set of approaches have relied upon perturbation theory [11] [12] [13]. As with the results of [6], perturbation theory requires relatively small  $U$  (Coulomb repulsion) or alternatively, temperatures far in excess of the Kondo temperature, and so presumably can access, at best, qualitative, not quantitative, features of the strongly coupled physics found in the Kondo regime of quantum dots at low temperatures.

These inherent difficulties with the out-equilibrium Anderson were circumvented in the study of a non-equilibrium Kondo impurity at its Toulouse point [14]. At this point, the model can be mapped to a system of non-interacting fermions, thus permitting an exact solution. It is unclear, however, how the Toulouse limit affects the underlying physics. Although the ordinary Kondo model shares the same IR fixed point as its Toulouse counterpart, we are interested in part in physics for large applied field, bias, and temperature, that is, in physics far away from this fixed point.

Given the limitations of these methods, one cannot help but notice that the Anderson model is exactly solvable. Indeed this integrability has already been exploited through Bethe ansatz solutions to compute thermodynamic quantities [15] [16] such as the specific heat and magnetic susceptibility. But what of transport quantities? A limited attempt to deduce information about transport properties from the Bethe ansatz solution of the *Kondo* model was made recently [17]. There the equilibrium impurity density of states that arises from the Bethe ansatz was studied. In general, the impurity density of states coming from the Bethe ansatz is unrelated to the spectral density of states arising from the dot correlator,  $\text{Im}\langle dd^\dagger \rangle$ . Indeed at zero temperature and zero field, it is clear the two are much different quantities (the heights of zero energy peaks in both quantities are controlled by far different energy scales). But in methodology of [17], it is this latter quantity,  $\text{Im}\langle dd^\dagger \rangle$ , that is directly related to transport [12][9][10]. Moreover, the context of their computation, as determined in [12][9][10], demands that the *non-equilibrium* properties of

$\text{Im}\langle dd^\dagger \rangle$  be computed. Given the general unavailability from integrability of information about correlators such as  $\text{Im}\langle dd^\dagger \rangle$ , a different approach is needed to extract transport properties from the exact solvability of the model. Here we advocate a Landauer-Büttiker approach to transport, and so are instead faced with the task of identifying scattering states in the context of integrability.

The key feature of an integrable system is the exact knowledge of eigenfunctions of the fully interacting Hamiltonian. In turn there is a well-defined notion of elementary excitations. In particular these excitations have an infinite lifetime: integrability forbids any decay processes from occurring. This arises from the infinite series of non-trivial conservation laws in the model. In some sense an integrable system is a superior version of a Fermi liquid.

In the Anderson model, there is such a set of excitations, as detailed in Sections 2 and 4. They are not on the face of it, however, particularly electronic. And if we are to understand the transport of the sea of electrons in the attached leads, we necessarily need scattering states which carry the quantum numbers of an electron. Rather the excitations divide into separate spin and charge sectors. The closest they come to being electronic is in bound states between excitations which can be thought of as bound states of electrons. This is not so unnatural. If one were to bosonize the Anderson model, one would find that the degrees of freedom separate into spin and charge bosons. But this is only one problem with the excitations arising from integrability. These excitations, as explained in Section 2, are a combination of degrees of freedom in *both* of the leads connected to the dot. And it is the case that this entanglement cannot always be simply reversed.

And so there is the difficulty. The scattering states are not necessarily electronic in nature and not confined to a single lead. Only if one can understand electronic excitations in an individual lead can one hope to make sense of scattering amplitudes off the dot. It is these two facts that have prevented the integrability of the Anderson model from being applied to transport quantities up to now.

However we have managed to circumvent these problems in a number of cases. In particular we have successfully described both scattering states at the Fermi surface for generic values of  $U$ ,  $\varepsilon_d$ , and  $\Gamma$ , and scattering at finite energies at the symmetric point of the Anderson model,  $U = -\varepsilon_d/2$ . There we argue that by correctly gluing together a spin and charge excitation, we are able to form an excitation that is electronic in nature. Moreover the excitations are such that one can understand them in terms of the individual leads and so compute reflection and transmission amplitudes of the excitation off the dot. We do so

in an argument akin to that used by N. Andrei [18] in computing the magnetoresistance in the Kondo model. There he argues that the scattering phase of an excitation can be identified with its impurity momentum. In turn this momentum is related to the impurity density of states as it appears in the Bethe ansatz and so can be directly computed.

We now turn to how we use these excitations to compute transport quantities. All such quantities could be expressed in terms of the scattering of asymptotically free electrons (i.e. electrons in the attached leads) off the quantum dot. However such scattering, in general, is not particularly simple. In general away from the Fermi surface such scattering will be inelastic and involve particle-hole production. We, however, recast the density of states of asymptotically free fermions in terms of the integrable excitations we have identified. Because of their integrability, their scattering is simple: their character does not change in scattering through the dot and their transport can be described individually: they scatter one-by-one through the dot.

It is however unlikely that the integrable electronic excitations we use in computing transport properties provide exact results in all cases - the issues involved here are subtle and will be discussed in detail in the next sections. In particular, it is unlikely the high energy limit of the excitations we construct are entirely confined to a single lead. However this methodology successfully passes a number of tests. The first test of our method comes in proving the Friedel sum rule. The Friedel sum rule relates the occupancy of spin  $\uparrow / \downarrow$  electrons on the quantum dot,  $n_{d\uparrow/\downarrow}$ , to the scattering phase of an electron of the same spin,  $\delta_{e\uparrow/\downarrow}$ , at the Fermi surface:

$$\delta_{e\uparrow/\downarrow} = 2\pi n_{\uparrow/\downarrow}. \quad (1.3)$$

It thus relates a dynamic quantity to a thermodynamic quantity. With this in hand, previous works have computed the linear response conductance from the knowledge of this occupancy, at least at  $H = 0$  [19] [20]. However such works do not make any attempt to explicitly identify the excitations that scatter according to the Friedel sum rule. Here we do so. We show that the scattering phase of the excitations we have identified to be the same as that predicted by the Friedel sum rule both in and out of a magnetic field. As we have reproduced the Friedel sum rule, we can say that the excitations we have identified coincide exactly with the free fermions *at the Fermi surface*.

Now while the Friedel sum rule only deals with excitations at the Fermi surface, our method goes beyond excitations directly at the Fermi surface, at least near the symmetric point of the Anderson model. To determine whether the excitations we have identified



together with their associated scattering amplitudes provide a complete solution of the problem, we compute the linear response conductance at finite temperature. At finite temperature, the excitations needed for the linear response conductance using a Landauer-Büttiker formalism exist over a range of energies. In particular, we compute the linear response conductance at the symmetric point ( $-U/2 = \varepsilon_d$ ) of the Anderson model as a function of temperature,  $T$ , and compare it to Costi et al.'s [21] numerical renormalization group (NRG) computation of this quantity and find excellent agreement. We thus are able to conclude that using our excitations away from the Fermi surface is a valid procedure.

Although our finite temperature computation suggests we have correctly identified the low (but finite) energy excitations at the symmetric point, we do not claim that our result is *exact*. Again our inability to make this claim hinges on the question of whether the integrable excitations we construct are entirely confined to a single lead and so make appropriate scattering states. Moreover we know that our prescription for scattering fails once we leave the Kondo regime where approximately one electron sits on the dot and enter the mixed valence regime of the Anderson model. This again suggests that near the symmetric point, our methods are merely highly accurate. The situation here is not dissimilar to form-factors computations of correlation and response functions, where integrable techniques can provide, if not the exact result (which would involve resumming an infinite number of contributions), controlled approximations of excellent accuracy, from the lowest energies through crossover regimes [22] [23].

The physical origin of the accurate reproduction of scattering at non-zero energies relative to the Fermi surface at the Anderson model's symmetric point lies in a separation of scales. At this point there are two relevant scales in the problem: one is the Kondo temperature,  $T_k$ , while the other is  $\sqrt{U\Gamma}$ , a function of the Coulomb repulsion,  $U$ , and the resonance width of the dot level,  $\Gamma$ . At the symmetric point,  $T_k \ll \sqrt{U\Gamma}$ . We exploit this fact to make our identification of integrable scattering states. But in turn this means that we expect errors in transport quantities involving scattering away from the Fermi surface of  $\mathcal{O}(T_k/\sqrt{U\Gamma})$ .

Bootstrapping from our success with the finite temperature linear response conductance, we look at the non-equilibrium conductance near the symmetric point both in and out of a magnetic field at zero temperature. In order to compute this conductance we again employ a Landauer-Büttiker formalism akin to that employed in computing the out-of-equilibrium conductance of interacting quantum Hall edges [24]. We imagine placing each lead at two differing chemical potentials,  $\mu_1$  and  $\mu_2$ . These differing voltages induce

different populations of free electrons in the leads. As with the finite temperature linear response problem, we recast these electrons in terms of our integrable scattering states. We then compute the (equilibrium) scattering amplitudes of scattering states in the leads. These scattering amplitudes then provide the probability for a state to tunnel from one lead to the other. Although the system is interacting, its integrability again implies the states scatter one-by-one. It is important to understand that this means of computation introduces no additional error into the calculation. The sole source of uncertainty is found in whether the scattering states that we construct are entirely confined to a single lead. But because of the excellent agreement of the finite T linear response conductance with the previous NRG results, we expect this error to be similarly insignificant in our non-equilibrium computations.

It is important to understand that this approach to the non-equilibrium physics differs from that used in [12][9][10] in a fundamental way. There the non-equilibrium conductance is expressed in terms of the non-equilibrium density of states of the impurity as determined from the correlator,  $\text{Im}\langle dd^\dagger \rangle$ . Here we have nothing direct to say about the non-equilibrium (or indeed, the equilibrium) behaviour of this quantity.

We must stress this as the reader may be confused by the fact we do use the impurity momentum (which is in turn related to the Bethe ansatz impurity density of states as explained in Section 2) to compute the scattering amplitudes of excitations off the dot. This confusion may be heightened in that we employ the equilibrium Bethe ansatz density of states in computing the scattering matrices. It would thus seem legitimate to ask why we do not need to use a non-equilibrium impurity density of states in computing the out of equilibrium conductance [25].

The answer lies in correctly understanding the basis of excitations by which we compute the conductance [26]. We are able to use the equilibrium scattering phases as we employ the basis that is naturally present when the system is equilibrated. However because of the integrability of the system, we can continue to employ this basis when we move the system out of equilibrium. These particles continue to scatter as they do in equilibrium. We note that if one were to compute out-of-equilibrium scattering matrices, one would find that they differ from their in-equilibrium counterparts by an overall phase alone. As transport quantities depend upon the absolute value of the scattering, this overall phase would then have no effect [26]. While the application of finite voltage does not effect the scattering of the excitations, it does change their distribution in the leads. And indeed we must and do take this into account.

The rationale behind this understanding has been tested beyond the various checks of these ideas applied by [24] in their computations of conductances of quantum Hall edges. Generically the thermodynamics of an integrable field theory can be computed using thermodynamic Bethe ansatz which employs zero temperature S-matrices (and not finite temperature S-matrices as might again be naïvely expected – the finite temperature distribution might be thought to *necessarily* dress the scattering). With the thermodynamics, one can determine the finite temperature scaling behaviour of a field theory. If in the UV or IR limit, the theory flows to a conformal field theory, the finite scaling behaviour in these limits is independently determined by the central charge,  $c$ , of the theory. That the two computations always agree provides strong evidence we are handling the problem correctly.

Turning to our non-equilibrium results, we find that they reproduce the expected gross features of the experimental differential conductance. When  $H = 0$  and we are near the symmetric point, the differential conductance is sharply peaked about its linear response value. The peak width is controlled by the scale,  $T_k$ , the Kondo temperature. We find that the peak is roughly symmetrical about  $V = 0$  in accordance with experiment [1].

In a non-zero field, Meir and Wingreen [10] predicted that the differential conductance would peak at  $eV = \pm H$ . We find such peaks with our techniques although our peaks are found shifted to values of  $e|V|$  notably smaller than  $|H|$ . Even in the limit of fields much larger than  $T_k$ , we do not find the peaks at  $|H|$ . This is again consistent with experiment [3]. We should not necessarily expect the peaks to occur exactly at  $eV = H$  as Meir and Wingreen’s prediction is predicated in part upon a second order perturbative result. Moreover our construction of the scattering states suggests that in the particular case of the differential magneto-conductance, our results become exact in the limit of large applied fields.

A portion of the results of this paper have been reported in [27]. Here in this work we provide far greater detail on the nature of our computations. The paper is so organized as follows. In Section 2 we introduce the continuum version of the two lead Anderson model. The two lead Anderson model is integrable as is. However we first map it onto a one lead problem. If we were to explicitly solve the two lead problem, we would find nevertheless that we would be implicitly implementing the map to the one lead case. Having done this we review the Bethe ansatz for the one lead Anderson model together with the excitations necessary to form the ground state at zero temperature. The remaining portion of Section 2 is devoted to identifying the excitations (both at and away from the Fermi surface) that

can be identified with scattering states and then computing their scattering amplitudes. We provide further details of the approximate nature of the scattering states so identified away from the Fermi surface. In the course of this discussion we demonstrate the Friedel sum rule.

In Section 3 we explore the behaviour of the  $T = 0$  linear response conductance both in and out of a magnetic field. Because Wiegmann and Tsvelick [28] computed expressions for the occupancy of the dot,  $n_{d\uparrow/\downarrow}$ , as a function of the gate voltage,  $\varepsilon_d$ , and  $H$  in a variety of regimes, and the Friedel sum rule relates the electron scattering phase to this occupancy, we can derive closed form expressions for the linear response conductance in these same regimes. Outside these regimes we compute the occupancy numerically. Using these results, we show how the linear response conductance behaves as function of  $\varepsilon_d$ .

We plot the linear response conductance as a function of the gate voltage,  $\varepsilon_d$ , in zero field in Figure 4. However the most interesting results of this section are found in our computations of the linear response conductance at finite  $H$ . In Figure 5 we plot the linear response conductance as function of  $\varepsilon_d$  for a variety of values of  $H$ . As  $H$  is increased from zero we see that the linear response conductance is suppressed as a result of the destruction of the Kondo effect in a finite field. We also see the structure of the conductance peak evolve from its zero field value to that of free fermions. With increasing  $H$ , the full width at half maximum becomes narrower, decreasing from its zero field value of  $U$  to its free-fermion value of  $2\Gamma$ . The peak height, in turn, decreases from its maximal value of  $2e^2/h$  to  $e^2/h$ . And finally the location of the peak shifts from  $\varepsilon_d = -U/2$  to  $H/2$  (we scale  $H$  here and throughout this paper such that  $g\mu_B = 1$ ), appropriate to a spin up free-fermion with a field-induced, shifted chemical potential. These results are encoded in Figure 6.

At the symmetric point  $U/2 = -\varepsilon_d$ , we provide a simple closed form expression for the conductance (see Section 4.2). We then find that the conductance deviates from its unitary maximum for small fields via

$$G = 2\frac{e^2}{h}\left(1 - \frac{\pi^2}{16}\frac{H^2}{T_k^2} + \mathcal{O}(H^4/T_k^4)\right). \quad (1.4)$$

This deviation from the maximal conductance is quadratic, appropriate for the controlling  $H = 0$  strongly coupled Fermi liquid fixed point. Here  $T_k$ , the Kondo temperature, is given in (3.16).

In Section 4 we compute the finite temperature linear response conductance at the symmetric point,  $U/2 = -\varepsilon_d$ . This requires recomputing the scattering of Section 2. At

finite temperature one must consider the thermal bath of all possible excitations. This highly non-trivial bath modifies the scattering. However doing so leads us to a highly pleasing result. We are able to reproduce Costi et al.'s NRG result for  $G$  as a function of  $T$  (see Figure 9). This is convincing evidence that we have correctly identified the scattering states (at least at the symmetric point of the dot). More specifically, we know the linear response conductance will again have a Fermi liquid form:

$$G(T) = 2\frac{e^2}{h}\left(1 - c\frac{T^2}{T_k^2} + \mathcal{O}(T^4/T_k^4)\right). \quad (1.5)$$

Costi et al. demonstrated in perturbation theory that the constant,  $c$ , takes the value,  $c = \pi^4/16 = 6.088$ . We compute in comparison  $c = 6.05 \pm .1$ . Beyond the low temperature Fermi liquid regime, we emphasize we are able to describe accurately the conductance in the crossover regime  $T \sim T_k$ .

We also compare the scaling curve for the finite temperature linear response conductance with the experimental data found in [1]. The comparison is plotted in Figure 10. We find the experimental measurements, even though taken away from the symmetric point of the dot (although still in its Kondo regime), agree well with our scaling curve. This suggests the Kondo regime of the dot exists over a wide range of gate voltages (i.e.  $\varepsilon_d$ ).

In Section 5 we move on to compute the non-equilibrium conductance at zero temperature. Again the scattering amplitudes need to be recomputed to take into account the change in the distributions of electrons in the leads induced by the finite bias. We also discuss subtleties with understanding how to think of a finite biased system in its one lead formulation. We then present results of the differential conductance both in and out of a magnetic field as discussed above.

We are able to derive a number of simple closed form results for the out-of-equilibrium conductance. The differential conductance in zero field at the symmetric point is computed to be

$$G(\mu_1, \mu_2) = 2\frac{e^2}{h} \frac{1}{\left(1 + \frac{\pi^2(\mu_1 - \mu_2)^2}{4T_k}\right)}, \quad (1.6)$$

a remarkably simple result. We are also able to characterize the peak in the differential conductance that develops in the presence of a magnetic field. The quantity most discussed in the literature, the bias at which the peak occurs, is given by the expression

$$eV_{\max} = -H\left(1 - \frac{1}{2\pi} \tan^{-1} \frac{1}{I^{-1} - b} + \dots\right), \quad (1.7)$$

$$I^{-1} - b = \frac{1}{\pi} \log\left(\frac{H}{2T_k} \sqrt{\frac{\pi e}{2}}\right),$$

valid for  $H \gg T_k$  and  $H \ll \sqrt{U\Gamma}$ . Because of the logarithmic dependence of  $b$  upon  $H$ , the position of the peak approaches  $eV = |H|$  extremely slowly. In addition to the location of the peak, we are also able to describe both the peak width and the height of the peak. The peak width is given by

$$e\Delta V = \frac{H}{2\pi} \left( \tan^{-1} \frac{1}{I^{-1} - 1/2 - b} - \tan^{-1} \frac{1}{I^{-1} + 1/2 - b} \right), \quad (1.8)$$

while the peak height is equal to

$$G_{\max} = \frac{e^2}{h} \left( \frac{3}{2} - \frac{(I^{-1} - b)}{\sqrt{4(I^{-1} - b) + 1}} \right). \quad (1.9)$$

We see that the height of the conductance peak approaches  $e^2/h$ , one half the unitary limit, in the asymptotic limit of large  $H$ . Interestingly, the non-equilibrium Kondo model in the Toulouse limit [14] also predicts a zero temperature differential magneto-conductance peak at  $eV = H$  which has a peak of  $e^2/h$ , one-half the unitary limit.

## 2. Basic Formalism

### 2.1. Description of the System

Pictured in Figure 2 is a sketch of the quantum dot connected to two leads. The Hamiltonian for this model in the continuum limit is given by

$$\mathcal{H} = \sum_{l\sigma} \int_{-\infty}^{\infty} dx \{ -ic_{l\sigma}^\dagger(x) \partial_x c_{l\sigma}(x) + V_l \delta(x) [c_{l\sigma}^\dagger(x) d_\sigma + d_\sigma^\dagger c_{l\sigma}(x)] \} + \varepsilon_d \sum_{\sigma} n_\sigma + U n_\uparrow n_\downarrow, \quad (2.1)$$

where  $n_\sigma = d_\sigma^\dagger d_\sigma$ . Here  $\sum_l$  is a sum over the two leads ( $l = 1, 2$ ). We have allowed for the possibility that the hopping matrix element,  $V_l$ , differs between the leads as is typical in any experimental realization. Rather than treating the leads as half-lines with both left and right moving fermions, we represent the leads as ‘unfolded’ with fermions that are solely right-moving. Fermions in either lead that are incident upon the dot are considered to lie in the region,  $x < 0$ , while those traveling away from the dot in either lead are found with  $x > 0$ . We represent this in Figure 2 by drawing the leads as elongated arcs.

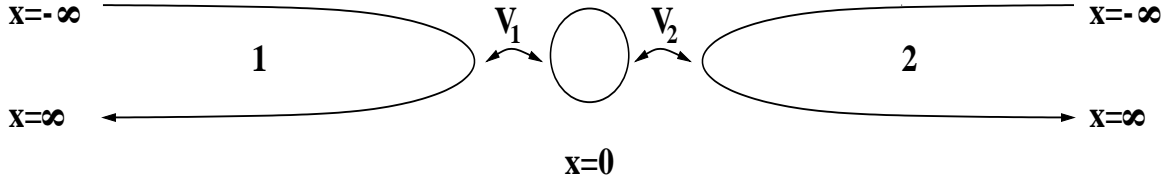


Figure 2: A sketch of two leads attached to a quantum dot.

We stress that there are no interactions in the leads (as opposed to the calculations in [24] for instance): the non-trivial physics of the problem arises solely from the strongly interacting dynamics of the dot.

It will be advantageous to reformulate this problem as a one-lead Anderson model (i.e. a single lead model). To do so, we introduce even/odd electrons:

$$c_{e/o} = \frac{1}{\sqrt{V_1^2 + V_2^2}} (V_{1/2} c_1 \pm V_{2/1} c_2). \quad (2.2)$$

Recasting  $\mathcal{H}$  in this new basis, the odd electron,  $c_o$ , decouples and we are left with

$$\begin{aligned} \mathcal{H} = \sum_{\sigma} \int dx \{ & -i c_{e\sigma}^{\dagger}(x) \partial_x c_{e\sigma}(x) + (V_1^2 + V_2^2)^{1/2} \delta(x) [c_{e\sigma}^{\dagger}(x) d_{\sigma} + d_{\sigma}^{\dagger} c_{e\sigma}(x)] \} + \\ & \varepsilon_d \sum_{\sigma} n_{\sigma} + U n_{\uparrow} n_{\downarrow}. \end{aligned} \quad (2.3)$$

We have thus reduced the problem to that solved using Bethe ansatz in a series of papers by Kawakami and Okiji [15] and Filyov, Wiegmann and Tsvelick [16].

With this reformulation of the model, we have to address the question of computing scattering amplitudes of electronic excitations in the original two lead problem. Naïvely it would seem we can do this. Let  $T(\varepsilon)$  and  $R(\varepsilon)$  be defined by:

$$\begin{aligned} T(\varepsilon) : & \text{transmission amplitude for an electronic excitation of energy, } \varepsilon, \\ & \text{to scatter from lead 1 to lead 2 (or 2 to 1),} \\ R(\varepsilon) : & \text{reflection amplitude for an electronic excitation of energy, } \varepsilon, \\ & \text{to scatter from lead 1 to lead 1 (or 2 to 2).} \end{aligned} \quad (2.4)$$

Assuming the amplitudes behave linearly under the even/odd map (2.2), we have (for  $V_1 = V_2$ )

$$\begin{aligned} e^{i\delta_e(\varepsilon)} &= R(\varepsilon) + T(\varepsilon); \\ e^{i\delta_o(\varepsilon)} &= 1 = R(\varepsilon) - T(\varepsilon). \end{aligned} \quad (2.5)$$

We then conclude that,

$$\begin{aligned} T(\varepsilon) &= \frac{e^{i\delta_e(\varepsilon)} - 1}{2}; \\ R(\varepsilon) &= \frac{e^{i\delta_e(\varepsilon)} + 1}{2}, \end{aligned} \tag{2.6}$$

govern scattering in the two lead problem. However not all electronic excitations behave linearly under the map (2.2) and so things are not always this simple. We will consider this in more detail in Section 2.4 and in particular Section 2.5.

As noted, in writing the above two equations, we have assumed  $V_1 = V_2$ . If  $V_1 \neq V_2$ , the transmission amplitude is scaled by the factor,

$$\frac{2V_1V_2}{V_1^2 + V_2^2}.$$

As this is a constant factor, it is always possible to rescale results to take into account an asymmetry in the dot-lead couplings. As such, we will assume throughout the paper that  $V_1 = V_2$ .

## 2.2. Bethe Ansatz Solution of the One-Lead Anderson Model

In order to understand the scattering between the two leads we will rely upon aspects of the one-lead Bethe ansatz solution found in [15] and [16]. As such we summarize briefly the results of this work. Applying the Bethe ansatz yields a set of quantization conditions describing a finite number of bare excitations in the system:

$$\begin{aligned} e^{ik_j L + i\delta(k_j)} &= \prod_{\alpha=1}^M \frac{g(k_j) - \lambda_\alpha + i/2}{g(k_j) - \lambda_\alpha - i/2}, \\ \prod_{j=1}^N \frac{\lambda_\alpha - g(k_j) + i/2}{\lambda_\alpha - g(k_j) - i/2} &= - \prod_{\beta=1}^M \frac{\lambda_\alpha - \lambda_\beta + i}{\lambda_\alpha - \lambda_\beta - i}, \end{aligned} \tag{2.7}$$

where

$$\begin{aligned} \delta(k) &= -2 \tan^{-1} \left( \frac{\Gamma}{(k - \varepsilon_d)} \right); \\ g(k) &= \frac{(k - \varepsilon_d - U/2)^2}{2U\Gamma}; \\ \Gamma &= (V_1^2 + V_2^2). \end{aligned} \tag{2.8}$$

As in all problems with an SU(2) symmetry, there are two types of excitations: charge (with rapidities,  $k$ ) and spin (with rapidities,  $\lambda$ ). Here  $N$  is the total number of particles



in the system, and  $M$  marks out the spin projection of the system,  $2S_z = N - 2M$  (in zero magnetic field,  $M = N/2$ ).

When  $\varepsilon_d > -U/2$ , the ground state of the system consists of the following set of excitations:

- i)  $N - 2M$  real  $k'_j$ s;
- ii)  $M$  real  $\lambda'_\alpha$ s;
- iii) associated with each of the  $M$   $\lambda'_\alpha$ s are two complex  $k'$ s,  $k_\pm^\alpha$ , described by

$$\begin{aligned} g(k_\pm^\alpha) &= g(x(\lambda_\alpha) \mp iy(\lambda_\alpha)) = \lambda_\alpha \pm i/2; \\ x(\lambda) &= U/2 + \varepsilon_d - \sqrt{U\Gamma}(\lambda + (\lambda^2 + 1/4)^{1/2})^{1/2}; \\ y(\lambda) &= \sqrt{U\Gamma}(-\lambda + (\lambda^2 + 1/4)^{1/2})^{1/2}. \end{aligned} \tag{2.9}$$

Although only valid for  $\varepsilon_d > -U/2$ , we can also understand the case,  $\varepsilon_d < -U/2$ , through a particle hole transformation. If we take the continuum limit of (2.9), we no longer deal with discrete values of  $\lambda$  and  $k$ , but rather go over to smooth distributions,  $\rho(k)$  for the real  $k_j$ 's, and  $\sigma(\lambda)$  for the  $\lambda_\alpha$ 's and their associated  $k_\pm^\alpha$ 's. To derive these distributions, we first take the log of (2.7):

$$\begin{aligned} k_j L + \delta(k_j) &= 2\pi N_j - \sum_{\beta=1}^M \theta_1(g(k_j) - \lambda_\beta); \\ 2\pi J_\alpha + \sum_{\beta=1}^M \theta_2(\lambda_\alpha - \lambda_\beta) + \sum_{j=1}^{N-2M} \theta_1(\lambda_\alpha - g(k_j)) & \\ &= -2Lx(\lambda_\alpha) - 2\text{Re}\delta(x(\lambda_\alpha) + iy(\lambda_\alpha)); \\ \theta_n(x) &= 2 \tan^{-1}\left(\frac{2}{n}x\right) + \pi. \end{aligned} \tag{2.10}$$

$N_j$  and  $J_\alpha$  are the quantum numbers of the charge and spin excitations respectively. Taking the thermodynamic limit (i.e.  $N, M, L \rightarrow \infty$  with  $N/L$  and  $M/L$  finite), followed by derivatives of the above, gives

$$\begin{aligned} \rho(k) &= \frac{1}{2\pi} + \frac{\Delta(k)}{L} + g'(k) \int_Q^{\tilde{Q}} d\lambda a_1(g(k) - \lambda)\sigma(\lambda); \\ \sigma(\lambda) &= -\frac{x'(\lambda)}{\pi} + \frac{\tilde{\Delta}(\lambda)}{L} - \int_Q^{\tilde{Q}} d\lambda' a_2(\lambda' - \lambda)\sigma(\lambda') - \int_{-D}^B dk a_1(\lambda - g(k))\rho(k), \end{aligned} \tag{2.11}$$

where

$$\begin{aligned}
\Delta(k) &= \frac{1}{2\pi} \partial_k \delta(k); \\
\tilde{\Delta}(\lambda) &= -\frac{1}{\pi} \partial_\lambda \text{Re} \delta(x(\lambda) + iy(\lambda)); \\
a_n(x) &= \frac{1}{2\pi} \partial_x \theta_n(x) = \frac{2n}{\pi} \frac{1}{(n^2 + 4x^2)}.
\end{aligned}
\tag{2.12}$$

Various limits appear in the above equations for the distributions.  $-D$  marks the lower allowed limit of the  $k$ 's while  $\tilde{Q}$  marks out the bandwidth of the  $\lambda$ 's. As each  $\lambda$  has a pair of complex  $k$ 's, its associated energy is  $2x(\lambda)$ . We thus determine  $\tilde{Q}$  by

$$x(\tilde{Q}) = -D. \tag{2.13}$$

Often it will be possible to replace  $\tilde{Q}$  and  $-D$  by  $\infty$  and  $-\infty$ .  $B$  and  $Q$  on the other hand give the spin and charge Fermi surfaces. They are determined by the constraints

$$\begin{aligned}
\frac{N - 2M}{L} &= \int_{-D}^B dk \rho(k); \\
\frac{M}{L} &= \int_Q^{\tilde{Q}} d\lambda \sigma(\lambda).
\end{aligned}
\tag{2.14}$$

### 2.3. Determination of the Scattering Phase at the Fermi Surface: The Friedel Sum Rule

In this section we examine the relationship between the scattering phase of electrons  $\delta_e(\epsilon)$  at the Fermi surface and the number of electrons on the dot and so verify the Friedel sum rule.

To determine  $\delta_e(\epsilon)$ , we employ an energetics argument of the sort used by N. Andrei in the computation of the magnetoresistance in the Kondo model [18]. Imagine adding an electron to the system. Through periodic boundary conditions, its momentum is quantized,  $p = 2\pi n/L$ . If the dot was absent, the quantization condition would be determined solely by the conditions in the bulk of the system and we would write,  $p_{\text{bulk}} = 2\pi n/L$ . Upon including the dot, this bulk momentum is shifted by a term scaling as  $1/L$ . The quantization condition is then rewritten as

$$p = \frac{2\pi n}{L} = p_{\text{bulk}} + \frac{\delta_e(\epsilon)}{L}, \tag{2.15}$$

where  $L$  is the system's length. The coefficient of the  $\frac{1}{L}$  term is identified with the scattering phase of the electron off the dot.

As we are interested in expressing  $\delta_e$  in terms of the number of electrons on the dot, it is useful to separate out from  $\rho(k)$  and  $\sigma(\lambda)$  the impurity contribution to the density of states. We thus write

$$\begin{aligned}\rho(k) &= \rho_{\text{bulk}}(k) + \frac{1}{L}\rho_{\text{imp}}(k); \\ \sigma(\lambda) &= \sigma_{\text{bulk}}(\lambda) + \frac{1}{L}\sigma_{\text{imp}}(\lambda).\end{aligned}\tag{2.16}$$

$\rho_{\text{bulk}}/\sigma_{\text{bulk}}$  represent the bulk contribution to the densities while  $\rho_{\text{imp}}/\sigma_{\text{imp}}$  determine the number of electrons of definite spin,  $n_{d\uparrow}/n_{d\downarrow}$ , sitting on the dot. From (2.14) we have

$$\begin{aligned}n_{d\uparrow} &= \int_Q^{\tilde{Q}} d\lambda \sigma_{\text{imp}}(\lambda) + \int_{-D}^B dk \rho_{\text{imp}}(k); \\ n_{d\downarrow} &= \int_Q^{\tilde{Q}} d\lambda \sigma_{\text{imp}}(\lambda).\end{aligned}\tag{2.17}$$

These relations will be key in verifying the Friedel sum rule. Substituting (2.16) into (2.11), we obtain separate equations for  $\rho_{\text{bulk}}/\rho_{\text{imp}}$  and  $\sigma_{\text{bulk}}/\sigma_{\text{imp}}$ :

$$\begin{aligned}\rho_{\text{bulk}}(k) &= \frac{1}{2\pi} + g'(k) \int_Q^{\tilde{Q}} d\lambda a_1(g(k) - \lambda)\sigma_{\text{bulk}}(\lambda); \\ \sigma_{\text{bulk}}(\lambda) &= -\frac{x'(\lambda)}{\pi} - \int_Q^{\tilde{Q}} d\lambda' a_2(\lambda' - \lambda)\sigma_{\text{bulk}}(\lambda') - \int_{-D}^B dk a_1(\lambda - g(k))\rho_{\text{bulk}}(k),\end{aligned}\tag{2.18}$$

and

$$\begin{aligned}\rho_{\text{imp}}(k) &= \Delta(k) + g'(k) \int_Q^{\tilde{Q}} d\lambda a_1(g(k) - \lambda)\sigma_{\text{imp}}(\lambda); \\ \sigma_{\text{imp}}(\lambda) &= \tilde{\Delta}(\lambda) - \int_Q^{\tilde{Q}} d\lambda' a_2(\lambda' - \lambda)\sigma_{\text{imp}}(\lambda') - \int_{-D}^B dk a_1(\lambda - g(k))\rho_{\text{imp}}(k).\end{aligned}\tag{2.19}$$

In Appendix A we give alternative forms to the above equations governing the density functionals. These alternatives are far more amenable to numerical analysis and in practice, the ones used in solving for the densities.

Having obtained the equations governing the impurity densities of state, we now focus on the scattering phase itself. From (2.10) we can read off the bulk momentum of a charge/spin excitation with quantum number  $N/J$  to be

$$\begin{aligned}p(k) &= \frac{2\pi N}{L} = k + \int_Q^{\tilde{Q}} d\lambda \sigma_{\text{bulk}}(\lambda)\theta_1(g(k) - \lambda); \\ p(\lambda) &= -\frac{2\pi J}{L} = 2x(\lambda) + \int_Q^{\tilde{Q}} d\lambda' \sigma_{\text{bulk}}(\lambda')\theta_2(\lambda - \lambda') + \int_{-D}^B dk \rho_{\text{bulk}}(k)\theta_1(\lambda - g(k)).\end{aligned}\tag{2.20}$$

We assume here  $\tan^{-1}$  in  $\theta_{1,2}$  varies from  $\pi/2$  to  $\pi/2$  so ensuring a simple relationship between the momentum and the energy functionals to be derived in the next subsection.

The impurity contribution to the momentum for each type of excitation can be similarly determined to be

$$\begin{aligned}
p_{\text{imp}}(k) &= \delta(k) + \int_Q^{\tilde{Q}} d\lambda \sigma_{\text{imp}}(\lambda)(\theta_1(g(k) - \lambda) - 2\pi); \\
p_{\text{imp}}(\lambda) &= 2Re\delta(x(\lambda) + iy(\lambda)) + \int_Q^{\tilde{Q}} d\lambda' \sigma_{\text{imp}}(\lambda')(\theta_2(\lambda - \lambda') - 2\pi) \\
&\quad + \int_{-D}^B dk \rho_{\text{imp}}(k)(\theta_1(\lambda - g(k)) - 2\pi).
\end{aligned} \tag{2.21}$$

Here we have chosen a different range for  $\tan^{-1}$  in  $\theta_{1,2}$  for describing the impurity momentum. Shifting back to the original range leads then to the appearance of the  $2\pi$ 's. This choice is governed by our ultimate desire to give the scattering phases in terms of the impurity momentum. In particular we want  $p_{\text{imp}}(k \rightarrow -\infty) = p_{\text{imp}}(\lambda \rightarrow \infty) = 0$ .

According to (2.15), we identify  $p_{\text{imp}}(k)$  with the scattering phase of a charge excitation and  $p_{\text{imp}}(\lambda)$  with the scattering phase of a spin excitation. By differentiating these expressions and comparing to (2.19), we obtain the relations

$$\begin{aligned}
\partial_k p_{\text{imp}}(k) &= 2\pi \rho_{\text{imp}}(k); \\
\partial_\lambda p_{\text{imp}}(\lambda) &= -2\pi \sigma_{\text{imp}}(\lambda).
\end{aligned} \tag{2.22}$$

Again we have relations crucial to verifying the Friedel sum rule.

In order to determine the scattering phase of an electron (as opposed to a spin or charge excitation), we must specify how to glue together a spin and a charge excitation to form the electron. The situation is analogous to adding a single particle excitation in the attractive Hubbard model [29]. Adding a single spin  $\uparrow$  electron to the system demands that we add a real  $k > B$  (charge) excitation. In doing so we create a hole at  $\lambda > Q$  in the spin distribution as the number of the available slots in the spin distribution is determined by the number of electrons in the system. Adding an electron to the system thus opens up an additional slot in the  $\lambda$ -distribution.

The electron scattering phase off the impurity is then the difference of the right-moving  $k$ -impurity momentum,  $p_{\text{imp}}(k)$ , and the left-moving  $\lambda$ -hole impurity momentum  $-p_{\text{imp}}(\lambda)$ :

$$\begin{aligned}
\delta_e^\uparrow &= p_{\text{imp}}^\uparrow = p_{\text{imp}}(k) + p_{\text{imp}}(\lambda); \\
&= 2\pi \int_{-D}^k dk' \rho_{\text{imp}}(k') + 2\pi \int_\lambda^{\tilde{Q}} d\lambda' \sigma_{\text{imp}}(\lambda'),
\end{aligned} \tag{2.23}$$

where we have used (2.22) in writing the last line. If the excitations are added/removed at the Fermi surfaces, i.e.  $k = B$ ,  $\lambda = Q$ , we obtain the Friedel sum rule for spin up electrons,

$$\delta_e^\uparrow = 2\pi \int_{-D}^B dk \rho_{\text{imp}}(k) + 2\pi \int_Q^{\tilde{Q}} d\lambda \sigma_{\text{imp}}(\lambda) = 2\pi n_{d\uparrow}, \quad (2.24)$$

where (2.17) has been used. The total energy of this excitation is  $\varepsilon(k = B) + \varepsilon(\lambda = Q) = 0$ , as it should be.

To determine the scattering of a spin down electron we employ particle-hole symmetry. A particle-hole transformation is implemented via

$$\begin{aligned} c_\uparrow^\dagger(k) &\rightarrow c_\downarrow(-k); \\ c_\downarrow^\dagger(k) &\rightarrow c_\uparrow(-k); \\ d_\uparrow^\dagger &\rightarrow d_\downarrow; \\ d_\downarrow^\dagger &\rightarrow d_\uparrow; \\ \varepsilon_d &\rightarrow -U - \varepsilon_d. \end{aligned} \quad (2.25)$$

Consequently the scattering phase of a spin  $\downarrow$  hole is related to that of a spin  $\uparrow$  electron via

$$\delta_{ho}^\downarrow(-U - \varepsilon_d) = \delta_e^\uparrow(\varepsilon_d). \quad (2.26)$$

The phase of this excitation is then

$$\delta_{ho}^\downarrow(-U - \varepsilon_d) = 2\pi \int_\lambda^{\tilde{Q}} d\lambda' \sigma_{\text{imp}}(\lambda') + 2\pi \int_{-D}^k dk' \rho_{\text{imp}}(k') = 2\pi n_{d\uparrow}(\varepsilon_d). \quad (2.27)$$

where the last equality holds if we take the hole to be at the Fermi surface,  $\lambda = Q$  and  $k = B$ . As  $n_{d\uparrow}(\varepsilon_d) = 1 - n_{d\downarrow}(-U - \varepsilon_d)$ , we have

$$\delta_{ho}^\downarrow(-U - \varepsilon_d) \bmod 2\pi = -n_{d\downarrow}(-U - \varepsilon_d). \quad (2.28)$$

At the Fermi surface, hole and electron scattering are identical (up to a sign) and so we verify the Friedel sum rule for spin down electrons.

The reader may be puzzled why we rely on a particle-hole transformation in computing the scattering amplitude for spin-down electrons. Although it would be desirable to do this computation directly, it does not seem to be possible. To construct a spin  $\downarrow$  electron

at the Fermi surface, it is natural to remove a  $k = B$  excitation while adding a  $\lambda = Q$  excitation. The corresponding scattering phase is then given by

$$\begin{aligned}
\delta_e^\downarrow &= p_{\text{imp}}^\downarrow \\
&= p_{\text{imp}}(k) + p_{\text{imp}}(\lambda) \\
&= 2\pi \int_{-D}^B dk \rho_{\text{imp}}(k) + 2\pi \int_Q^{\tilde{Q}} d\lambda' \sigma_{\text{imp}}(\lambda') \\
&= 2\pi n_{d\uparrow}.
\end{aligned} \tag{2.29}$$

But this is obviously not what we want - a manifest violation of the Friedel sum rule. Rather by comparing (2.29) with (2.27), the scattering indicates we have constructed a spin  $\downarrow$  electron not at  $\varepsilon_d$  but at the particle-hole conjugate point,  $-U - \varepsilon_d$ . Why this is so it is not entirely clear. However one can notice that the  $k$ -excitations are not only charge excitations, but are in some sense unbound spin  $\uparrow$  electrons (the number of  $k$ -excitations is directly proportional to the magnetization of the system). So in removing a  $k$ -excitation to form the spin  $\downarrow$  electron, we are in some sense creating a spin  $\uparrow$  hole. And a spin  $\uparrow$  hole at chemical potential,  $\varepsilon_d$ , will scatter as a spin  $\downarrow$  electron at  $-U - \varepsilon_d$ .

This entire discussion has concerned itself with proving the Friedel sum rule for the one-lead Anderson model. However we can argue that it applies, appropriately revised, to the two-lead model. More precisely, we can argue that the excitations at the Fermi surface behave linearly under the map (2.2) and so have two-lead scattering amplitudes given by (2.6). This will be detailed in the following two sections.

In appendix B we give an alternate derivation of the scattering phase that focuses upon the impurity energy of an excitation as opposed to its impurity momentum. In doing so, we elucidate subtleties not explicitly discussed in [28]. We also give a third derivation of the scattering phase in Appendix C by directly considering the dressing of the bare scattering.

#### 2.4. Excitations Away From the Fermi Surface in the Kondo Regime

In the previous section we were mainly concerned with scattering at the Fermi surface. However as made clear by taking  $k \neq B$ ,  $\lambda \neq Q$ , we can look at scattering above the Fermi surface.

It is tempting to ask first whether the non interacting electrons in the lead can still be described in this formalism (by electrons we mean the standard plane wave excitations

of appropriate spin and charge). Here it is useful to recall some well known results from many-body theory: Langreth, in verifying the Friedel sum rule for  $H = 0$  [30], computed the ratio of the elastic inverse lifetime,  $\tau_{el}^{-1}$ , of a plane wave mode to that of its total inverse lifetime,  $\tau^{-1}$ , finding

$$\frac{\tau_{el}^{-1}(\varepsilon)}{\tau^{-1}(\varepsilon)} = \frac{\Gamma}{2\text{Im}\Sigma(\varepsilon)}, \quad (2.30)$$

where  $\Sigma(\varepsilon)$  is the self-energy for the dot electron Green's function. At the Fermi surface,

$$\text{Im}\Sigma(\varepsilon = 0) = \frac{\Gamma}{2}, \quad (2.31)$$

and there are no inelastic processes. However away from the Fermi surface

$$\text{Im}\Sigma(\varepsilon) = \frac{\Gamma}{2} + c\varepsilon^2, \quad c > 0, \quad (2.32)$$

and  $\tau_{el}^{-1} < \tau^{-1}$ , so electrons with energies above the Fermi surface do not scatter elastically.

On the other hand, the simple excitations we construct within the integrable description by gluing spin and charge excitations will necessarily scatter elastically: beyond the Fermi surface, they cannot be the free electrons one would initially like to describe. In and of itself, this does not matter as all we are interested in at the end is charge transport, irrespective of what kind of objects actually do carry this charge. A similar situation occurs in the fractional quantum Hall effect [24], where the integrability approach uses quasi-particles which are neither electrons nor Laughlin quasi-particles. This approach merely provides a more convenient basis for the space of excitations, chosen such that scattering at the impurity is as simple as possible. However we do have to concern ourselves with rewriting the original free electrons in terms of the integrable scattering basis. As indicated in the introduction we are not able to provide an answer to this problem in its entirety.

Our approach will then be to build excitations which are “electronic”, that is carry the same quantum numbers as electrons, but scatter simply (i.e. elastically) at the impurity - they will also scatter in a simple, factorized way among themselves, although their S-matrix is non trivial (it is not  $S = -1$  anymore). One can certainly think of these excitations as dressed electrons.

This being understood, another difficulty remains: the potential parameter space of electronic excitations, i.e.  $(k, \lambda)$ , is two dimensional (provided we neglect other solutions of the Bethe ansatz, see Section 2.6), whereas we naturally want the space to be one dimensional. For the moment, we can only make the necessary dimensional reduction

when we are in the Kondo regime of the Anderson model. The first step in doing so is to determine the energy-momentum of an excitation labelled by  $(k, \lambda)$ .

We already know the momentum of the excitations from (2.20). We thus must only compute the energies. To facilitate the calculation of excitation energies, it is useful to decompose  $\rho(k)$  and  $\sigma(\lambda)$  into particle and hole densities:

$$\begin{aligned}\rho_{p/h}(k) &= \theta(\pm B \mp k)\rho(k); \\ \sigma_{p/h}(\lambda) &= \theta(\mp Q \pm \lambda)\sigma(\lambda).\end{aligned}\tag{2.33}$$

Now imagine varying  $\rho_{p/h}$  and  $\sigma_{p/h}$  and asking what is the corresponding variation in the energy. We can write this variation in two ways: one in terms of the bare energies and one in terms of new functions,  $\varepsilon^\pm(k)$  and  $\varepsilon^\pm(\lambda)$ , governing the dressed energies:

$$\begin{aligned}\delta E &= L \int dk \{ \varepsilon^+(k)\delta\rho_p(k) - \varepsilon^-(k)\delta\rho_h(k) \} + L \int d\lambda \{ \varepsilon^+(\lambda)\delta\sigma_p(\lambda) - \varepsilon^-(\lambda)\delta\sigma_h(\lambda) \} \\ &= L \int dk \left( k - \frac{H}{2} \right) \delta\rho_p(k) + 2L \int d\lambda x(\lambda)\delta\sigma_p(\lambda).\end{aligned}\tag{2.34}$$

The variations on  $\delta\rho_{p/h}$  and  $\delta\sigma_{p/h}$  are not independent. From (2.11) we see

$$\begin{aligned}\delta\rho_p(k) + \delta\rho_h(k) &= g'(k) \int d\lambda \delta\sigma_p(\lambda) a_1(g(k) - \lambda); \\ \delta\sigma_p(\lambda) + \delta\sigma_h(\lambda) &= - \int d\lambda' \delta\sigma_p(\lambda') a_2(\lambda' - \lambda) - \int dk \delta\rho_p(k) a_1(\lambda - g(k)).\end{aligned}\tag{2.35}$$

Substituting (2.35) into (2.34), we obtain

$$\begin{aligned}\varepsilon^+(k) + \varepsilon^-(k) &= k - \frac{H}{2} - \int d\lambda \varepsilon^-(\lambda) a_1(\lambda - g(k)); \\ \varepsilon^+(\lambda) + \varepsilon^-(\lambda) &= 2x(\lambda) - \int d\lambda' \varepsilon^-(\lambda') a_2(\lambda' - \lambda) \\ &\quad + \int dk g'(k) \varepsilon^-(k) a_1(g(k) - \lambda).\end{aligned}\tag{2.36}$$

$\varepsilon^\pm(\lambda)$  and  $\varepsilon^\pm(k)$  are characterized by

$$\begin{aligned}\varepsilon^+(\lambda) &= \theta(Q - \lambda)(\varepsilon^+(\lambda) + \varepsilon^-(\lambda)) > 0; \\ \varepsilon^-(\lambda) &= \theta(\lambda - Q)(\varepsilon^+(\lambda) + \varepsilon^-(\lambda)) < 0; \\ \varepsilon^+(k) &= \theta(k - B)(\varepsilon^+(k) + \varepsilon^-(k)) > 0; \\ \varepsilon^-(k) &= \theta(B - k)(\varepsilon^+(k) + \varepsilon^-(k)) < 0.\end{aligned}\tag{2.37}$$



The functions,  $\varepsilon = \varepsilon^+ + \varepsilon^-$ , are continuous and monotonic.  $\varepsilon^\pm$  have been defined such that  $\varepsilon^+(k/\lambda)$  is the cost of adding an excitation at  $k/\lambda$  while  $-\varepsilon^-(k/\lambda)$  is the energy needed to create a hole at  $k/\lambda$ . Again in Appendix A, we give alternative forms to the above equations governing the energy functionals which are more amenable to numerical analysis.

Having determined the energy of the excitation, we can easily relate it to its corresponding momentum. We consider the case of  $H = 0$  first. Comparing (2.20) and (2.36), and using  $\partial_k \varepsilon(k) = 2\pi \rho_{\text{bulk}}(k)$  and  $\partial_\lambda \varepsilon(\lambda) = -2\pi \sigma_{\text{bulk}}(\lambda)$ , we see

$$\begin{aligned} p_{\text{bulk}}(k) &= \varepsilon(k); \\ p_{\text{bulk}}(\lambda) &= \varepsilon(\lambda), \end{aligned} \tag{2.38}$$

where  $p_{\text{bulk}}$  is the portion of momentum not scaling as  $1/L$ .

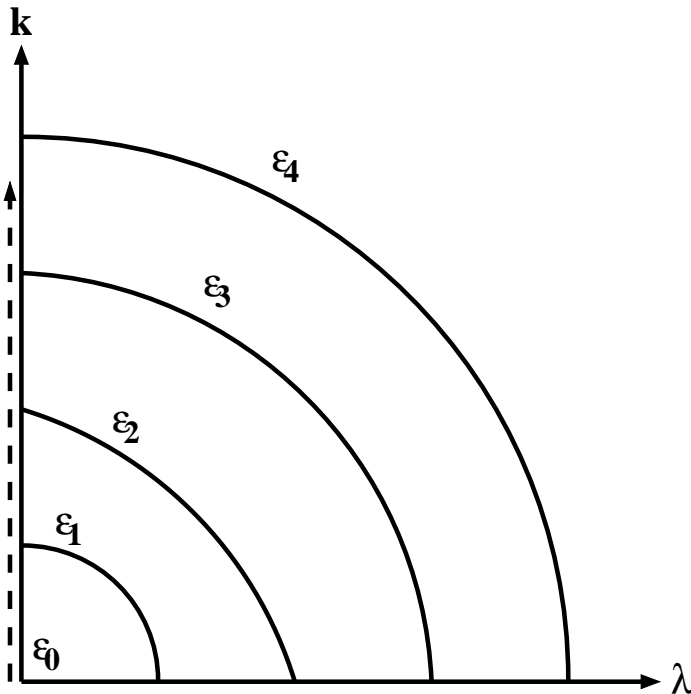


Figure 3: A cartoon of the parameter space describing electronic excitations. The drawing supposes that  $\varepsilon_0 = 0 < \varepsilon_1 < \varepsilon_2 < \varepsilon_3 < \varepsilon_4$ . Each curve represents a set of the excitations that share the same energy  $\varepsilon$ . Only in the case,  $\varepsilon_0 = 0$ , i.e. when we are at the Fermi surface, is the pair  $(k, \lambda)$  uniquely specified. The dashed line marks out the ansatz we employ in the Kondo regime.

With this in hand, we can parameterize the scattering phases of electronic excitations away from the Fermi surface. Suppose we want to characterize a spin  $\uparrow$  electron with energy,  $\varepsilon_{el}$ . (This is sufficiently general for  $H = 0$  as we know spin  $\downarrow$  electrons will scatter identically.) The possible  $k$  and  $\lambda$  forming this excitation must satisfy

$$\varepsilon(k) - \varepsilon(\lambda) = \varepsilon_{el}. \quad (2.39)$$

Given (2.38), this choice automatically satisfies  $\varepsilon_{el} = p_{el}$  (up to  $1/L$  corrections).

This parameterization leaves an unresolved issue. It does not in general uniquely specify a particular pair  $(k, \lambda)$ , crucial if we are to actually compute quantities involving information away from the Fermi surface. We have schematically illustrated the degeneracy of choices in Figure 3: as the energy is increased the multiplicity of pairs  $(k, \lambda)$  correspondingly increases.

In certain cases, however, the specification is unique. At the Fermi surface, the degeneracy of pairs is lifted. This already illustrated in Figure 3. However there is another case not captured by the cartoon in Figure 3 where the specification is unique. We have only a single possible pair  $(k, \lambda)$  for each energy in the case of spin  $\uparrow$  hole scattering in finite magnetic field at the symmetric point of the model. The reason behind the reduction of the parameter space for this case will be made clear in what follows.

For the other cases where the choice is not unique, the question becomes on what operative principle do we reduce the space. The key that we have identified to reducing the parameter space is determining how the excitations behave under the map (2.2). Only if they behave linearly under the map are they of use for it is only then that we can compute their scattering amplitudes in the two-lead picture via (2.6).

Although we have refined the question, we cannot in general determine whether a given excitation unfolds linearly in the case when there are multiple possible pairs  $(k, \lambda)$ . We can however make some progress when we are in the Kondo regime of the Anderson model (i.e.  $U + 2\varepsilon_d \sim 0$ ). In this regime we expect the scattering phase to vary on the scale of the Kondo temperature,  $T_k$ . The electron scattering phase is determined by  $\rho_{\text{imp}}$  and  $\sigma_{\text{imp}}$ , the two impurity densities. Of the two, only  $\rho_{\text{imp}}$  varies on scales on the order of  $T_k$ . In contrast,  $\sigma_{\text{imp}}$  is controlled by the much larger scale  $\sqrt{U\Gamma}$ . Thus in computing electronic scattering phases away from the Fermi surface at zero temperature, it is natural

to keep  $\lambda = Q$ , its Fermi surface value, and vary  $k$ . Specifically, to describe an electron of energy,  $\varepsilon_{el}$ , we chose  $(k, \lambda)$  such that

$$\begin{aligned} k \text{ particle, } \quad \varepsilon(k) &= \varepsilon_{el}; \\ \lambda \text{ hole at } \lambda &= Q. \end{aligned} \quad (2.40)$$

With this ansatz, we then have restricted the two dimensional phase space,  $(\lambda, k)$ , of potential excitations carrying the quantum numbers of an electron to an one dimensional subspace. Hence the scattering phases of electrons of energy,  $\varepsilon_{el}$ , above the Fermi surface at  $H = 0$  are given by

$$\delta_e^\uparrow(\varepsilon_{el}) = \delta_e^\downarrow(\varepsilon_{el}) = 2\pi \int_{-D}^k dk' \rho_{\text{imp}}(k') + 2\pi \int_Q^{\tilde{Q}} d\lambda \sigma_{\text{imp}}(\lambda), \quad \varepsilon(k) = \varepsilon_{el}. \quad (2.41)$$

When  $H \neq 0$ , we still have a simple relation between the energy and momentum, i.e., we have

$$\begin{aligned} \varepsilon(k) &= p(k) - \frac{H}{2}; \\ \varepsilon(\lambda) &= p(\lambda). \end{aligned} \quad (2.42)$$

Hence with  $H \neq 0$  we are still faced with an oversized parameter space. But we conjecture similar relations to those in (2.40) hold in constructing the electronic spin  $\uparrow$  excitations:

$$\begin{aligned} \uparrow \text{ electron : } k \text{ particle, } \quad \varepsilon(k) &= \varepsilon_{el}; \\ \lambda \text{ hole at } \lambda &= Q. \end{aligned} \quad (2.43)$$

The scattering phase of this excitation is accordingly

$$\delta_e^\uparrow(\varepsilon_{el}) = 2\pi \int_{-D}^k dk' \rho_{\text{imp}}(k') + 2\pi \int_Q^{\tilde{Q}} d\lambda \sigma_{\text{imp}}(\lambda), \quad \varepsilon(k) = \varepsilon_{el}. \quad (2.44)$$

With  $H \neq 0$  and consequently  $\varepsilon^-(k)$  not identically zero, we can construct spin  $\uparrow$  hole states by removing a  $k$ -state and a  $\lambda$ -hole. The scattering phase of spin  $\uparrow$  holes is then equal to

$$\begin{aligned} \delta_{ho}^\uparrow(\varepsilon_{ho} > 0) &= p_{\text{imp}}(k) + p_{\text{imp}}(\lambda); \\ &= 2\pi \int_{-D}^k dk' \rho_{\text{imp}}(k') + 2\pi \int_Q^{\tilde{Q}} d\lambda' \sigma_{\text{imp}}(\lambda'), \quad \varepsilon(k) = -\varepsilon_{ho}. \end{aligned} \quad (2.45)$$

For this particular excitation we do not need the scattering ansatz. If we are to remove a  $\lambda$ -hole we must do it for  $\lambda < Q$ . However at the symmetric point  $Q = -\infty$  and so

the choice is unique. This fact will allow us to conclude that in the large field limit, our computation of the differential magneto-conductance becomes exact. We also point out that as  $\varepsilon(k)$  is bounded below, i.e.  $\varepsilon(k = -D) = -H$ , we are limited in the energy range  $([0, H])$  in which we can construct spin  $\uparrow$  holes.

With  $H \neq 0$ , we must compute the scattering of spin  $\downarrow$  objects separately. To do so we again employ a particle-hole transformation. We so obtain

$$\begin{aligned}\delta_e^\downarrow(\varepsilon_{el}, -U - \varepsilon_d) &= \delta_{ho}^\uparrow(\varepsilon_{ho} = \varepsilon_{el}, \varepsilon_d); \\ \delta_{ho}^\downarrow(\varepsilon_{ho}, -U - \varepsilon_d) &= \delta_e^\uparrow(\varepsilon_{el} = \varepsilon_{ho}, \varepsilon_d).\end{aligned}\tag{2.46}$$

Unlike scattering at the Fermi surface where we could infer behaviour at  $\varepsilon_d > -U/2$  from behaviour at  $\varepsilon_d < -U/2$ , we cannot do so for scattering away from the Fermi surface. Thus when we need to compute explicitly the scattering of spin  $\downarrow$  objects, say in computing the magneto-conductance out of equilibrium, we will be restricted to the symmetric point  $\varepsilon_d = -U/2$ .

### 2.5. Returning to the Two-Lead Problem

In this section we explore in more depth the map between the one and two lead models and its attendant problems. To review the map in more formal terms call  $E_{e,o}$  the integrable excitations in the even and odd leads. We then describe the factorized scattering by the relations

$$\begin{aligned}E_e D &= e^{i\delta_e} D E_e \\ E_o D &= e^{i\delta_o} D E_o,\end{aligned}\tag{2.47}$$

where  $D$  is a formal symbol representing the impurity. Again the phase,  $\delta_e$ , is non trivial, while  $\delta_o = 0$ . Under the map (2.2), integrable excitations in the two lead picture are given by

$$E_{1,2} = E_e \pm E_o.\tag{2.48}$$

Scattering of an excitation in the first lead is then described by

$$E_1 D = R D E_1 + T D E_2;$$

or

$$(E_e + E_o) D = R D (E_e + E_o) + T D (E_e - E_o),\tag{2.49}$$

where consistency with (2.47) demands that the transmission and reflection amplitudes,  $R$  and  $T$ , satisfy  $R+T = e^{i\delta_e}$  and  $R-T = e^{i\delta_o}$ . An implicit assumption in this determination

of the scattering in the two lead picture is that the superposition  $E_o + E_e$  of an electronic excitation in the even sector and an electronic excitation in the odd sector carries unit charge in lead 1 and no charge in lead 2. For an arbitrary fermionic excitation in the even and odd leads this will not be the case. For example, imagine a electronic excitation in the even lead, that if decomposed into a plane wave basis of free electrons, consists in part of particle-hole excitations:

$$E_e = \sum_k a_k c_{ek}^\dagger |\text{Fermi sea}\rangle + \sum_{k,k_p,k_h} a_{kk_pk_h} c_{ek}^\dagger c_{ek_p}^\dagger c_{ek_h} |\text{Fermi sea}\rangle + \dots, \quad (2.50)$$

where here  $c_{ek}$  is a plane wave electron in the even lead with wave vector  $k$ . The linear combination  $E_e + E_o$ , where the excitation,  $E_o$ , is arrived at from (2.50) through  $c_e \rightarrow c_o$ , does then not carry unit charge in lead 1. Rather it carries indefinite charge in both leads. In this case the excitation does not transform between the two pictures as indicated by (2.48) and its scattering cannot be expected to be described by (2.49). If  $E_e$  was strictly a linear combination of terms of the form  $c_{ek}^\dagger |\text{Fermi sea}\rangle$ , this problem would not surface.

Thus in order to exploit the map between the two pictures, we must limit ourself to excitations that behave linearly under the map as described in (2.48). There are then two questions to be answered. Do such excitations in general exist? And if they do exist, are they sufficient for our purposes, the description of transport properties. We have two arguments that excitations with scattering described by (2.48) do exist. More precisely we have two arguments giving that excitations falling along some line in the two dimensional  $(k, \lambda)$  parameter space have such scattering. Moreover, we argue that the scattering of such excitations is sufficient to determine transport properties.

The first argument relies upon the transformation properties of the Fermi field,  $c(x)$ . Recall that in order to implement the map between the one and two lead pictures, it is  $c(x)$  that is transformed, i.e.

$$c_e(x) \rightarrow \frac{1}{\sqrt{2}}(c_1(x) \pm c_2(x)).$$

Thus any integrable excitation  $E_e$  that has a finite matrix element with  $c_e$ , i.e.

$$\langle c_e | E_e \rangle \neq 0,$$

must also behave linearly under the map from one to two leads. To see this more explicitly imagine making a mode expansion of the field,  $c_e(x)$ , in terms of the integrable excitations. As  $E_e$  couples to  $c_e$ ,  $E_e$  must appear in this expansion,

$$c_e(x) = \sum_r a_r e^{ip_r x} E_{er} + \dots, \quad (2.51)$$

where  $E_e$  is one of the  $E_{er}$ 's. As  $c_e$  and  $E_e$  are linearly related, they must share the same transformation properties. This guarantees that any excitation appearing in the above mode expansion will have scattering described by (2.49).

But we can say more on the basis of the properties of  $c_e(x)$ . Because the underlying model is essentially free, we know the single particle spectral function of the model will be given by

$$\langle c_e c_e(0) \rangle(E, p) \propto \delta(E - p).$$

Thus for any given energy  $E = p$ , we know that some integrable excitation with this energy and momentum must appear in the mode expansion (2.50). In terms of the two dimensional parameter space,  $(k, \lambda)$ , this implies that there is at least one line in this space describing excitations transforming as (2.48) and scattering as (2.49).

The second argument for the existence of this line in the  $(k, \lambda)$  parameter space relies upon combining the properties of the low energy sector of the theory with the equivalence of the integrable excitation we have constructed at the Fermi surface with the corresponding plane wave electron excitation. Given our reliance on this equivalence, it deserves further exploration.

This equivalence is, of course, strongly suggested by our ability to reproduce the Friedel sum rule and the fact Langreth [30] demonstrated that plane wave electrons at the Fermi surface scatter elastically, the hallmark of integrable excitations. Nevertheless, the statement that the integrable excitation coincides with a plane wave electron needs further clarification. If we denote the wave function of the integrable excitation as  $\psi_{\text{int}}(x, x_1, \dots, x_N)$ , where  $x$  is the coordinate of the excitation and the  $x_i$  are the coordinates of the electrons in the Fermi sea, and  $\psi_{\text{free el.}}(x, x_1, \dots, x_N)$  as the many-body wave function of the corresponding plane wave electron plus Fermi sea, we know that the orthogonality catastrophe implies the matrix element,  $\langle \text{int} | \text{free el.} \rangle$ , equals

$$\langle \text{int} | \text{free el.} \rangle = \int_{-\infty}^{\infty} dx dx_1 \cdots dx_N \psi_{\text{int}}^*(x, x_1, \dots, x_N) \psi_{\text{free el.}}(x, x_1, \dots, x_N) = \mathcal{O}(1/L),$$

and so vanishes in the thermodynamic limit. Thus it would seem that that in fact that the two excitations do not coincide.

However we are not interested in matrix elements involving full eigenstates of the Hamiltonian, but matrix elements involving asymptotic scattering states defined far from the impurity. These are the states of concern in applying a Landauer-Buttiker formalism. With such states, we would evaluate the above matrix elements by restricting  $x, x_i \ll 0$  or

$x, x_i \gg 0$ , depending on whether the state is in-going or out-going. With such a restriction, the orthogonality catastrophe does not apply and

$$\langle \text{int} | \text{free el.} \rangle = 1 + \mathcal{O}(1/L).$$

In this sense the excitations coincide.

With this equivalence so understood, the two excitations, the integrable excitation and the plane wave share the same transformation property (2.48) under the map. We now exploit this fact by combining it with the behaviour of the low energy sector of the theory. In this sector we can take a scaling limit and obtain a relativistic theory invariant under Lorentz transformations. Under such transformations, we can imagine boosting the integrable excitations at the Fermi surface, obtaining in the process an excitation with finite energy and momentum. However the transformation properties of the excitation cannot be altered by the boost. As such the boosted excitation will still transform via (2.48) under the map. This again implies that there is a line in  $(k, \lambda)$  parameter space describing excitations transforming in the desired fashion. In this case moving along this line amounts to making a Lorentz boost.

Having argued that there do exist excitations transforming as (2.48), we now have to address whether the existence of such excitations is sufficient for our computations of transport properties. We can answer in the affirmative. To compute any given transport quantity in the Landauer-Buttiker approach, we need to sum up transmission amplitudes over some given energy range. For example, if we were to compute the zero temperature out-of-equilibrium conductance, this energy range would be determined by the difference of chemical potentials in the two leads. Now imagine looking at a particular infinitesimal energy interval within this range. As we know the density of states of the free electron in the lead, and we know that the interactions in the problem do not affect this particular quantity, we know precisely how much charge lies in this interval. Now we are able to construct an integrable state that transforms via (2.48) with an energy in this interval and with the same density of states as the free particles. Thus our integrable state completely exhausts the charge lying within this infinitesimal interval. Given that we are able to compute its transmission amplitude (2.49), we can compute the contribution of this infinitesimal energy interval to the transport quantity.

As a corollary to this, the manifold other integrable states arising from the Bethe ansatz equations are then not needed for the computation of transport properties. We

do not need to account for the  $(k, \lambda)$  states that do not transform as (2.48). We also do not need to worry about states consisting of  $(k, \lambda)$  excitations together with particle-hole excitations of  $k$  and  $\lambda$ , or indeed excitations involving more complicated string solutions of the Bethe ansatz equations. The inclusion of such states in the computation of any transport quantity would amount to a double counting, given that the line of  $(k, \lambda)$  states transforming as (2.48) completely exhausts the density of states of free electrons in the leads.

Given all of this, we still must stress that our computation of scattering amplitudes away from the Fermi surface is in general only approximate. Although we understand that there exists a line of excitations in the  $(k, \lambda)$  parameter space for which we understand and can compute scattering, we do not know which line. Rather, at the symmetric point of the model we have only an ansatz of how this line cuts through parameter space. However we again stress that this ansatz is supported by the nature of the two scales in the Kondo regime,  $T_k$  and  $\sqrt{UT}$ . Moreover our ansatz appears to be extremely good given its agreement with Costi et al.'s NRG results.

Fortuitously there is one case where this ansatz is exact: the description of spin  $\uparrow$  holes. There, the  $(k, \lambda)$  parameter space is one-dimensional from the start and no ansatz is needed. We point out that the scattering of such holes provides by far and away the main contribution to the differential magneto-conductance at large fields,  $H$ . As such we expect the differential magneto-conductance to be exact at asymptotically large fields.

In order to determine for all cases how the line of linearly transforming excitations cuts through the  $(k, \lambda)$  parameter space we would have to have complete control of the change of basis between the free electrons and the integrable excitations. There must presumably exist a complete set of such excitations providing a proper change of basis of the form

$$|E\rangle = \sum c_{n, F_1 \dots F_k} |F_1, \dots, F_k\rangle. \quad (2.52)$$

Here, the notation is highly symbolic:  $E$  stands for any possible integrable excitation, while  $F_i$  stands for free electrons with some spin and energy with the sum over the number,  $k$ , the types, and the energies of such excitations. Presumably, there are some complex selection rules making it possible to match the number of degrees of freedom on the left and on the right of (2.52). At this point however, an exact understanding of (2.52) is beyond our reach.



### 3. Linear Response Conductance at $T = 0$

In this section we discuss the linear response conductance both in and out of a magnetic field at zero temperature. We of course note that none of Section 2 is necessary to compute the linear response conductance at  $T = 0$ . Although we have demonstrated the Friedel sum rule using integrability, all we need for this quantity is the occupancy of the dot as a function of various parameters, something available from the original Bethe ansatz work on the one-lead Anderson model. However, the behaviour of the linear response conductance as predicted by the Bethe ansatz has never been adequately explored, particularly in the case with a magnetic field. Indeed in the original work of Ng and Lee [7] showing that the Friedel sum rule could be applied to quantum dots, they employ a Hartree-Fock approximation in estimating the dot occupancy and so obtain some qualitatively incorrect predictions as to the behaviour of the conductance.

Generally, the linear response conductance equals

$$G = \frac{e^2}{h} (|T_{\uparrow}|^2(\varepsilon = 0) + |T_{\downarrow}|^2(\varepsilon = 0)), \quad (3.1)$$

where  $T_{\uparrow/\downarrow}(\varepsilon = 0)$  is the scattering amplitude at the Fermi surface:

$$|T_{\uparrow/\downarrow}(\varepsilon = 0)|^2 = \sin^2(\pi n_{d\uparrow/\downarrow}). \quad (3.2)$$

In the case with  $H = 0$ , the number of electrons on the dot as a function of  $\varepsilon_d$ , the gate voltage, can be computed exactly, as has been done by [28]. When  $H \neq 0$ , the equations become more difficult to analyze and in general only numerical solutions are available. However at the symmetric point, it is again possible to compute in closed form the number of spin  $\uparrow / \downarrow$  electrons on the dot [28], and so arrive at an analytic expression for  $G$ . We first consider the case with  $H = 0$ .

#### 3.1. $H = 0$ Linear Response Conductance

In this case the Friedel sum rule tells us

$$|T_{\uparrow/\downarrow}|^2 = \sin^2\left(\frac{\delta_{\uparrow/\downarrow}(\varepsilon = 0)}{2}\right), \quad (3.3)$$

where the phase,  $\delta_{\uparrow/\downarrow}$ , is equal to

$$\delta_{\uparrow/\downarrow} = 2\pi n_{d\uparrow/\downarrow}. \quad (3.4)$$

The number of electrons,  $n_{d\uparrow/\downarrow}$ , on the dot when  $H = 0$  simplifies to

$$n_{d\uparrow/\downarrow} = \int_Q^{\tilde{Q}} d\lambda \sigma_{\text{imp}}(\lambda). \quad (3.5)$$

$\sigma_{\text{imp}}(\lambda)$  in turn is given by (2.19) with the charge Fermi surface,  $B$ , set to the bottom of the band,  $-D$ ,

$$\sigma_{\text{imp}}(\lambda) = \tilde{\Delta}(\lambda) - \int_Q^{\tilde{Q}} d\lambda' a_2(\lambda' - \lambda) \sigma_{\text{imp}}(\lambda'). \quad (3.6)$$

The Fermi surface,  $Q$ , of the spin excitations is determined by the equations

$$\begin{aligned} \frac{N}{L} &= \int_Q^{\tilde{Q}} d\lambda \sigma(\lambda); \\ \sigma(\lambda) &= -\frac{x'(\lambda)}{\pi} - \int_Q^{\tilde{Q}} d\lambda' a_2(\lambda' - \lambda) \sigma(\lambda'). \end{aligned} \quad (3.7)$$

These equations are solved explicitly over most of the relevant parameter range in [28] using a Wiener-Hopf technique.

The solution breaks down into three cases according to the value of  $Q$  describing the Fermi surface:

**case i:** If we are close to the symmetric point ( $U/2 + \varepsilon_d \ll \sqrt{U\Gamma}$ ) then  $Q \ll 0$  (at the symmetric point,  $Q = -\infty$ ) and we have

$$n_{d\uparrow/\downarrow} = \frac{1}{2} - \frac{1}{\pi\sqrt{2}} \sum_{n=0}^{\infty} \frac{(-1)^n}{(2n+1)} G_+(i\pi(2n+1)) \int_{-\infty}^{\infty} dk \Delta(k) e^{-(2n+1)\pi(g(k)-Q)}, \quad (3.8)$$

where  $G_+$  arises in factoring the kernel of the integral equation, (3.6):

$$G_+(\omega) = \frac{\sqrt{2\pi}}{\Gamma(\frac{1}{2} - \frac{i\omega}{2\pi})} \left( \frac{-i\omega + \varepsilon}{2\pi e} \right)^{\frac{-i\omega}{2\pi}}. \quad (3.9)$$

We include above an extra factor of  $e$  omitted from [28] through a typo.  $Q$  is determined implicitly by the equation

$$\frac{2\varepsilon_d + U}{\sqrt{2U\Gamma}} = \frac{\sqrt{2}}{\pi} \sum_{n=0}^{\infty} \frac{(-1)^n}{(2n+1)^{3/2}} e^{\pi Q(2n+1)} G_+(i\pi(2n+1)). \quad (3.10)$$

This differs from [28] by a factor of 2. This same factor of 2 is missing from eqn. 8.2.38 of [28] which should, we believe, read

$$\frac{1}{\pi}(\varepsilon_d + U/2) = \int_{-\infty}^Q d\lambda \sigma(\lambda). \quad (3.11)$$

**case ii:** In the next case the location of the Fermi surface satisfies the constraint

$$0 < Q < I^{-1} \equiv \frac{U}{8\Gamma} - \frac{\Gamma}{2U}. \quad (3.12)$$

In this case  $n_{d\uparrow/\downarrow}$  is computed to be

$$n_{d\uparrow/\downarrow} = 2 - \sqrt{2} + \frac{\pi}{6\sqrt{2}}(I^{-1} - Q) - \frac{\pi^2\sqrt{2}}{(24)^2}(I^{-1} - Q)^2 + \mathcal{O}((I^{-1} - Q)^3). \quad (3.13)$$

The first two terms are found in [28] although we disagree by a factor of 2 in the term of  $\mathcal{O}(I^{-1} - Q)$  while the remaining term was computed by the authors alone.

**case iii:** In the final case we are far from the symmetric point such that  $(U/2 + \varepsilon_d) \gg \sqrt{U\Gamma}$  and  $Q > I^{-1} \equiv -1(U/8\Gamma - \Gamma/(2U))$ . We then have instead

$$n_{d\uparrow/\downarrow} = \frac{1}{2\pi^{3/2}} \int_0^\infty \frac{dw}{w} \Gamma(1/2 + w) e^{2\pi w(\frac{1}{T} - Q)} \sin(2\pi w) \left(\frac{w}{e}\right)^{-w}, \quad (3.14)$$

with  $Q$  in this case determined by

$$\begin{aligned} Q &= q^* + \frac{1}{2\pi} \log(2\pi e q^*), \\ \sqrt{q^*} &= \frac{\varepsilon_d + U/2}{\sqrt{2U\Gamma}}. \end{aligned} \quad (3.15)$$

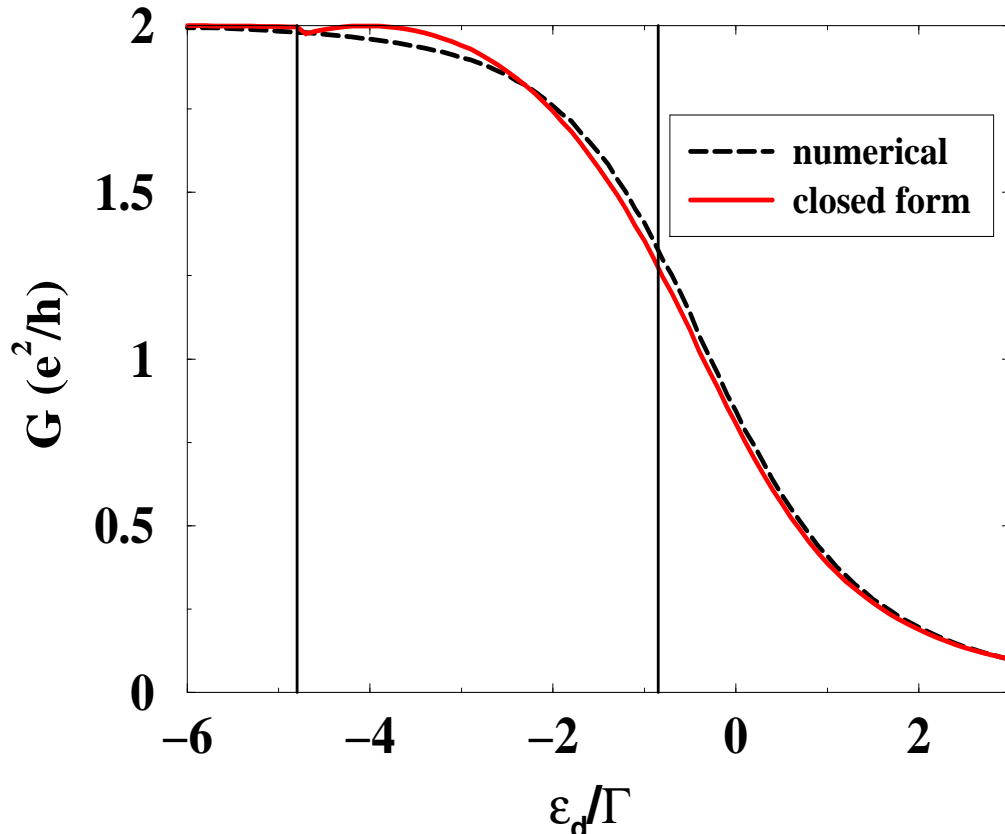


Figure 4: A plot of the linear response conductance at zero temperature in zero magnetic field. The parameters used are  $U = .75$  and  $\Gamma = U/12$ . The dashed line marks out the conductivity derived from a numerical solution of  $n_d$  while the solid line represents the closed form solution described in this section.

In Figure 4 is plotted the linear response conductance as a function of the dot chemical potential,  $\varepsilon_d > -U/2$  (for  $\varepsilon_d < -U/2$  particle-hole symmetry tells us the plot is a mirror image about the  $\varepsilon_d = -U/2$  axis), according to this closed form solution. For the purposes of comparison, we also present the conductance derived from a numerical evaluation of the equations determining  $n_d$ . The vertical lines divide the plot according to the three cases of the closed form solution. We see that this solution best matches the numerical solution in cases i and iii. We also see that the solution makes a discontinuous transition from case i to case ii, a consequence of the approximate nature of the solution in case ii.

As expected the linear response conductance rises smoothly from zero at large, positive values of  $\varepsilon_d$  to its maximum possible value,  $2e^2/h$ , at the symmetric point of the model,

$U/2 = -\varepsilon_d$ . The ratio of the values of  $U$  and  $\Gamma$  chosen for this plot correspond to that of the experimental realization of a quantum dot discussed in [1]<sup>1</sup>.

### 3.2. $H \neq 0$ Linear Response Conductance

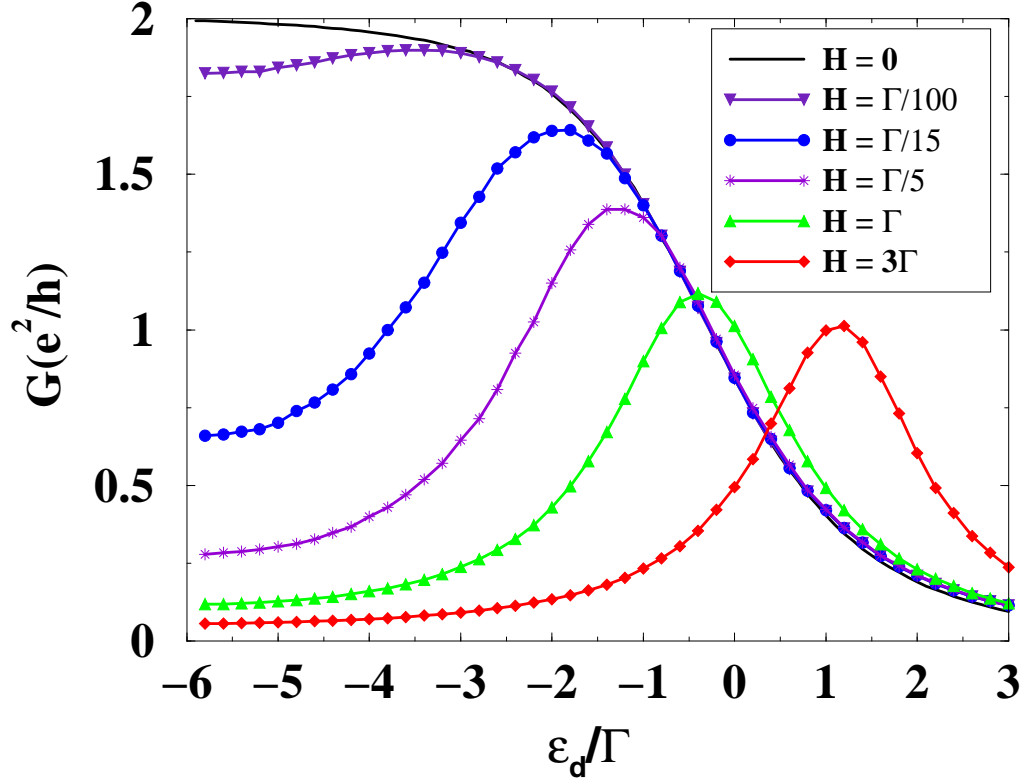


Figure 5: A plot of the linear response conductance at zero temperature for various values of the magnetic field. By particle-hole symmetry, the conductance for values of  $\varepsilon_d < -U/2$  is obtained by taking the plot's mirror image about the axis  $\varepsilon_d = -U/2$ . The parameters used are  $U = .75/\pi D$  ( $D$  being the bandwidth) and  $\Gamma = U/12$ . For these parameters, the Kondo temperature at the symmetric point is  $T_k = .02508\Gamma$ .

*Solution Away from the Symmetric Point ( $\varepsilon_d > -U/2$ ):*

Again the transmission amplitude of the electrons is given by (3.3) and (3.4). But in

---

<sup>1</sup> Note that our definition of  $\Gamma$  is related to that of [1] by  $\Gamma = \Gamma_{[1]}/2$ .

this case

$$\begin{aligned}
n_{d\uparrow} &= \int_{-D}^B dk \rho_{\text{imp}}(k) + \int_Q^{\tilde{Q}} d\lambda \sigma_{\text{imp}}(\lambda) \\
n_{d\downarrow} &= \int_Q^{\tilde{Q}} d\lambda \sigma_{\text{imp}}(\lambda),
\end{aligned}
\tag{3.16}$$

where  $\rho_{\text{imp}}$  and  $\sigma_{\text{imp}}$  are given by (2.19).

In general the equations for  $\rho_{\text{imp}}$  and  $\sigma_{\text{imp}}$  cannot be solved analytically. Therefore we resort to numerical solutions. In Figure 5 we plot the result. Presented there is the linear response conductance as a function of  $\varepsilon_d$  for a variety of magnetic fields ranging from  $H = 0$  to  $H = 3\Gamma$ .

As  $H$  is increased from zero, we see two effects: the value of  $\varepsilon_d$  marking the conductance peak shifts away from the symmetric point,  $\varepsilon_d = -U/2 (= -6\Gamma)$  while the magnitude of the peak decreases. This is as expected. The Kondo temperature for the model is given by [31] [28]:

$$T_k = \sqrt{\frac{U\Gamma}{2}} e^{\pi(\varepsilon_d(\varepsilon_d+U)-\Gamma^2)/(2\Gamma U)},
\tag{3.17}$$

and so varies strongly as a function of the dot chemical potential. When  $H > T_k$  we expect the Kondo effect to be suppressed and any consequent enhancement in  $G$  to disappear. For values of  $\varepsilon_d$  away from the symmetric point,  $T_k$  is relatively large and thus strong fields are needed to suppress the conductance. Closer to the symmetric point,  $T_k$  is exponentially suppressed and weak fields are sufficient to destroy the Kondo effect.

When  $H = 0$ , a conductance maximum of  $2e^2/h$  occurs at the symmetric point. At the symmetric point,  $n_{d\uparrow/\downarrow} = 1/2$ , and so each spin species makes a corresponding  $e^2/h$  contribution to  $G$ . As  $H$  is increased to large positive values, the gate voltage,  $\varepsilon_d$ , at which  $n_{d\uparrow/\downarrow} = 1/2$  splits leading to a corresponding split in the conductance resonance. For example for large  $H$  the resonance associated with the spin  $\uparrow$  electrons is approximately  $e^2/h$  and occurs at  $H/2$ .

We see for example in Figure 5 that when  $H = \Gamma/100$  the Kondo temperature is never exceeded regardless of the value of the gate voltage and so we see little consequent suppression of the conductance. However for the next largest value of  $H$ ,  $H = \Gamma/15$ , the Kondo temperature is exceeded in the Kondo regime and we see a corresponding depression in the conductance in this regime. For the largest value of  $H = 3\Gamma$ , we see as expected that the peak value is approximately  $e^2/h$  and that it occurs roughly at  $\varepsilon_d = H/2$ .

We note that the linear response conductance curves are symmetric about their peak value. This differs from the prediction based upon a Hartree-Fock computation of Ng and Lee [7]. But it is in agreement with Meir and Wingreen [9].

The conclusions in the above discussion are reiterated in Figure 6. There we plot the behaviour of the conductance peak as the magnetic field is increased from zero. In the top panel of Figure 6 we see that the location of the peak rapidly moves away from  $\varepsilon_d = -U/2$  towards the large field value of  $H/2$ . The straight line in this panel indicates the behaviour of the peak if interactions were absent. Similarly we see the peak height in the middle panel of Figure 6 change from its maximal value of  $2e^2/h$  at  $H = 0$  to  $e^2/h$  at large fields corresponding to a contribution to the conductance of a single spin species. And finally in the bottommost panel of Figure 6 we examine the width of the peak. At  $H = 0$  the width of the peak is approximately  $12\Gamma$ . However in the large field limit this settles down to  $2\Gamma$  appropriate to the conductance being governed by the Breit-Wigner formula

$$G = \frac{e^2}{h} \frac{\Gamma^2}{\Gamma^2 + (\varepsilon_d - H/2)^2}, \quad (3.18)$$

appropriate to a single non-interacting electron species.

*Solution at the Symmetric Point, ( $\varepsilon_d = -U/2$ ):*

Although we cannot in general express the magneto-conductance in closed form, we can do so at the symmetric point. At the symmetric point, the Fermi surface of the spin excitations,  $Q$ , goes to  $\infty$ . The density equations then simplify to

$$\begin{aligned} \rho_{\text{bulk}}(k) &= \frac{1}{2\pi} + g'(k) \int_{-\infty}^{\infty} d\lambda a_1(g(k) - \lambda) \sigma_{\text{bulk}}(\lambda); \\ \sigma_{\text{bulk}}(\lambda) &= -\frac{x'(\lambda)}{\pi} - \int_{-\infty}^{\infty} a_2(\lambda' - \lambda) \sigma_{\text{bulk}}(\lambda') - \int_{-D}^B dk a_1(\lambda - g(k)) \rho_{\text{bulk}}(k), \end{aligned} \quad (3.19)$$

and

$$\begin{aligned} \rho_{\text{imp}}(k) &= \Delta(k) + g'(k) \int_{-\infty}^{\infty} d\lambda a_1(g(k) - \lambda) \sigma_{\text{imp}}(\lambda); \\ \sigma_{\text{imp}}(\lambda) &= \tilde{\Delta}(\lambda) - \int_{-\infty}^{\infty} d\lambda a_2(\lambda' - \lambda) \sigma_{\text{imp}}(\lambda') - \int_{-D}^B dk a_1(\lambda - g(k)) \rho_{\text{imp}}(k). \end{aligned} \quad (3.20)$$

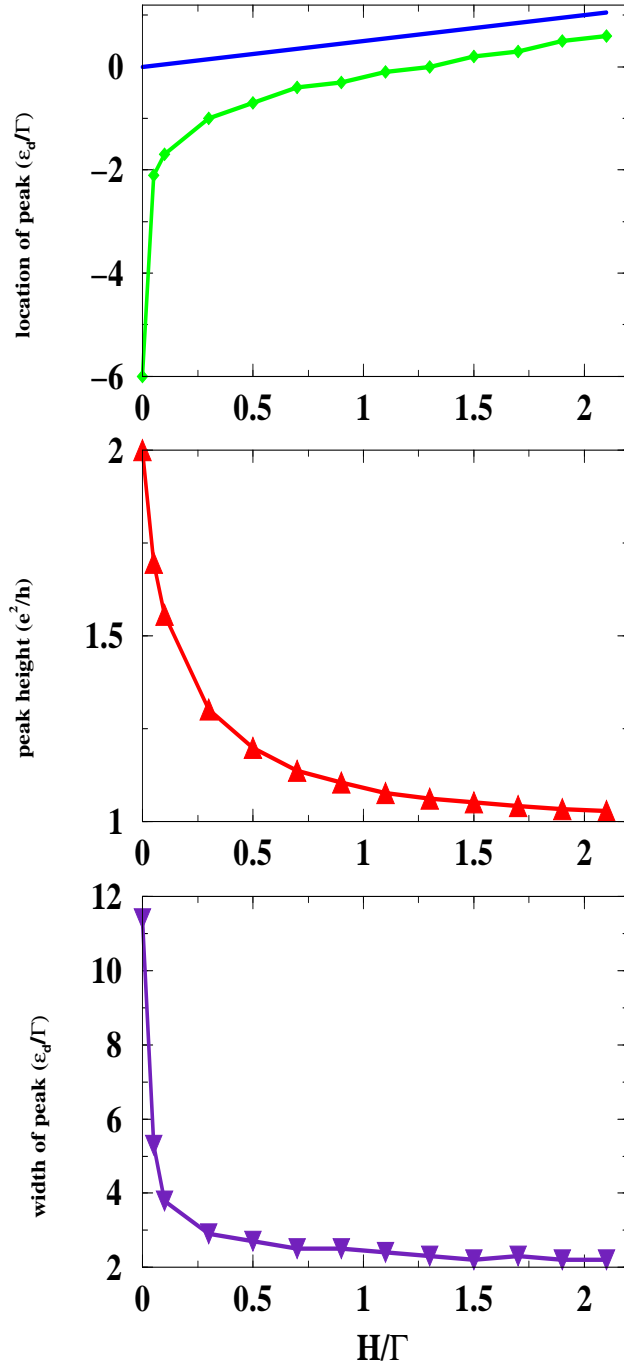


Figure 6: Plots of how the conductance peak evolves with increasing magnetic field. In the top panel is a plot of the location of the peak while the middle panel records the peak height and the bottom panel gives the peak width. The parameters used are  $U = .75/\pi D$  ( $D$  being the bandwidth) and  $\Gamma = U/12$ .



Here the limit  $B$  is determined by

$$\frac{2S_z}{L} = \frac{H}{2\pi} = \int_{-D}^B dk \rho(k). \quad (3.21)$$

As the electrons in the leads are non-interacting, the first equality is a result of Pauli-paramagnetism.

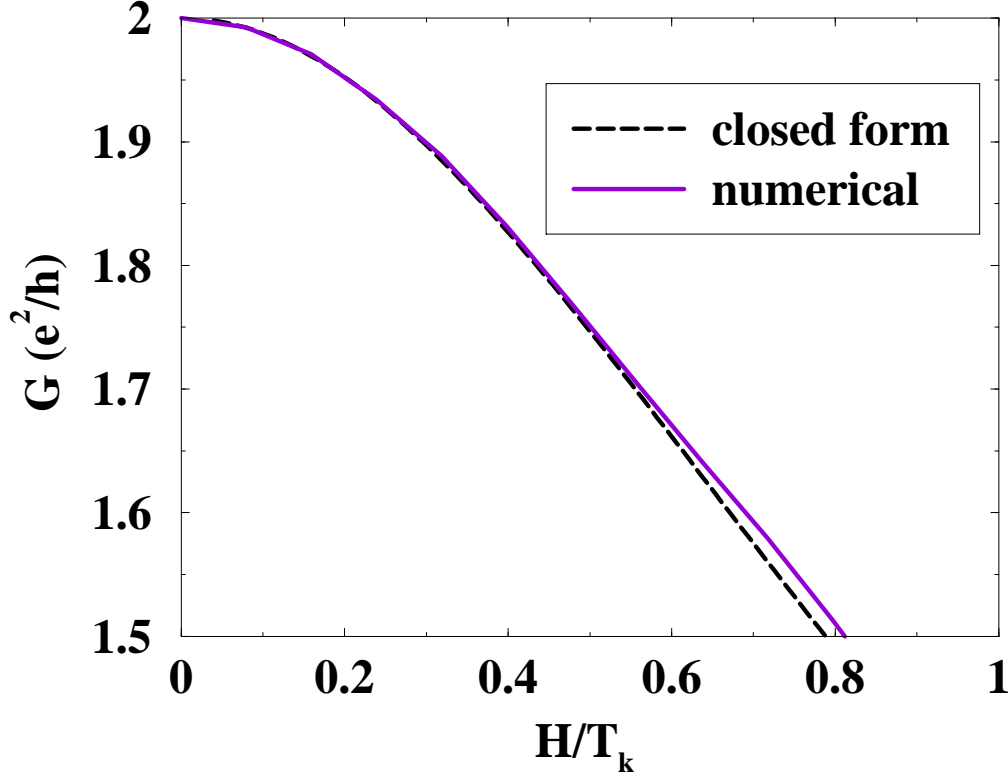


Figure 7: A plot of the linear response conductance at zero temperature at the symmetric point ( $\varepsilon_d = -U/2$ ) as a function of magnetic field. The parameters used are  $U = .75$  and  $\Gamma = U/12$ . The dashed line marks out the conductivity derived from a numerical solution of  $n_d$  while the solid line represents the closed form solution described in this section.

The phase shifts are given by

$$\begin{aligned} \delta_{e\uparrow} = 2\pi - \delta_{e\downarrow} &= 2\pi \int_Q^{\tilde{Q}} d\lambda \sigma_{\text{imp}}(\lambda) + 2\pi \int_{-\infty}^B dk \rho_{\text{imp}}(k) \\ &= \pi + \pi \int_{-\infty}^B dk \rho_{\text{imp}}(k), \end{aligned} \quad (3.22)$$

which follows as

$$\int_{-\infty}^{\infty} d\lambda \sigma_{\text{imp}}(\lambda) = \frac{1}{2} - \frac{1}{2} \int_{-\infty}^B dk \rho_{\text{imp}}(k). \quad (3.23)$$

This is established by integrating,  $\int_{-\infty}^{\infty}$ , (3.20). We can thus focus solely upon the  $k$ -distribution.

In order to evaluate the phase shift in the equation above, we are thus interested in computing the integral,

$$\int_{-\infty}^B dk \rho_{\text{imp}}(k) = 2M_i, \quad (3.24)$$

which, as indicated, is directly related to the impurity magnetization,  $M_i$ . Using the same Wiener-Hopf technique, [28] determined this integral in the case  $T_k > H$ , to be

$$2M_i = \frac{\sqrt{2}}{\pi} \sum_{n=0}^{\infty} \frac{G_+(i\pi(2n+1))}{(2n+1)} (-1)^n e^{-\pi(2n+1)(b-1/I)}, \quad (3.25)$$

$$b = \frac{1}{\pi} \log\left(\frac{2}{H} \sqrt{\frac{U\Gamma}{\pi e}}\right).$$

Combining this with the expression for the Kondo temperature in (3.17), we have for the scattering phases at leading order in  $H/T_k$

$$\delta_{e\uparrow} = 2\pi - \delta_{e\downarrow} = \pi\left(1 + \frac{H}{2T_k}\right), \quad (3.26)$$

which in turn gives the magneto-conductance as

$$G(H) = 2\frac{e^2}{h} \left(1 - \frac{\pi^2}{16} \left(\frac{H}{T_k}\right)^2 + \mathcal{O}\left(\frac{H}{T_k}\right)^4\right). \quad (3.27)$$

The quadratic deviation from the maximal conductance has the expected Fermi liquid form.

In Figure 7 is plotted how the magnitude of the linear response conductance at the symmetric point changes as a function of  $H/T_k$  (for small  $H$ ) according to this solution. We plot it against the numerical solution and we obtain agreement at worst of 1.5%. The disagreement becomes larger as  $H$  increases as the closed form solution is only valid at  $H < T_k \propto e^{-1/I}$ . Beyond  $H > T_k$ , we rely entirely on a numerical solution to determine the magneto-conductance. We plot the behaviour of  $G(H)$  in Figure 8 up to  $H = \Gamma$ .

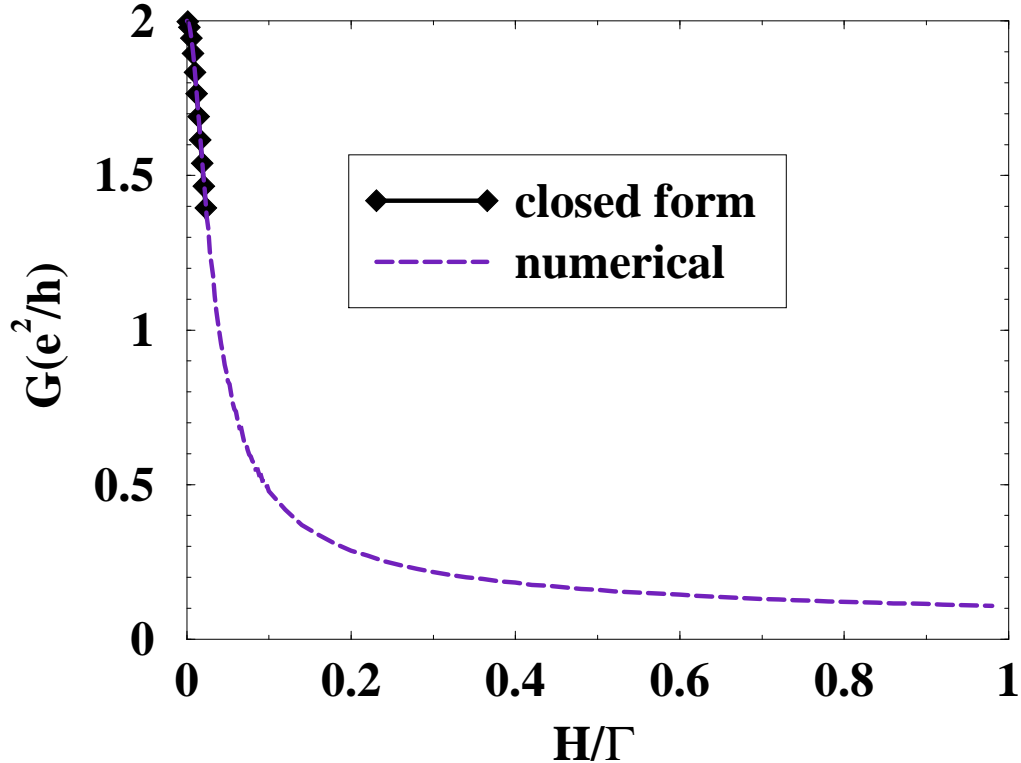


Figure 8: A plot of the linear response conductance at zero temperature at the symmetric point ( $\varepsilon_d = -U/2$ ) as a function of magnetic field. The parameters used are  $U = .75$  and  $\Gamma = U/12$ . The dashed line marks out the conductivity derived from a numerical solution of  $n_d$  while the solid line represents the closed form solution described in this section.

#### 4. Linear Response Conductance at Finite Temperature

In the previous section we focused upon scattering at the Fermi surface. In this section, we discuss a problem that requires us to understand scattering at finite energy: the linear response conductance as a function of temperature. We compare it to Costi et al.'s NRG results and find excellent agreement. This is important as it indicates we have an essentially correct description of the low energy scattering states, i.e. an excellent approximation to the right hand side of (2.52).

Computing the linear response conductance at finite  $T$  is a complicated matter. Even though we only consider glued charge and spin excitations as explained in Section 2, we now have to compute their scattering matrix - the  $1/L$  correction of their associated momenta -

in the presence of a “thermalized ground state”. This ground state is no longer composed of merely real  $k$  states and 2-string bound states of spin and charge as it was at  $T = 0$ . Rather all the possible solutions of the Bethe ansatz equations of the model make an appearance. Thus to begin the computation of the scattering amplitudes at finite  $T$ , we give the complete list of excitations in the model.

It is useful to understand how the following calculation differs from the exact computation of the conductances in the fractional quantum Hall problem [24]. The logic of [24] would first require the identification of all the excitations above the zero temperature ground state. We then would need to compute both the bulk and impurity scattering matrices of these excitations. Having done this, the second step would be to turn on the temperature. The thermalized ground state would then consist of seas of all these excitations with their distributions determined by a thermodynamic Bethe ansatz, employing the zero temperature S-matrices. Finally, the conductance would be determined by the zero temperature impurity scattering matrices as in [24]. A potential difficulty in this approach would come in understanding the gluing necessary to form excitations carrying electronic quantum numbers as it only such excitations that can be mapped back to the two-lead picture.

Whatever the likelihood for success, one can see that this way of proceeding requires considerable technical expenditure. It turns out to be easier to determine the thermalized ground state directly from the Bethe ansatz, i.e., by dealing with bare excitations rather than first determining the zero temperature ground state, classifying its “physical” or “dressed” excitations, and expressing the thermalized ground state in terms of these excitations. On the other hand, with the quantum Hall edges, it was the natural way to proceed as the initial data one had at hand (with no calculations whatsoever) is precisely the excitations about the zero temperature ground state together with their S-matrices, both bulk and impurity.

To proceed then, the first step is to identify all solutions of the Bethe ansatz equations. These are of three types: real  $k$ -states, spin complexes associated with complex  $k$ 's (both of which we have seen as the ground state at zero temperature is composed of such excitations) and spin complexes not associated with complex  $k$ 's. Below we give a more specific description together with the quantum numbers carried by each excitation. The spin quantum numbers are measured relative to a vacuum carrying spin  $N/2$  where  $N$  is the number of particles in the system.

i) real  $k$ 's: These appear in the ground state at  $T=0$  in the presence of a magnetic field.

They carry charge  $e$  and no spin.

ii)  $n$ -spin complex with no associated  $k$ 's: An  $n$ -complex involves  $n$   $\lambda$ 's organized as

$$\lambda^{nj} = \lambda^n + i\left(\frac{n+1}{2} - j\right), \quad j = 1, \dots, n. \quad (4.1)$$

Here  $\lambda^n$  is a real rapidity and is known as the centre of the complex. The  $n$ -spin complex carries spin  $-n/2$ .

iii)  $n$ -spin complex with  $2n$  associated complex  $k$ 's: The  $n$ -complex is organized as before

$$\lambda^{nj} = \lambda^n + i\left(\frac{n+1}{2} - j\right), \quad j = 1, \dots, n. \quad (4.2)$$

but now there are two  $k$ 's associated with each  $\lambda^{nj}$

$$\begin{aligned} g(k^{+nj}) &= \lambda^n + i\left(\frac{n}{2} + 1 - j\right); \\ & \qquad \qquad \qquad j = 1, \dots, n; \\ g(k^{-nj}) &= \lambda^n + i\left(\frac{n}{2} - j\right). \end{aligned} \quad (4.3)$$

These excitations carry charge  $2ne$  and spin  $-n/2$ . The simplest of these excitations ( $n=1$ ) appear in the ground state at zero temperature. Now the claim is that these are solutions to the Bethe ansatz equations (2.7) and (2.8) and indeed they are in the thermodynamic limit (the object of our concern) [28].

We can derive equations constraining the particle/hole densities of these various ex-

citations in the same fashion we arrive at (2.11) from (2.7) and (2.8). The result is

$$\begin{aligned}
\rho_p(k) + \rho_h(k) &= \frac{1}{2\pi} + \frac{\Delta(k)}{L} + g'(k) \sum_{n=1}^{\infty} \int_{-\infty}^{\infty} d\lambda a_n(g(k) - \lambda)(\sigma_{pn}(\lambda) + \sigma'_{pn}(\lambda)); \\
\sigma_{hn}(\lambda) &= -\frac{x'_n(\lambda)}{\pi} + \frac{\widetilde{\Delta}_n(\lambda)}{L} - \int_{-\infty}^{\infty} a_n(\lambda - g(k))\rho_p(k) \\
&\quad - \sum_{m=1}^{\infty} \int_{-\infty}^{\infty} d\lambda' A_{nm}(\lambda - \lambda')\sigma_{pm}(\lambda'); \\
\sigma'_{hn}(\lambda) &= \int_{-\infty}^{\infty} a_n(\lambda - g(k))\rho_p(k) - \sum_{m=1}^{\infty} \int_{-\infty}^{\infty} d\lambda' A_{nm}(\lambda - \lambda')\sigma'_{pm}(\lambda'); \\
x_n(\lambda) &= \sqrt{2U\Gamma} \operatorname{Re} \left( \lambda + i\frac{n}{2} \right)^{1/2} + n\left(\frac{U}{2} + \varepsilon_d\right) \\
\widetilde{\Delta}_n(\lambda) &= -\frac{1}{\pi} \partial_\lambda \delta_n(\lambda) \equiv -\frac{1}{\pi} \partial_\lambda \operatorname{Re} \delta(-\sqrt{2U\Gamma} (\lambda + i\frac{n}{2})^{1/2} + U/2 + \varepsilon_d) \\
&\quad - \frac{1}{2\pi} \partial_\lambda \sum_{k=1}^{n-1} \left\{ \delta(-\sqrt{2U\Gamma} (\lambda + \frac{i}{2}(n-2k))^{1/2} + U/2 + \varepsilon_d) \right. \\
&\quad \left. + \delta(\sqrt{2U\Gamma} (\lambda + \frac{i}{2}(n-2k))^{1/2} + U/2 + \varepsilon_d) \right\}.
\end{aligned} \tag{4.4}$$

The kernels in the density equations are given by

$$\begin{aligned}
a_n(\lambda) &= \frac{2n}{\pi} \frac{1}{(n^2 + 4\lambda^2)}; \\
A_{nm}(\lambda) &= \delta_{nm} \delta(\lambda) + a_{|n-m|}(\lambda) + 2 \sum_{k=1}^{\min(n,m)-1} a_{|n-m|+2k}(\lambda) + a_{n+m}(\lambda).
\end{aligned} \tag{4.5}$$

Here  $\rho_{p/h}$  is as before while  $\sigma_{p/hn}$  denotes the particle/hole densities of n-strings associated with complex k's (in Section 2 we denoted  $\sigma_{p/h1}$  by  $\sigma_{p/h}$ ) and  $\sigma'_{p/hn}$  denotes particle/hole densities of n-strings not so associated.

As stated in the introduction of this section, we construct the electronic excitations in the same fashion as at zero temperature, the only difference being that the excitations are now over the thermal ground state, not the  $T = 0$  ground state. In order to describe the scattering amplitudes we thus need to specify the impurity momentum of the  $\rho(k)$  and  $\sigma_1(\lambda)$  excitations. The finite temperature momenta for such excitations are as follows

(compare (2.20)):

$$\begin{aligned}
p^{\text{imp}}(k) &= \delta(k) + \sum_{n=1}^{\infty} \int_{-\infty}^{\infty} (\theta_n(g(k) - \lambda) - 2\pi)(\sigma_{pn}^{\text{imp}}(\lambda) + \sigma'_{pn}{}^{\text{imp}}(\lambda)); \\
p_1^{\text{imp}}(\lambda) &= 2\delta_1(\lambda) + \int_{-\infty}^{\infty} dk \rho_p^{\text{imp}}(k)(\theta_1(\lambda - g(k)) - 2\pi) \\
&\quad + \sum_{m=1}^{\infty} \int d\lambda' (\Sigma_{1m}(\lambda - \lambda')) \sigma_{pm}^{\text{imp}}(\lambda'),
\end{aligned} \tag{4.6}$$

with  $\Sigma_{nm}$  given by

$$\Sigma_{nm}(\lambda) = (\theta_{|n-m|}(\lambda) - 2\pi) + 2 \sum_{k=1}^{\min(n,m)-1} (\theta_{|n-m|+2k}(\lambda) - 2\pi) + (\theta_{n+m}(\lambda) - 2\pi). \tag{4.7}$$

We again can read off the  $\frac{1}{L}$  contributions to the momenta and the densities and arrive at the all important relations:

$$\begin{aligned}
\partial_k p^{\text{imp}}(k) &= 2\pi \rho^{\text{imp}}(k); \\
\partial_\lambda p_1^{\text{imp}}(\lambda) &= -2\pi \sigma^{\text{imp}}(\lambda),
\end{aligned} \tag{4.8}$$

still valid at finite temperatures. The scattering phases, as they are given (as in Section 2) from the impurity momenta,  $p^{\text{imp}}(k)$  and  $p_1^{\text{imp}}(\lambda)$ , can be computed from a knowledge of  $\rho^{\text{imp}}$  and  $\sigma_1^{\text{imp}}$ . For example, a spin up excitation constructed from a charge excitation,  $k$ , and a  $n = 1$  spin-charge complex,  $\lambda$ , has a scattering phase of the form

$$\begin{aligned}
\delta_e^\uparrow &= p^{\text{imp}}(k) + p_1^{\text{imp}}(\lambda); \\
&= 2\pi \int_{-D}^k dk \rho^{\text{imp}}(k) + 2\pi \int_\lambda^{\tilde{Q}} d\lambda' \sigma_1^{\text{imp}}(\lambda'),
\end{aligned} \tag{4.9}$$

identical to (2.23).

Another piece of the prescription of computing the scattering amplitudes at finite temperature is the energy associated with the charge and spin excitations. The energies

of the various excitations can be derived as in Section 2 with the result

$$\begin{aligned}
\varepsilon(k) &= k + T \sum_{n=1}^{\infty} \int_{-\infty}^{\infty} d\lambda \log\left(\frac{f(-\varepsilon'_n(\lambda))}{f(-\varepsilon_n(\lambda))}\right) a_n(\lambda - g(k)); \\
\log(f(\varepsilon_n(\lambda))) &= -\frac{2}{T} x_n(\lambda) - \int_{-\infty}^{\infty} dk g'(k) \log(f(-\varepsilon(k))) a_n(g(k) - \lambda) \\
&\quad + \sum_{m=1}^{\infty} \int d\lambda' A_{nm}(\lambda - \lambda') \log(f(-\varepsilon_m(\lambda'))); \\
\log(f(\varepsilon'_n(\lambda))) &= - \int_{-\infty}^{\infty} dk g'(k) \log(f(-\varepsilon(k))) a_n(g(k) - \lambda) \\
&\quad + \sum_{m=1}^{\infty} \int d\lambda' A_{nm}(\lambda - \lambda') \log(f(-\varepsilon'_m(\lambda'))),
\end{aligned} \tag{4.10}$$

where  $f(\varepsilon) = (1 + \exp(\varepsilon/T))^{-1}$  is the Fermi distribution. These equations are arrived at by relating the densities to the energies via

$$\begin{aligned}
\exp(\varepsilon(k)/T) &= \rho_h(k)/\rho_p(k); \\
\exp(\varepsilon_n(\lambda)/T) &= \sigma_{nh}(\lambda)/\sigma_{np}(\lambda); \\
\exp(\varepsilon'_n(\lambda)/T) &= \sigma'_{nh}(\lambda)/\sigma'_{np}(\lambda).
\end{aligned} \tag{4.11}$$

This relation is chosen so that the energies determine the particle/hole distributions in the same fashion that they do in the case of non-interacting fermionic particles, i.e.,

$$\rho_p(k) = (\rho_p(k) + \rho_h(k)) f(\varepsilon(k)), \tag{4.12}$$

and likewise for  $\sigma_{np/h}$  and  $\sigma'_{np/h}$ . This definition is completely consistent with that at zero temperature. Taking  $T \rightarrow 0$  in the above recovers (2.36). This is a general feature of energy functionals in a thermodynamic Bethe ansatz analysis. However here the energies are related to the densities in an additional way indicative that the bulk of the system (i.e. the leads) is indeed non-interacting:

$$\begin{aligned}
\rho_{p/h}(k) &= \frac{1}{2\pi} \partial_k \varepsilon(k) f(\pm \varepsilon(k)); \\
\sigma_{np/h}(\lambda) &= -\frac{1}{2\pi} \partial_\lambda \varepsilon_n(\lambda) f(\pm \varepsilon_n(\lambda)); \\
\sigma'_{np/h}(\lambda) &= \frac{1}{2\pi} \partial_\lambda \varepsilon'_n(\lambda) f(\pm \varepsilon'_n(\lambda)).
\end{aligned} \tag{4.13}$$

Having specified the energy functionals, we can now determine the particular  $k$  and  $\lambda$  we choose in creating an electron. As  $H = 0$ , we will simply focus on spin  $\uparrow$  electrons. In



forming a spin  $\uparrow$  electron we add a  $k$ -excitation in  $\rho(k)$  and a  $\lambda$  hole in  $\sigma_1(\lambda)$ . The energy of the electron is then

$$\varepsilon_{el} = \varepsilon(k) - \varepsilon(\lambda). \quad (4.14)$$

We again will only allow  $k$  to vary in varying  $\varepsilon_{el}$  while fixing  $\lambda$  to some  $\lambda_o$ . While at  $T = 0$  we fixed  $\lambda$  to be  $Q$ , its value at the Fermi surface, this is not appropriate at finite temperature as the Fermi surface has become blurred. However we have another way to characterize the correct choice for  $\lambda$ , at least at the symmetric point, which we give in the following subsection.

We are now ready to specify the final equation governing the finite temperature linear response conductance. Given that we construct the electronic excitations by gluing together a fixed spin excitation,  $\lambda_o$ , and a range of  $k$  excitations, these excitations are distributed according to the Fermi distribution, as they must be. Thus the conductance at finite  $T$  is given by

$$G(T) = 2 \frac{e^2}{h} \int_{-\infty}^{\infty} d\varepsilon_{el} (-\partial_{\varepsilon_{el}} f(\varepsilon_{el})) |T(\varepsilon_{el})|^2; \quad (4.15)$$

$$|T(\varepsilon_{el})|^2 = \sin^2\left(\frac{1}{2}\delta_{el}(\varepsilon_{el} = \varepsilon(k) - \varepsilon(\lambda_o), T)\right).$$

Here, the first formula is the standard Landauer-Büttiker formula applied to the electronic excitations discussed in Section 2, while the second formula follows from the expression of  $|T(\varepsilon_{el})|^2$  in terms of phase shifts in the even and odd leads, and  $\delta_{el}$  is given by (4.9) with  $\lambda = \lambda_o$ . Finally, we have used the key result that the density of states (per unit of energy) for the electronic excitations is a constant as follows from (4.13).

#### 4.1. Computation at the Symmetric Point

So far we have discussed the computation of  $G(T)$  in general terms. In this section we specialize to the symmetric point ( $\varepsilon_d = -U/2$ ). There are two reasons to do so. At the symmetric point the equations become more amenable to analysis. However more importantly, it is only at the symmetric point that we are able to compute the conductance, for it is only at this point that we can compute electron scattering for arbitrary energy, as required by (4.15).

The problem is a technical one. The energy functional,  $\varepsilon(k)$  is bounded below. For example, as the analysis of [32] [33] and [34] shows, at the symmetric point  $\varepsilon(k)$  satisfies

$$\varepsilon(k) \geq -T \log(3). \quad (4.16)$$

Thus we are unable to compute directly electron scattering phases for energies below  $\varepsilon(k = -D) - \varepsilon(\lambda = \lambda_o)$ . Rather for energies below this, we must compute hole scattering and relate this to particle scattering via

$$\delta_e^\dagger(\varepsilon_{el}, \varepsilon_d) = \delta_{ho}^\dagger(\varepsilon_{ho} = \varepsilon_{el}, -U - \varepsilon_d), \quad (4.17)$$

valid when  $H = 0$ . In order to exploit then this relation, we need  $\varepsilon_d = -U - \varepsilon_d$ , i.e.  $\varepsilon_d = -U/2$ . To compute  $\delta_{ho}^\dagger$ , we remove a  $k$  and a  $\lambda$ -hole. Thus akin to (2.45) we have

$$\delta_{ho}^\dagger(\varepsilon_{ho}) = 2\pi \int_{-D}^k dk' \rho_{\text{imp}}(k') + 2\pi \int_{\lambda_o}^{\tilde{Q}} d\lambda' \sigma_{\text{imp}}(\lambda'), \quad \varepsilon(k) = -\varepsilon_{ho} + \varepsilon(\lambda = \lambda_o), \quad (4.18)$$

with the difference,  $\lambda_o \neq Q$  and  $\varepsilon(\lambda_o) \neq 0$ .

With this, we can now consider the simplifications in the structure of the equations that arise at the symmetric point. Following [28], we can recast the equations defining the energy functionals in a universal form for energies comparable to  $T_k$ , the Kondo temperature. Define

$$\begin{aligned} \phi_n(\lambda) &= \frac{1}{T} \varepsilon_n \left( \lambda - \frac{1}{\pi} \log\left(\frac{2A}{T}\right) \right); \\ \phi'_1(g(k)) &= -\frac{1}{T} \varepsilon(-g(k) + \frac{1}{\pi} \log\left(\frac{2A}{T}\right)); \\ \phi'_{n+1}(\lambda) &= \frac{1}{T} \varepsilon'_n \left( -\lambda + \frac{1}{\pi} \log\left(\frac{2A}{T}\right) \right); \\ A &= \frac{\sqrt{2U\Gamma}}{2\pi}. \end{aligned} \quad (4.19)$$

In our definition of  $\phi'_1$ , we rely upon the fact that in the energy range we are interested in,  $\varepsilon(k)$  depends solely upon  $g(k)$ . With these definitions,  $\phi_n$  and  $\phi'_n$  satisfy the equations

$$\xi_n(\lambda) = - \int_{-\infty}^{\infty} d\lambda' s(\lambda - \lambda') \log(f(T\xi_{n-1}(\lambda))f(T\xi_{n+1}(\lambda))) - \delta_{n1} e^{\pi\lambda}, \quad (4.20)$$

where  $\xi_n = \phi_n$  or  $\phi'_n$  and  $s(\lambda) = \cosh^{-1}(\pi\lambda)/2$ . These equations have been analyzed by [32] [33] and [34]. In practice they are highly accurate in determining energies up to scales of 10's of  $T_k$ 's. This is a consequence of two scales existing in the problem,  $T_k$  and  $\sqrt{U\Gamma}$ . These equations focus on the first scale while throwing out information on the second. But because  $T_k \ll \sqrt{U\Gamma}$  in the Kondo regime, this approximation is extremely good.

With these equations in hand, we can determine the choice of  $\lambda_o$ . At the symmetric point we expect the scattering phase to be symmetric in energy, i.e.

$$\delta_{el}(\varepsilon) = \delta_{el}(-\varepsilon), \quad (4.21)$$

regardless of the temperature. We thus fix  $\lambda = \lambda_o$  such that (4.21) is satisfied.

We now derive the specific equations for the impurity densities at the symmetric point. These equations have the initial form

$$\begin{aligned}
\rho^{\text{imp}}(k) &= \Delta(k) + g'(k) \sum_{n=1}^{\infty} \int_{-\infty}^{\infty} d\lambda a_n(g(k) - \lambda) (\sigma_{pn}^{\text{imp}} + \sigma_{pn}^{\prime\text{imp}})(\lambda); \\
\sigma_{hn}^{\text{imp}}(\lambda) &= \tilde{\Delta}_n(\lambda) - \int_{-\infty}^{\infty} dk \rho_p^{\text{imp}}(k) a_n(\lambda - g(k)) \\
&\quad - \int_{-\infty}^{\infty} d\lambda' \sum_{m=1}^{\infty} A_{nm}(\lambda - \lambda') \sigma_{pm}^{\text{imp}}(\lambda'); \\
\sigma_{hn}^{\prime\text{imp}}(\lambda) &= \int_{-\infty}^{\infty} dk \rho_p^{\text{imp}}(k) a_n(\lambda - g(k)) - \int_{-\infty}^{\infty} d\lambda' \sum_{m=1}^{\infty} A_{nm}(\lambda - \lambda') \sigma_{pm}^{\prime\text{imp}}(\lambda').
\end{aligned} \tag{4.22}$$

We will recast these equations in a simpler form. We use the inverse of the matrix  $A_{nm}$ ,

$$A_{nm}^{-1}(\lambda) = \delta_{nm} \delta(\lambda) - s(\lambda) (\delta_{nm+1} + \delta_{nm-1}), \tag{4.23}$$

together with the equalities

$$\begin{aligned}
\delta_{n1} s(\lambda - \lambda'') &= \int_{-\infty}^{\infty} d\lambda' A_{nm}^{-1}(\lambda - \lambda') a_m(\lambda' - \lambda''), \\
\tilde{\Delta}_n(\lambda) &= \int_{-\infty}^{\infty} dk \Delta(k) a_n(\lambda - g(k)),
\end{aligned} \tag{4.24}$$

to rewrite (4.22) as

$$\begin{aligned}
\rho^{\text{imp}}(k) &= \Delta(k) + g'(k) \int_{-\infty}^{\infty} d\lambda s(\lambda - g(k)) \tilde{\Delta}_1(\lambda) \\
&\quad - g'(k) \int_{-\infty}^{\infty} d\lambda s(\lambda - g(k)) (\sigma_{h1}^{\text{imp}}(\lambda) + \sigma_{h1}^{\prime\text{imp}}(\lambda)); \\
\sigma_{pn}^{\text{imp}}(\lambda) + \sigma_{hn}^{\text{imp}}(\lambda) &= \int_{-\infty}^{\infty} d\lambda' s(\lambda - \lambda') (\sigma_{hn+1}^{\text{imp}}(\lambda') + \sigma_{hn-1}^{\text{imp}}(\lambda')) \\
&\quad + \delta_{n1} \int_{-\infty}^{\infty} dk \rho_h^{\text{imp}}(k) s(\lambda - g(k)); \\
\sigma_{pn}^{\prime\text{imp}}(\lambda) + \sigma_{hn}^{\prime\text{imp}}(\lambda) &= \int_{-\infty}^{\infty} d\lambda' s(\lambda - \lambda') (\sigma_{hn+1}^{\prime\text{imp}}(\lambda') + \sigma_{hn-1}^{\prime\text{imp}}(\lambda')) \\
&\quad + \delta_{n1} \int_{-\infty}^{\infty} dk \rho_p^{\text{imp}}(k) s(\lambda - g(k)).
\end{aligned} \tag{4.25}$$

We can further simplify these equations. For energies  $\ll \sqrt{U\Gamma}$ , it is an excellent approximation to take

$$-\frac{g'(k)}{2} \frac{1}{\cosh(\pi(g(k) - I^{-1}))} = \Delta(k) + g'(k) \int_{-\infty}^{\infty} s(\lambda - g(k)) \tilde{\Delta}_1(\lambda);$$

$$I^{-1} = \frac{U}{8\Gamma} - \frac{\Gamma}{2U}.$$
(4.26)

Together with this approximation we can take

$$\sigma_{h1}^{\text{imp}} = 0;$$

$$\sigma_m^{\text{imp}} = 0, \quad m > 1.$$
(4.27)

These densities are identically zero at zero temperature and are governed by the energy scale  $\sqrt{U\Gamma}$ . Since we work at temperatures far below this scale, they can be safely approximated as zero. With this, the density and energy equations can be solved numerically through iteration.

We do so and plot in Figure 9,  $G$  as a function of  $T/T_k$ . Comparing to the NRG computation of Costi et al., we find excellent agreement for energies up to several  $T_k$ , the regime where one would expect the NRG, by its very nature, to be most robust. We emphasize that this agreement is achieved with no fitting parameters. Our definition of the Kondo temperature,  $T_k$ , is the same as that used by Costi et al. Because of the Fermi liquid nature of this problem, we know the functional form of the conductance at  $T \ll T_k$  is

$$G(T/T_k) = \frac{2e^2}{h} \left(1 - c \frac{T^2}{T_k^2} + \dots\right).$$
(4.28)

Costi et al. [21], based upon results borrowed from [35] and [36], computed  $c$  to be

$$c = \frac{\pi^4}{16} = 6.088\dots$$
(4.29)

We find numerically

$$c = 6.05 \pm .1.$$
(4.30)

We have arrived at this value by fitting the plot in the region  $T/T_k < .1$ . The error is systematic in nature, arising from the arbitrary nature of deciding the region over which to fit.

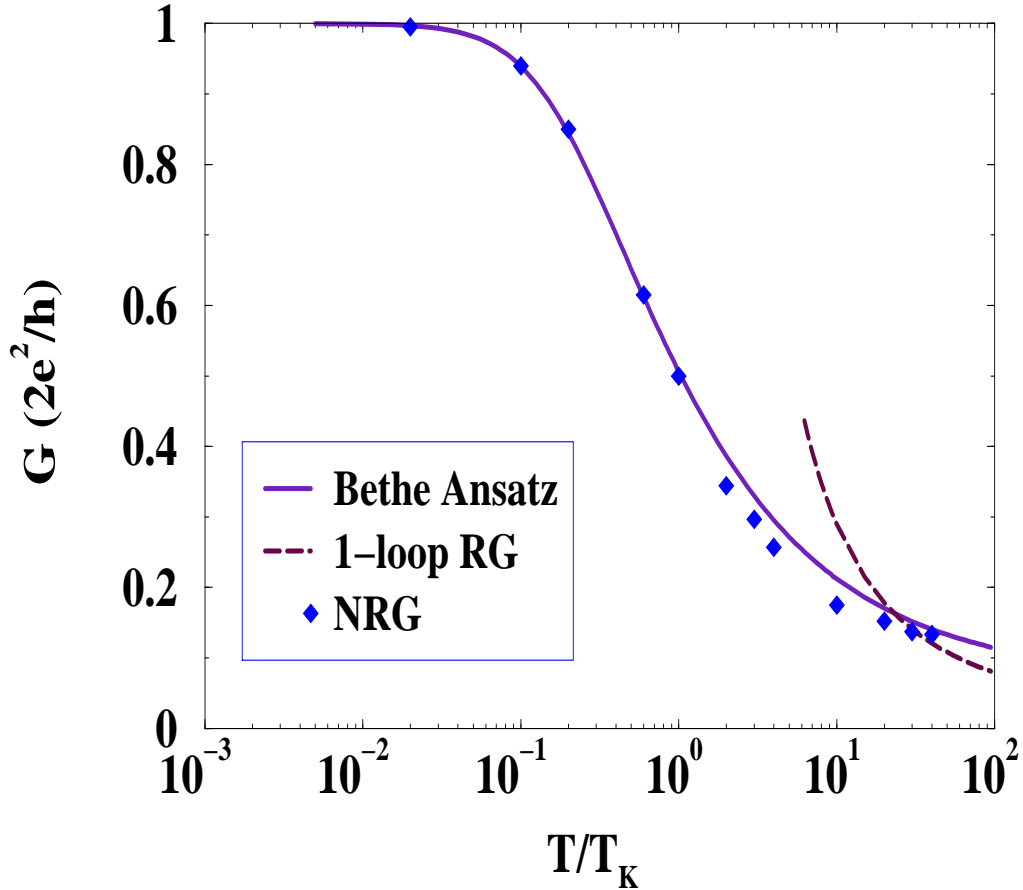


Figure 9: A plot of the scaling curve for the conductance as a function of  $T/T_k$ .  $T_k$  is as defined in Costi et al.'s work and so there are no free parameters. Our computation was carried out at the symmetric point in the Anderson model,  $U + 2\varepsilon_d = 0$ .

We also compare our results in Figure 9 with [13]. It appears that the logarithmic dependence in  $G$ ,

$$G \sim 1/\log^2(T/T_k),$$

characteristic of weak coupling and arising from a one-loop RG [13], should only be expected to become qualitatively descriptive for values of  $T/T_k$  in excess of about 20. This observation will play a role in our determination of the validity of our computation of the zero field differential conductance in the next section.

The quality of the fit is a good indicator of the validity of our approach in the Kondo regime. We expect from arguments given in Section 2 that our methodology should be

characterized by errors of order  $\mathcal{O}(T_k/\sqrt{UT}) \ll 1$  and as such we should see an exact match between our scaling curve and the NRG results. We are thus uncertain whether the slight discrepancy between ours and Costi et al.'s results at large  $T$  is a consequence of the some unguessed shortcoming in our approach, some problem with the NRG, or some difficulty with our numerics. While we cannot speak to the first two, we do note that our handling of the numerics opens up the possibility for error at large  $T/T_k$ ; the numerics are fashioned so to more readily reproduce the low temperature behaviour.

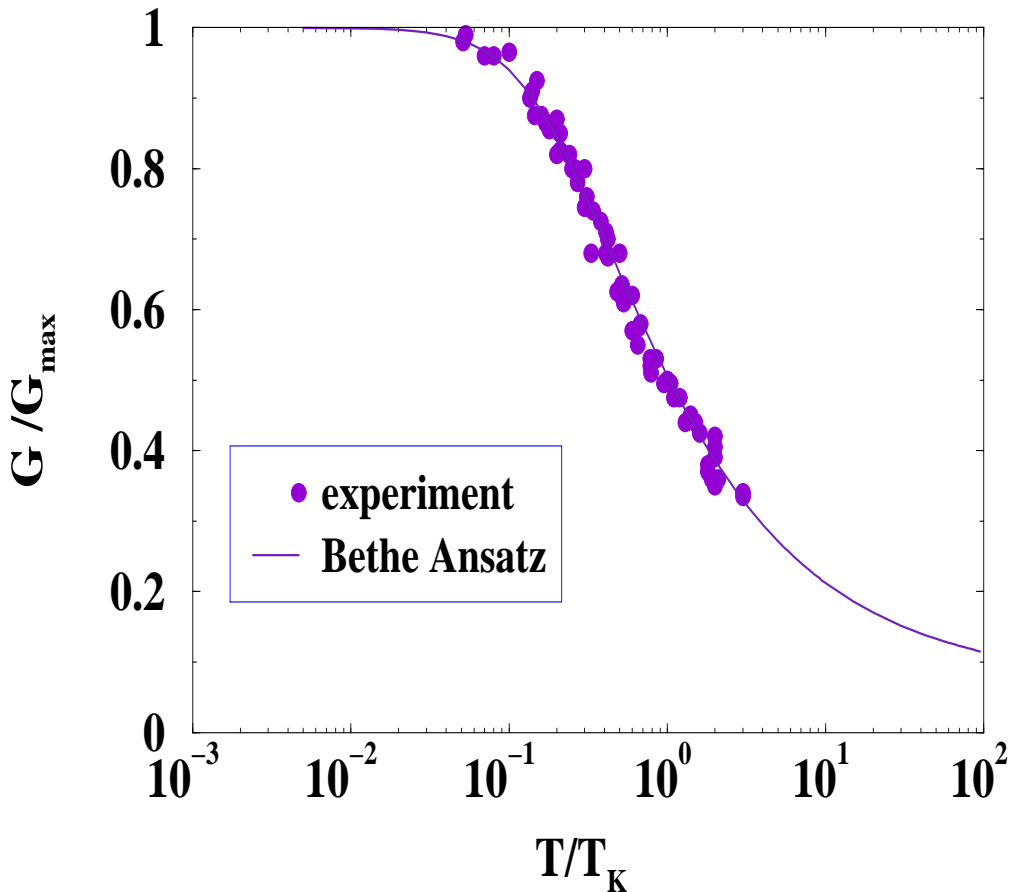


Figure 10: A comparison of the data from [1] with the computed scaling curve for the conductance. We now plot on the abscissa the ratio of the conductance with the maximal possible conductance. For the experimental realization in [1], the dot-lead couplings,  $V_{1,2}$ , are asymmetric, and the conductance does not achieve its unitary maximum,  $2e^2/h$ . However the scaling behaviour of  $G/G_{\max}$  is expected to be the same.

We end this section by comparing in Figure 10 our scaling curve with the experimental results of [1]. We see that we find excellent agreement. We point however that while we compute the scaling curve at the symmetric point ( $U/2 + \varepsilon_d = 0$ ) of the Anderson model, the data in [1] was taken away from the symmetric point but still in the dot's Kondo regime. (The Kondo temperature obtains an exponentially suppressed minimum at the symmetric point and so is usually below the temperature that can be experimentally realized. In order to experimentally see Kondo physics one then must move away from the symmetric point.) The continuing applicability of our scaling curve suggests a certain robustness to the scaling behaviour.

## 5. Out-of-Equilibrium Conductance

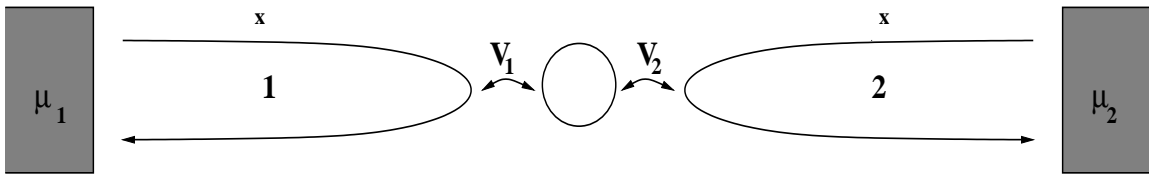


Figure 11: A sketch of two leads attached to a quantum dot. Each lead is, as indicated, at differing chemical potentials.

### 5.1. Basic Formalism

In order to compute the non-equilibrium conductance we imagine placing the reservoirs attached to each lead at differing chemical potentials as pictured in Figure 11. This on the face of it poses a problem. In doing so we add a term to the Hamiltonian of the form

$$\mathcal{H}_\mu = \mu_1 \int dx c_1^\dagger(x)c_1(x) + \mu_2 \int dx c_2^\dagger(x)c_2(x). \quad (5.1)$$

This term does not behave well under the map into the even/odd electron basis in as much as the odd electron no longer decouples. It would thus seem it is not possible to employ the results of the previous sections in analyzing the out-of-equilibrium system.

However we must ask what we need to compute the non-equilibrium conductance. We need to know the distribution of particles in each of the two reservoirs. And we need to know the scattering amplitudes of said particles. For the particle distributions, we note

that the particles in the two reservoirs do not interact with one another. Knowledge of one distribution is not needed to determine the other. Thus to compute the distribution of particles in reservoir 1 we can set  $\mu_2$  to be whatever is convenient and likewise for the determination of the distribution in reservoir 2. This is notably different from what occurs in the scattering of quasi-particles between quantum Hall edges. In the boundary sine-Gordon formulation of this problem, the two reservoirs, one reservoir of positive solitons and one of negative solitons, do interact with one another. The above device would thus not work in this context.

We emphasize again that the distribution of particles we compute are not the plane wave modes of an electron but rather are “dressed” electrons. But they do share several features with plane wave electrons. Beyond carrying the same quantum numbers of electrons, they share the same constant density of states as a function of energy as the plane wave electron modes. Moreover their dispersion relationship is the same as the plane wave modes.

Having dealt with the computation of the distributions we now turn to the scattering. Here there is no problem. As we are using an integrable basis, we are able to compute the scattering in the context of the in-equilibrium model. The scattering of the basis of integrable excitations is unaffected by the differing chemical potentials in the leads. We could, if we wished, adopt a basis of (dressed) excitations that was aware of the finite voltage. Although technically challenging, we could also compute the corresponding scattering amplitudes. Such amplitudes, however, would only differ from the original by an overall phase. As the conductance depends upon the absolute value of the scattering matrices, our answer would go unchanged. The sole consequence of  $\mu_1 \neq \mu_2$  is then felt in the distributions. In this sense then, the problem *is* akin to scattering between quantum Hall edges.

We now proceed with the actual calculation. Here we keep  $\mu_1$  constant and imagine varying  $\mu_2$  alone. The computation divides itself into two cases:  $\mu_1 > \mu_2$  and  $\mu_2 > \mu_1$ . We examine the former first.



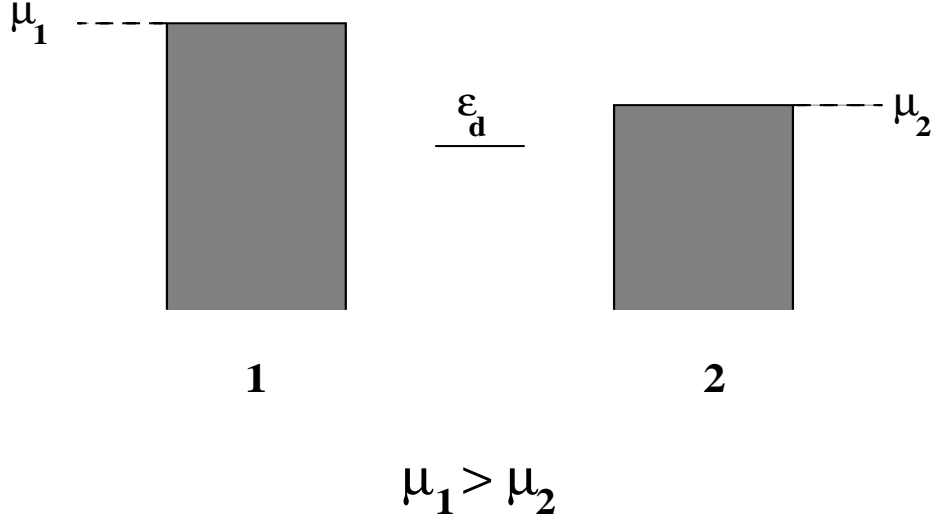


Figure 12: A sketch of the distribution of particles in the leads when  $\mu_1 > \mu_2$ .

The case  $\mu_1 > \mu_2$  is pictured in Figure 12. As we are at zero-temperature, particles will only diffuse from lead 1 to lead 2. The current is thus given by

$$J(\mu_1, \mu_2) = \frac{e}{h} \int_{\mu_2 - \mu_1}^0 d\varepsilon (|T_{\uparrow}^{1 \rightarrow 2}(\varepsilon, \mu_1)|^2 + |T_{\downarrow}^{1 \rightarrow 2}(\varepsilon, \mu_1)|^2). \quad (5.2)$$

We have expressed the current as an integral over all energies ranging from zero to  $\mu_2 - \mu_1$ . We note that the above integral reflects that the density of states as a function of energy is constant. Our particular choice of limits in the above integral is a consequence of our conventions: our equations governing the energy of the excitations (see (2.36)) give the Fermi energy of lead 1 as 0. It is only in this energy range that particles are available to scatter in lead 1 and that are not Pauli blocked in lead 2. We choose energies to parameterize the particles as opposed to either of the parameters  $k$  or  $\lambda$ . These latter parameters are not convenient in determining Pauli blocking in that with  $\mu_1 \neq \mu_2$  the energy functionals for the leads are also not equal, i.e.  $\varepsilon_1(k/\lambda) \neq \varepsilon_2(k/\lambda)$ . We note that even though  $\mu_1$  and  $\mu_2$  are bare chemical potentials, they are the correct ones to use in determining the current. They are not renormalized by interactions, understandably, as there are no interactions in the bulk.<sup>2</sup>

<sup>2</sup> Technically this may be seen as follows. Changing the chemical potential in a lead by  $\Delta\mu$  yields a change in the number of particles,  $\Delta N = \frac{\Delta\mu}{\pi}$ . The density of states per unit energy of the  $\lambda$ -particles filling the ground state is  $\sigma(\varepsilon) = \frac{1}{2\pi}$ . As each  $\lambda$ -particle is a bound state of two particles, the shift in the Fermi energy induced by the change in chemical potential is precisely  $\Delta\mu$ .

It is worthwhile commenting on the dependence of the current  $J$  upon  $\mu_1$  and  $\mu_2$ . Although the limits governing the energy range of excitations contributing to transport are a function of the difference,  $\mu_1 - \mu_2$ , of chemical potentials, the current's dependence upon  $\mu_1$  and  $\mu_2$  is more complicated. This reflects the dependence of the transmission amplitude,  $T^{1 \rightarrow 2}$ , upon  $\mu_1$  alone. In particular, in the Kondo regime of this problem, the Kondo temperature that appears in the expressions for the current will be a function of  $\mu_1 - \varepsilon_d$  and will not depend at all upon  $\mu_2$ .

Appearing in (5.2) are the electron scattering probabilities,  $T^{1 \rightarrow 2}$ , from lead 1 to lead 2. The amplitude,  $T^{1 \rightarrow 2}$ , is given from (2.6):

$$|T^{1 \rightarrow 2}(\varepsilon, \mu_1)|^2 = \sin^2\left(\frac{1}{2}\delta^1(\varepsilon_{ho} = -\varepsilon, \varepsilon_d - \mu_1)\right). \quad (5.3)$$

The phase for an electron below the Fermi surface, as indicated above, is computed by exciting the corresponding hole. As indicated in the introduction to this section, scattering in this case is determined solely by the dynamics in lead 1.

To compute  $\delta_{ho}$  involves exploiting particle-hole transformations. As such it is worthwhile to consider the cases of zero  $H$  and non-zero  $H$  separately. With  $H = 0$ , we can compute the scattering of a spin  $\downarrow$  hole by relating it to a spin  $\uparrow$  electron. According to (2.25) and (2.41), we have

$$\begin{aligned} \delta_{ho}^{1\downarrow}(\varepsilon_{ho} > \mu_1, \varepsilon_d - \mu_1) &= \delta_e^{1\uparrow}(\varepsilon_{el} = \varepsilon_{ho}, -U - \varepsilon_d + \mu_1) \\ &= 2\pi \int_{-D}^k dk \rho_{\text{imp}}^1(k) + 2\pi \int_Q^{\tilde{Q}} d\lambda \sigma_{\text{imp}}^1(\lambda), \quad \varepsilon^1(k) = \varepsilon_{ho} - \mu_1. \end{aligned} \quad (5.4)$$

Here the energies,  $\varepsilon_{el} - \mu_1$  and  $\varepsilon_{ho} - \mu_1$ , are measured relative to the Fermi surface in lead 1. By the  $SU(2)$  spin symmetry we then know  $\delta_{ho}^{1\downarrow}(\varepsilon_{ho}) = \delta_{ho}^{1\uparrow}(\varepsilon_{ho})$ . Because of the behaviour of  $\varepsilon_d$  under a particle-hole transformation, we can only directly compute out-of-equilibrium conductances when  $\varepsilon_d - \mu_1 < -U/2$ , unusual in that it is on the other side of the particle-hole symmetric point.

When  $H$  is nonzero the situation is more complicated. We no longer can equate spin  $\uparrow$  and spin  $\downarrow$  scattering. However we now can compute spin  $\uparrow$  hole scattering directly. From (2.45) we have

$$\delta_{ho}^{1\uparrow}(\varepsilon_{ho} > \mu_1, \varepsilon_d - \mu_1) = 2\pi \int_{-D}^k dk' \rho_{\text{imp}}^1(k') + 2\pi \int_Q^{\tilde{Q}} d\lambda \sigma_{\text{imp}}^1(\lambda), \quad \varepsilon^1(k) = -(\varepsilon_{ho} - \mu_1). \quad (5.5)$$

Because the bottom bound on  $\varepsilon^1(k)$  is  $-H$ , we are limited to computing spin  $\uparrow$  hole scattering for energies,  $0 < \varepsilon < H$ . For spin  $\downarrow$  hole scattering we resort to the particle-hole transformation used above:

$$\begin{aligned} \delta_{ho}^{1\downarrow}(\varepsilon_{ho} > \mu_1, \varepsilon_d - \mu_1) &= \delta_e^{1\uparrow}(\varepsilon_{el} = \varepsilon_{ho}, -U - \varepsilon_d + \mu_1) \\ &= 2\pi \int_{-D}^k dk' \rho_{\text{imp}}^1(k') + 2\pi \int_Q^{\tilde{Q}} d\lambda \sigma_{\text{imp}}^1(\lambda), \quad \varepsilon^1(k) = \varepsilon_{ho} - \mu_1. \end{aligned} \quad (5.6)$$

We have no similar constraint on the energy range for spin  $\downarrow$  scattering. But we can see another issue arises. We are able to compute spin  $\uparrow$  hole scattering for a dot chemical potential,  $\varepsilon_d - \mu_1 > -U/2$ , while for spin  $\downarrow$  hole scattering we can only perform the computation for  $\varepsilon_d - \mu_1 < -U/2$ . We are thus limited in the case of non-zero  $H$  to the symmetric point,  $\varepsilon_d - \mu_1 = -U/2$ . But given our belief that our ansatz for the scattering states is only valid near the symmetric point, this constraint costs us little.

To compute the energy functional relating the parameter  $k$  to the energy we employ the equations,

$$\begin{aligned} \varepsilon^1(k) &= k - \frac{H}{2} - \mu_1 - \int_Q^{\tilde{Q}} d\lambda \varepsilon^1(\lambda) a_1(\lambda - g(k)); \\ \varepsilon^1(\lambda) &= 2x(\lambda) - 2\mu_1 - \int_Q^{\tilde{Q}} d\lambda' \varepsilon^1(\lambda') a_2(\lambda' - \lambda) \\ &\quad + \int_{-D}^B dk g'(k) \varepsilon^1(k) a_1(g(k) - \lambda). \end{aligned} \quad (5.7)$$

These equations are identical to those of (2.36) but for the presence of  $\mu_1$ . The Fermi surfaces,  $Q$  and  $B$ , are determined as before by

$$\begin{aligned} \varepsilon^1(\lambda = Q) &= 0; \\ \varepsilon^1(k = B) &= 0, \end{aligned} \quad (5.8)$$

that is, the energy functionals are defined such that the Fermi energy is always zero.

Computing the differential conductance then amounts to computing  $-e\partial_{\mu_2} J$ :

$$G(\mu_1, \mu_2) = -e\partial_{\mu_2} J(\mu_1, \mu_2) = \frac{e^2}{h} (|T_{\uparrow}^{1\rightarrow 2}(\varepsilon = \mu_2 - \mu_1, \mu_1)|^2 + |T_{\downarrow}^{1\rightarrow 2}(\varepsilon = \mu_2 - \mu_1, \mu_1)|^2). \quad (5.9)$$

As the particle distribution and correspondent scattering in lead 1 are, as discussed above, only dependent upon  $\mu_1$ ,  $G$  has a particularly simple form: there are no terms of the form  $\partial_{\mu_2} |T|^2$ .

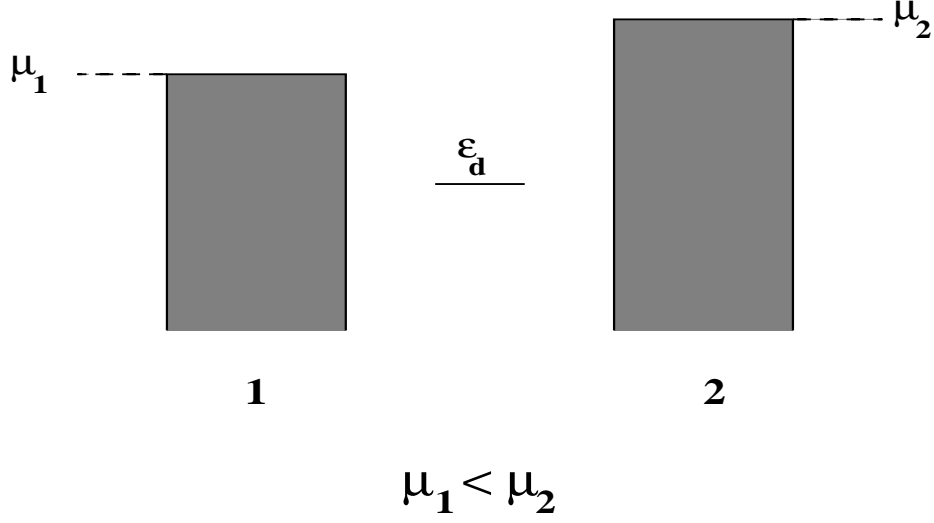


Figure 13: A sketch of the distribution of particles in the leads when  $\mu_1 < \mu_2$ .

In the second case,  $\mu_2 > \mu_1$  (pictured in Figure 13), such terms do come into play. Here, the current has the form

$$J(\mu_1, \mu_2) = -\frac{e}{h} \int_{\mu_1 - \mu_2}^0 d\varepsilon (|T_{\uparrow}^{2 \rightarrow 1}(\varepsilon, \mu_2)|^2 + |T_{\downarrow}^{2 \rightarrow 1}(\varepsilon, \mu_2)|^2). \quad (5.10)$$

In this case particles scatter from lead 2 to lead 1. The choice of limits in the above integral now reflects that the Fermi energy in lead 2 has been taken to be zero.  $T^{2 \rightarrow 1}$  can be determined by the same set of equations, (5.3) to (5.6), but with the energies and densities defined in lead 2. The expression for the differential conductance is more complicated than previously as the scattering matrices are determined on the basis of distributions in leads 2 and so the scattering varies as  $\mu_2$  is varied. We thus have

$$G = -e \partial_{\mu_2} J = \frac{e^2}{h} (|T_{\uparrow}^{2 \rightarrow 1}(\varepsilon = \mu_1 - \mu_2, \mu_2)|^2 + |T_{\downarrow}^{2 \rightarrow 1}(\varepsilon = \mu_1 - \mu_2, \mu_2)|^2) + \frac{e^2}{h} \int_{\mu_1 - \mu_2}^0 d\varepsilon (\partial_{\mu_2} |T_{\uparrow}^{2 \rightarrow 1}(\varepsilon, \mu_2)|^2 + \partial_{\mu_2} |T_{\downarrow}^{2 \rightarrow 1}(\varepsilon, \mu_2)|^2). \quad (5.11)$$

Here  $T^{2 \rightarrow 1}$  is given by

$$|T^{2 \rightarrow 1}|^2 = \sin^2\left(\frac{1}{2} \delta_{ho}(-\varepsilon, \varepsilon_d - \mu_2)\right) = \sin^2\left(\frac{1}{2} \delta_{el}(-\varepsilon, -\varepsilon_d + \mu_2 - U)\right). \quad (5.12)$$

We thus see explicitly  $\partial_{\mu_2} |T^{2 \rightarrow 1}|^2$  is non-zero. When  $H \neq 0$  recall we can only compute  $T_{\uparrow}$  and  $T_{\downarrow}$  only at the symmetric point. Given that we are varying  $\mu_2$ , and so varying the

effective dot chemical potential, we cannot compute the differential conductance for non-zero  $H$  in the case,  $\mu_2 > \mu_1$ . Moreover we are restricted to the region where  $\varepsilon_d - \mu_2 < -U/2$ , also as discussed previously.

We again comment upon the dependence of the current upon  $\mu_1$  and  $\mu_2$ . As with the case  $\mu_1 > \mu_2$ , the current is not simply a function of the difference of the two chemical potentials. In this case however the scattering amplitudes depend solely upon  $\mu_2$  not  $\mu_1$ . In particular in the Kondo regime, the Kondo temperature is determined by difference of  $\mu_2$  with the dot chemical potential  $\varepsilon_d$ .

As  $\delta_{ho}$  is given by an equation akin to (5.5), we can compute  $\partial_{\mu_2}|T^{2 \rightarrow 1}|^2$  to be

$$\begin{aligned} \partial_{\mu_2}|T^{2 \rightarrow 1}(\varepsilon, \mu_2)|^2 &= \frac{1}{2} \sin(p_{\text{imp}}(Q) + p_{\text{imp}}(k))(\partial_{\mu_2}p_{\text{imp}}(Q) + \partial_{\mu_2}p_{\text{imp}}(k)); \\ \partial_{\mu_2}p_{\text{imp}}(Q) &= 2\pi \int_Q^\infty d\lambda \partial_{\mu_2}\sigma_{\text{imp}}(\lambda, -\varepsilon_d + \mu_2 - U); \\ \partial_{\mu_2}p_{\text{imp}}(k) &= 2\pi \int_{-\infty}^k dk' \partial_{\mu_2}\rho_{\text{imp}}(k', -\varepsilon_d + \mu_2 - U), \quad \varepsilon_2(k) = -\varepsilon. \end{aligned} \quad (5.13)$$

From the density equations in Appendix A (see A.6), we find that with  $H = 0$ ,  $\partial_{\mu_2}\sigma_{\text{imp}}(\lambda)$  and  $\partial_{\mu_2}\rho_{\text{imp}}(k)$  satisfy

$$\partial_{\mu_2}\sigma_{\text{imp}}(\lambda) = 0; \quad (5.14)$$

$$\begin{aligned} \partial_{\mu_2}\rho_{\text{imp}}(k) &= \partial_{\mu_2}\Delta(k, -\varepsilon_d + \mu_2 - U) + \frac{1}{U\Gamma} \int_{-\infty}^Q d\lambda \sigma_{\text{imp}}(\lambda) s(\lambda - g(k)) \\ &\quad - (\partial_k g(k))^2 \int_{-\infty}^Q d\lambda \sigma_{\text{imp}}(\lambda) s'(\lambda - g(k)) - \frac{1}{U\Gamma} \int_{-\infty}^\infty dk' \Delta(k') R(g(k) - g(k')) \\ &\quad - (\partial_k g(k))^2 \int_{-\infty}^\infty dk' \Delta(k') R'(g(k) - g(k')), \end{aligned} \quad (5.15)$$

where here  $g(k) = (k + \varepsilon_d - \mu_2 + U/2)^2 / (2U\Gamma)$ . In computing  $\partial_{\mu_2}T$ , we have neglected contributions from  $\partial_{\mu_2}Q$ . We can see from the energy equations of (5.7) and (5.8) that

$$\partial_{\mu_2}Q \neq 0. \quad (5.16)$$

However,  $Q$ , determining the Fermi surface relative to the bottom of the band, is reflective of energy scales on the order of the bandwidth whereas we consider changes in  $\mu_2$  of  $\mathcal{O}(T_k)$ . Hence  $\partial_{\mu_2}Q$  is negligible.

## 5.2. Differential Conductance at $H = 0$

The differential conductance in zero field is expected to fall off rapidly with a scale,  $\sim T_k$ , from its linear response value near the symmetric point of  $\sim 2e^2/h$ . The characteristics of this peak are related to the peak, the Kondo resonance, in the spectral weight of the impurity density of states as determined by the Bethe ansatz. This is similar to the findings of [9][12][10] where they cast all transport properties in terms of the impurity density of states though as determined by  $\text{Im}\langle dd^\dagger \rangle$ . With the Landauer-Buttiker approach we have adopted, all scattering quantities are ultimately related to the equilibrium density of states; the non-equilibrium density of states plays no part in the computation marking an important difference with [9][12][10]. At the symmetric point we are able to derive in the case of negative bias,  $\mu_2 > \mu_1$ , a closed form expression for the differential conductance. Away from the symmetric point we must rely upon a numerical solution of the associated integral equations.

### i) Results at the Symmetric Point

At the symmetric point (and hence only the case  $\mu_1 > \mu_2$  assuming  $\mu_2$  is being varied), we derive a closed form expression for the current and differential conductance. At the symmetric point,  $\rho_{\text{imp}}$  is given by [28]:

$$\begin{aligned} \rho_{\text{imp}}(k < 0) = & -\frac{g'(k)}{2} \frac{1}{\cosh(\pi(g(k) - I^{-1}))} \\ & - g'(k) \sum_{n=0}^{\infty} e^{-\pi g(k)(1+2n)} \int dk' e^{-\pi g(k')(1+2n)} \text{Re}\Delta(ik'). \end{aligned} \quad (5.17)$$

In order to make use of this expression we need to parameterize  $k$  in terms of the energy  $\varepsilon(k)$ . For energies not far in excess of  $T_k$  we find in solving (5.2) with  $H = 0$ ,

$$\varepsilon(k < 0) - \mu_1 = \varepsilon^1(k < 0) = \frac{\sqrt{2U\Gamma}}{\pi} e^{-\pi g(k)}. \quad (5.18)$$

Hence the scattering phase is given by

$$\begin{aligned}
\delta_{ho}^1(\varepsilon, \varepsilon_d - \mu_1 = -U/2) &= \delta_{el}^1(\varepsilon, -U/2) \\
&= 2\pi \int_{-\infty}^{\infty} d\lambda \sigma_{\text{imp}}(\lambda) + 2\pi \int_{-\infty}^k dk' \rho_{\text{imp}}(k') \\
&= \frac{3}{2}\pi - \sin^{-1} \left( \frac{1 - (\varepsilon - \mu_1)^2 / \tilde{T}_k^2}{1 + (\varepsilon - \mu_1)^2 / \tilde{T}_k^2} \right) \\
&\quad + 2 \sum_{n=0}^{\infty} \frac{1}{1+2n} \left( \frac{\pi(\varepsilon - \mu_1)}{\sqrt{2U\Gamma}} \right)^{1+2n} \int dk e^{-\pi g(k)(1+2n)} \text{Re}[\Delta(ik)],
\end{aligned} \tag{5.19}$$

where

$$\tilde{T}_k = \frac{2}{\pi} T_k = \frac{2}{\pi} \sqrt{\frac{U\Gamma}{2}} e^{\pi((\varepsilon_d - \mu_1)(\varepsilon_d - \mu_1 + U) - \Gamma^2)/(2\Gamma U)}.$$

The latter term in the above is negligible when  $(\varepsilon - \mu_1) \sim T_k$  as  $T_k \ll \sqrt{U\Gamma}$ .

With this we can compute the current and the differential conductance:

$$\begin{aligned}
J(\mu_1, \mu_2) &= -2 \frac{e}{h} \tilde{T}_k \tan^{-1} \left( \frac{\mu_2 - \mu_1}{\tilde{T}_k} \right); \\
G(\mu_1, \mu_2) &= -e \partial_{\mu_2} J(\mu_2) = 2 \frac{e^2}{h} \frac{1}{(1 + (\mu_2 - \mu_1)^2 / \tilde{T}_k^2)}.
\end{aligned} \tag{5.20}$$

The simplicity of these results is striking. In our approach, it is directly related to the simple form of the dressed scattering phase (5.19), which only comes about at the end of a complex calculation. It is not clear to us whether there is a more direct way to obtain the results (5.20).

We observe that no  $\log(\mu/T_k)$  terms appear in the above expressions for the current and conductance whereas we might expect such terms for large  $\mu/T_k$ . In this regime such terms appear in weak coupling perturbative computations [13]. However we have already established with our finite temperature calculation that weak coupling perturbation theory is not even qualitatively accurate until one exceeds scales of  $T/T_k \sim 20$ . We expect the differential conductance to be governed by similar considerations. Correspondingly, we would conclude that our scattering ansatz as applied to the zero field differential conductance is at least good for energies up to  $T/T_k \sim 20$ .

Given that we are at the symmetric point, we would expect to be able to make contact with low energy scattering in the Kondo model as this model should produce identical

results to the Anderson model in the low energy regime. At low energies we have

$$\begin{aligned}\delta_{ho}^1(\varepsilon, \varepsilon_d - \mu_1 = -U/2) &= \frac{3}{2}\pi - \sin^{-1}\left(\frac{1 - (\varepsilon - \mu_1)^2/\widetilde{T}_k^2}{1 + (\varepsilon - \mu_1)^2/\widetilde{T}_k^2}\right); \\ &= \pi + 2 \tan^{-1}((\varepsilon - \mu_1)/\widetilde{T}_k).\end{aligned}\tag{5.21}$$

This latter form is identical to that found for spin excitations in the Kondo model [28]. In the exact solution of the Kondo model, the role assigned to ‘charge’ and ‘spin’ excitations differs from that of the Anderson model. In the Kondo model the charge excitations are non-interacting and so variations in the scattering phase occur solely because of changes in the spin sector. In this sense it is not surprising that we find the scattering phase of electronic excitations in the Anderson model is equal to the scattering phase of spin excitations in the Kondo model. If we were to compute transport properties directly in a two lead Kondo model, this equivalence suggests how we would have to formulate the scattering ansatz that governs the gluing together of excitations from the two sectors (in the case of the Anderson model, this is discussed in detail in Section 2). To compute the finite energy scattering phase for the case of the Kondo model, we would leave  $k$  at its Fermi surface value while varying  $\lambda$ , the exact opposite of what we find in the Anderson model.

It is also instructive to recast the impurity density of states so that it is a function of energy:

$$\rho_{\text{imp}}(\varepsilon) = \frac{1}{\pi\widetilde{T}_k} \frac{1}{1 + \varepsilon^2/\widetilde{T}_k^2}.\tag{5.22}$$

We see then that the impurity density of states is sharply peaked about zero energy with a peak height proportional to  $1/\widetilde{T}_k$ . The spectral density of states as determined from the dot correlator,  $\text{Im}\langle dd^\dagger \rangle$ , is also sharply peaked around zero energy. In contrast however, its peak height is proportional to  $1/\Gamma$ , a wildly different energy scale than the one governing the Bethe ansatz impurity density of states. The two quantities then are clearly different thus undermining an important premise of [17].

## ii) Results Away From the Symmetric Point

Pictured below is a plot of the differential conductance in zero magnetic field. We see that the expected qualitative features appear, namely the differential conductance sharply varies on energy scales related to the Kondo temperature,  $T_k$ .



Although we are not exactly at the symmetric point, we must remain close in order to keep true to our methodology of identifying scattering states. If, for example, we were to compute the differential conductance in the mixed valence regime of the Anderson model, we would find our results unphysical. Our construction of the scattering states was predicated on the knowledge that in the Kondo regime the scattering phase varies on the smallest scale in the problem, the Kondo temperature, and that in turn, only the impurity density of states for the  $k$ -excitations is governed by this scale. In the mixed valence regime all of these assumptions breakdown.

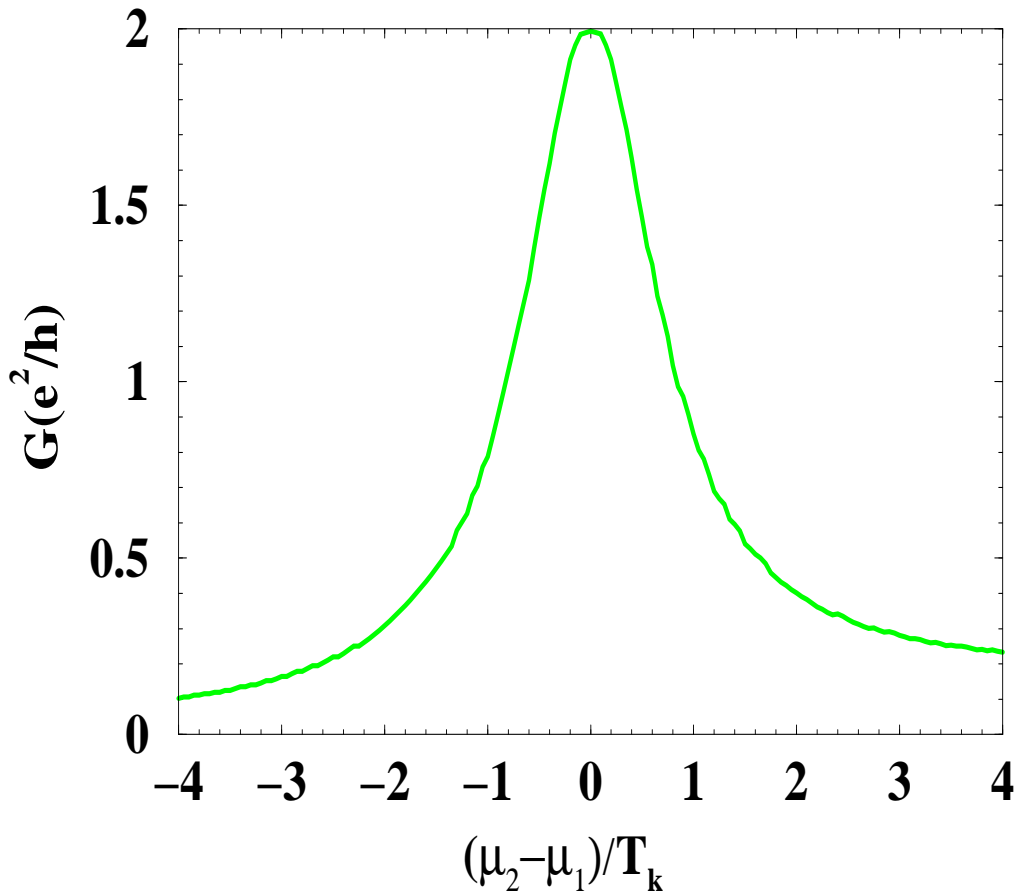


Figure 14: A plot of the differential conductance in zero magnetic field. The value of the parameters used in the plot are  $\Gamma = .05$ ,  $U = 10\Gamma$ , and  $\varepsilon_d = -5.2\Gamma$ , where we set the energy scale in terms of the bandwidth,  $D = \pi$ .

We see that the differential conductance curve in Figure 14 is asymmetric about  $\mu_2 - \mu_1 = 0$ . This is a consequence of the asymmetry introduced by variations in the

effective Kondo temperature. In the regime  $\mu_1 > \mu_2$ ,  $T_k$  does not vary as it is solely a function of  $\mu_1 - \varepsilon_d$  and we have assumed only  $\mu_2$  is changing. However in the regime  $\mu_2 > \mu_1$ ,  $T_k$  now depends upon  $\mu_2 - \varepsilon_d$  and so changes in  $\mu_2$  lead to changes in  $T_k$ . Hence the asymmetry in behaviour.

### 5.3. Results at the Symmetric Point for $H \neq 0$

At the symmetric point we develop closed form expressions for the differential conductance. As stated previously, the nature of our construction of the scattering states suggests that our results for the differential magneto-conductance to become exact as  $H/T_k$  becomes large. Our results are in rough accordance with [10] - we find that for fields,  $H > T_k$ , the  $H=0$  differential conductance peak at zero bias divides in two, one peak for each spin species. Roughly speaking, the origin of the split in the differential conductance arises from a similar bifurcation in the impurity density of states. The spectral weight of the Kondo resonance present at  $\omega = 0$  when  $H = 0$  divides into two resonances near  $eV \sim \pm H$ , again one associated with each spin species. The peak at negative bias,  $\mu_2 < \mu_1$ , corresponds to a spin  $\uparrow$  resonance while the peak occurring with  $\mu_2 > \mu_1$  is associated with a spin  $\downarrow$  resonance. Given our ability to work only at  $\mu_2 < \mu_1$  at the symmetric point, we explore the former alone.

For fields  $H \gg T_k$ , this peak is found at a bias close to  $-H$ . However unlike [10] we find the differential conductance peak does not occur exactly at  $eV = -H$ . This is not surprising as this result was predicated upon a second order perturbative computation. We find instead that the peak is shifted to values of  $e|V|$  smaller than  $H$ . For large fields we can develop closed form expressions for the position, height, and width of the conductance peaks. A related computation was done in [17] in the context of the Kondo model. However there the analysis was restricted to the peaks in the *equilibrium impurity density of states* as determined by the Bethe ansatz and not the conductance per se. As discussed previously, the two are not directly or obviously related, as indeed is clear from the work here.

In order to proceed with the computation, we review the constituent elements. The scattering phase for spin  $\uparrow$  hole scattering is given by

$$\delta_{ho}^\uparrow(\varepsilon_{ho} > \mu_1) = 2\pi \int_{-D}^k dk' \rho_{\text{imp}}^1(k') + 2\pi \int_{-\infty}^{\tilde{Q}} \sigma_{\text{imp}}^1(\lambda), \quad \varepsilon^1(k) = -(\varepsilon_{ho} - \mu_1). \quad (5.23)$$

Using (3.23), we can write the phase solely in terms of  $\rho_{\text{imp}}$ :

$$\delta_{ho}^{\uparrow}(\varepsilon_{ho} > \mu_1) = 2\pi \int_{-D}^k dk' \rho_{\text{imp}}^1(k') + \pi(1 - \int_{-D}^B dk \rho_{\text{imp}}^1(k)), \quad \varepsilon^1(k) = -(\varepsilon_{ho} - \mu_1). \quad (5.24)$$

The scattering phase for spin  $\downarrow$  hole scattering is found to be

$$\delta_{ho}^{\downarrow}(\varepsilon_{ho} > \mu_1) = 2\pi \int_{-D}^k dk' \rho_{\text{imp}}^1(k') + \pi(1 - \int_{-D}^B dk \rho_{\text{imp}}^1(k)), \quad \varepsilon^1(k) = \varepsilon_{ho} - \mu_1, \quad (5.25)$$

through a particle-hole transformation.

For  $H$  satisfying  $H \ll T_k$ , we can arrive at a closed form expression for the differential magneto-conductance. With  $H \ll T_k$ , the impurity density of states for the  $k$ -excitations retains its zero field form,

$$\rho_{\text{imp}}(k) = -\frac{k}{U\Gamma} \frac{1}{2 \cosh(\pi(g(k) - I^{-1}))}. \quad (5.26)$$

The impurity density is unperturbed by the field at first approximation as its spectral weight is found at the scale,  $T_k$ , while the presence of the field only affects energies far below this by assumption. On the other hand the energy is shifted by a constant from its zero field value (again taking  $\mu_1 = 0$ ):

$$\begin{aligned} \varepsilon^1(k) &= \frac{\sqrt{2U\Gamma}}{\pi} e^{-\pi g(k)} - H/2, \quad k \gg B; \\ \varepsilon^1(k) &= \frac{\sqrt{2U\Gamma}}{\pi} e^{-\pi g(k)} - H, \quad k \ll B. \end{aligned} \quad (5.27)$$

For  $k \gg B$  the energy is shifted by the bare energy of a spin in a magnetic field,  $H/2$ . For  $k \ll B$ , the effect of the field upon  $\varepsilon^1(k)$  can be determined by rewriting the energy,  $\varepsilon^1(k) \rightarrow \varepsilon^1(k) - H$  and substituting into (A.11). We then find that the field,  $H$ , disappears from the the equation, leaving us to conclude that energy is shifted by a dressed magnetic energy,  $H$ .

Using these forms for the energy and the impurity density, the spin  $\uparrow$  scattering phase reduces to

$$\delta_{ho}^{\uparrow}(\varepsilon_{ho} > \mu_1) = \frac{5}{4}\pi - \sin^{-1} \left( \frac{1 - (\varepsilon_{ho} - \mu_1 - H)^2/\tilde{T}_k^2}{1 + (\varepsilon_{ho} - \mu_1 - H)^2/\tilde{T}_k^2} \right) + \frac{1}{2} \sin^{-1} \left( \frac{1 - H^2/\tilde{T}_k^2}{1 + H^2/\tilde{T}_k^2} \right), \quad (5.28)$$

while for spin  $\downarrow$  scattering, we have

$$\delta_{ho}^{\downarrow}(\varepsilon_{ho} > \mu_1) = \frac{5}{4}\pi - \sin^{-1} \left( \frac{1 - (\varepsilon_{ho} - \mu_1 + H/2)^2/\tilde{T}_k^2}{1 + (\varepsilon_{ho} - \mu_1 + H/2)^2/\tilde{T}_k^2} \right) + \frac{1}{2} \sin^{-1} \left( \frac{1 - H^2/(4\tilde{T}_k^2)}{1 + H^2/(4\tilde{T}_k^2)} \right). \quad (5.29)$$

With this we can compute the differential conductance

$$\begin{aligned}
G(\mu_1, \mu_2) &= \frac{e^2}{h} \left[ 1 + \frac{1}{2} \frac{1 + (H^2 - (\mu_2 - \mu_1)^2)/\tilde{T}_k^2}{(1 + H^2/\tilde{T}_k^2)^{1/2}(1 + (\mu_2 - \mu_1 + H)^2/\tilde{T}_k^2)} \right. \\
&\quad \left. + \frac{1}{2} \frac{1 + (H^2/4 - (\mu_2 - \mu_1)^2)/\tilde{T}_k^2}{(1 + H^2/4\tilde{T}_k^2)^{1/2}(1 + (\mu_2 - \mu_1 - H/2)^2/\tilde{T}_k^2)} \right]; \quad (5.30) \\
\tilde{T}_k &= \frac{2}{\pi} \sqrt{\frac{U\Gamma}{2}} e^{\pi((\varepsilon_d - \mu_1)(\varepsilon_d - \mu_1 + U) - \Gamma^2)/(2\Gamma U)}.
\end{aligned}$$

Taking  $H \rightarrow 0$  recovers (5.20).

For values of  $H > T_k$ , we must resort to a Wiener-Hopf analysis of the scattering phases. The details have been relegated to Appendix D where exact forms of the scattering phase and the energy,  $\varepsilon(k)$ , can be found. Here however we summarize their asymptotic forms. For  $k \ll B$  and  $H \gg T_k$ , the energy  $\varepsilon^1(k)$  as given in (D.8) takes the form

$$\begin{aligned}
\varepsilon^1(k) &= -H \left( 1 - \frac{1}{2\pi} \tan^{-1} \frac{1}{g(k) - b} \right. \\
&\quad - \frac{1}{4\pi^2} \frac{1}{1 + (g(k) - b)^2} \left[ \frac{\psi(1/2)}{\Gamma(1/2)} + 1 - (g(k) - b) \tan^{-1} \left( \frac{1}{g(k) - b} \right) \right. \\
&\quad \quad \quad \left. \left. + C + \frac{1}{2} \log(4\pi^2(1 + (g(k) - b)^2)) \right] \right) \quad (5.31) \\
&\quad + \frac{\sqrt{2\Gamma U}}{\pi^2} \left( \frac{1}{\sqrt{2e\pi}} \frac{e^{-b\pi}}{1 + (g(k) - b)^2} + e^{-\pi g(k)} \tan^{-1} \left( \frac{1}{g(k) - b} \right) \right) \\
&\quad + \mathcal{O}((g(k) - b)^{-3}),
\end{aligned}$$

where  $C = .577216\dots$  is Euler's constant and  $b$  is given by

$$b = \frac{1}{\pi} \log\left(\frac{2}{H} \sqrt{\frac{U\Gamma}{\pi e}}\right). \quad (5.32)$$

Note that only the first two terms in the above expansion are at leading order but we need include the remaining terms in order to obtain reasonable estimates of the properties of the conductance peak. Under similar conditions for  $k$  and  $H$  we obtain an expression for

$\int dk \rho_{\text{imp}}$ :

$$\begin{aligned}
2\pi \int_{-\infty}^k dk \rho_{\text{imp}} &= \pi + 2 \tan^{-1}(2(I^{-1} - g(k))); \quad (5.33) \\
I^{-1} &= \frac{U}{8\Gamma} - \frac{\Gamma}{2U},
\end{aligned}$$

where again  $I^{-1}$  determines the Kondo temperature,  $T_k \sim e^{-\pi I}$ .

Combining this analysis with numerical work and the results in (5.30) allow us to plot in Figure 15 the magneto-conductance for a variety of values of  $H/T_k$ . As explained earlier, we are only able to compute the magneto-conductance for biases satisfying  $\mu_2 < \mu_1$ . Nonetheless we expect the differential conductance to be roughly symmetric about the  $V = 0$  axis.

We see that for  $H \gg T_k$  the behaviour of the differential conductance is in rough accordance with the predictions of Wingreen and Meir [10], that is, there is a peak approximately at  $\mu_2 - \mu_1 \sim H$  for  $H \gg T_k$ . However, as we have already noted, the peak occurs at a bias noticeably smaller than  $H$  while [10] finds the peak to occur exactly at  $H$ . As  $H$  is decreased this peak moves to smaller ratios of  $(\mu_1 - \mu_2)/H$  before disappearing altogether at  $H \sim T_k$ . For values of  $H \ll T_k$ , the differential conductance does not appreciably change from its linear response value for voltage biases of the same order of magnitude as  $H$ . We also see that as  $H$  is increased the width of the peak narrows and the height of the peak approaches the value of  $e^2/h$  indicating that only a single spin species (in this case spin  $\uparrow$ ) is contributing to the conductance.

We now analyze the properties of the differential conductance peak for values of  $H \gg T_k$ . As we have already noted in Section 2, we expect our results to be exact in the regime that  $H/T_k$  becomes asymptotically large. In this regime the differential magneto-conductance is determined solely by the spin  $\uparrow$  hole scattering which we are exactly able to determine: no scattering ansatz is needed here.

For  $H/T_k \gg 1$ , we can write the scattering phases as follows:

$$\begin{aligned}
\delta_{ho}^{\uparrow}(\varepsilon_{ho} > \mu_1) &= 2\pi \int_{-D}^k dk' \rho_{\text{imp}}^1(k') + \pi(1 - \int_{-D}^B dk \rho_{\text{imp}}^1(k)) \\
&\approx \pi + 2 \tan^{-1}(2(I^{-1} - g(k))); \\
\delta_{ho}^{\downarrow}(\varepsilon_{ho} > \mu_1) &= 2\pi \int_{-D}^k dk' \rho_{\text{imp}}^1(k') + \pi(1 - \int_{-D}^B dk \rho_{\text{imp}}^1(k)) \\
&\approx \frac{3}{2}\pi + \tan^{-1}(2(I^{-1} - b)).
\end{aligned} \tag{5.34}$$

In the first of the above equations, the second integral has been neglected relative to the first, valid for  $H \gg T_k$ . We also make the approximation that the spin  $\downarrow$  conductance varies inappreciably from its Fermi surface value as the bias is varied. Thus we set  $k = B$  in the second of the equations. As the conductance of the spin  $\downarrow$  species for large  $eV \sim H \gg T_k$  is constant, the peak maximum occurs when

$$\delta_{ho}^{\uparrow}(\varepsilon_{ho} > \mu_1) = \pi. \tag{5.35}$$

This in turn implies the condition

$$g(k) = I^{-1}, \quad (5.36)$$

and so from (5.31) the bias at which the maximum occurs is

$$eV_{\max} = \varepsilon^1(k = -\sqrt{2U\Gamma}I^{-1}) = -H \left( 1 - \frac{1}{2\pi} \tan^{-1} \frac{1}{I^{-1} - b} + \dots \right), \quad (5.37)$$

$$I^{-1} - b = \frac{1}{\pi} \log \left( \frac{H}{2T_k} \sqrt{\frac{\pi e}{2}} \right),$$

where  $\dots$  indicates we have not written out all the terms arising from (5.31). The half maxima of the peak occur when  $\delta_{ho}^\uparrow(\varepsilon_{ho} > \mu_1) = \frac{\pi}{2}/\frac{3\pi}{2}$ , which in turn implies

$$g(k) = I^{-1} \pm 1/2. \quad (5.38)$$

Hence the peak width equals

$$e\Delta V = \varepsilon^1(k = -\sqrt{2U\Gamma}(I^{-1} - 1/2)) - \varepsilon^1(k = -\sqrt{2U\Gamma}(I^{-1} + 1/2));$$

$$= \frac{H}{2\pi} \left( \tan^{-1} \frac{1}{I^{-1} - \frac{1}{2} - b} - \tan^{-1} \frac{1}{I^{-1} + \frac{1}{2} - b} \right) + \dots. \quad (5.39)$$

Finally we can estimate the peak height. The peak maximum will be characterized by the maximal conductance of the spin  $\uparrow$  electrons ( $e^2/h$ ) together with the associated conductance of the spin  $\downarrow$  electrons. The latter will vary only slightly from its Fermi surface value as already discussed. Hence the height of the peak is given by

$$G_{\max} = \frac{e^2}{h} \left( 1 + \sin^2 \left( \frac{1}{2} \delta_{ho}^\downarrow(\varepsilon = \varepsilon_F) \right) \right)$$

$$= \frac{e^2}{h} \left( \frac{3}{2} - \frac{(I^{-1} - b)}{\sqrt{4(I^{-1} - b)^2 + 1}} \right). \quad (5.40)$$

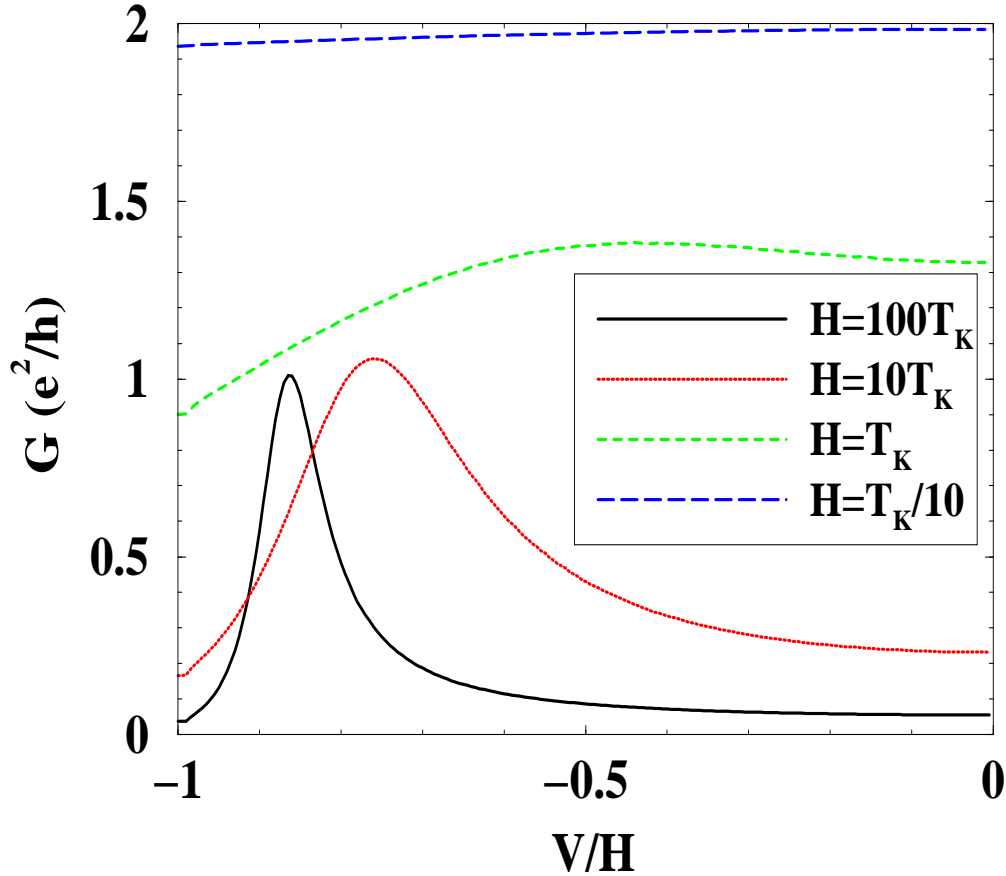


Figure 15: A plot of the differential conductance in a magnetic field at the symmetric point. The value of the parameters used in the plot are  $\Gamma = .05$  and  $U = 10\Gamma$ .

The results for the location and width of the differential conductance peak are similar to those found by Moore and Wen [17] to characterize the location and width of peaks appearing in the equilibrium Bethe ansatz impurity density of states for the Kondo model. In the large  $H$  limit, the impurity density of states as found in the Bethe ansatz then evidently shares certain properties with the non-equilibrium spectral density of states defined from the dot correlator,  $\text{Im}\langle dd^\dagger \rangle$ . However [17] makes no prediction as to the height of the differential conductance peak. We in general do not expect the height of the peak in the Bethe ansatz impurity density of states to be related to the height of the spectral density arising from  $\text{Im}\langle dd^\dagger \rangle$ . We already know that no such relationship exists at  $H = 0$  (see Section 5.2i) and there is no reason to expect it to appear at finite  $H$ .

In Figure 16 we plot how peak characteristics evolve with increasing  $H$ . For comparison, we plot both the asymptotic forms ((5.36)-(5.38)) for the peak characteristics against

the exact results. We see that the location of the peak slowly approaches  $eV = -H$  with increasing  $H$ . This approach will be logarithmic in  $H$  as

$$\frac{eV_{\max}}{H} + 1 \sim \frac{1}{2\pi} \frac{1}{I^{-1} - b}, \quad (5.41)$$

and  $b \sim -\log(H)$ . Similarly the height of the peak approaches  $e^2/h$  but again logarithmically in  $H$ . We note that the asymptotic forms reproduce the exact results with remarkable accuracy even in the region,  $H \sim T_k$ , where the assumptions of their derivation do not necessarily hold.



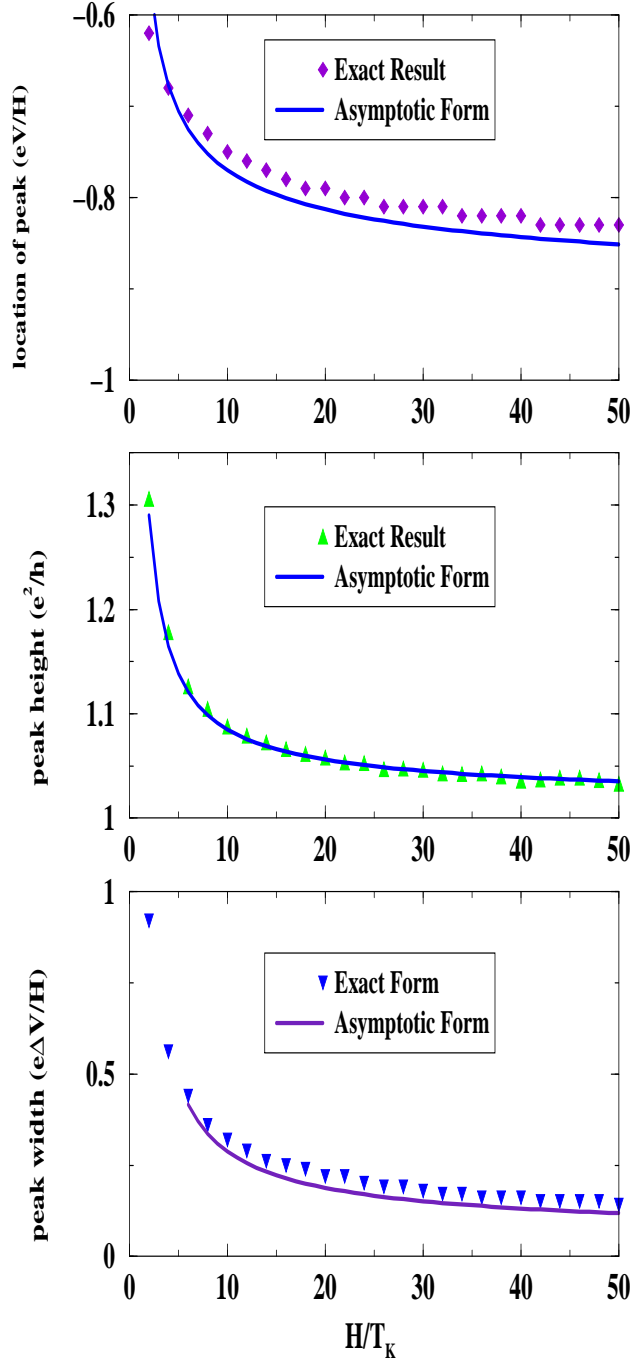


Figure 16: Plots describing the evolution of the differential conductance peak with increasing magnetic field. In the top panel is a plot of the location of the peak while the middle panel records the peak height and the bottom panel gives the peak width. The parameters used are  $U = .75/\pi D$  ( $D$  being the bandwidth) and  $\Gamma = U/12$ .

## 6. Concluding Remarks

Computing transport properties in a strongly interacting system is a difficult challenge. In this paper we have attacked the problem by combining a Landauer-Buttiker approach together with data from integrability. We have thus been able to provide a description of the scattering states in the theory that have led to several successes. We have verified the Friedel sum rule and provided a quantitative description of the linear response conductance at  $T=0$  both in and out of a magnetic field. Our most striking result has, however, been the computation of the finite temperature linear response conductance scaling curve. This result is predicated upon an accurate description of the scattering states away from the Fermi surface. As such we have also been able to compute the out-of-equilibrium current, again both in and out of a magnetic field. In particular, we have provided a quantitative description of the differential magneto-conductance. Given the nature of our construction of the scattering states, we believe our computation of this latter quantity to become exact in the large field limit.

While our technique bears a degree of resemblance to the successful, exact treatment of interacting quantum Hall edges [24], the technical complexity of the two-lead Anderson model has prevented us from finding a definitive solution of the problem in all regimes. However, we have still been able to use integrability to find extremely good approximations to the exact results in the cases of greatest experimental interest. The situation here is not altogether different from the use of form-factors in calculating correlation functions: although the techniques of integrability do not (yet) generically lead to closed form expressions, they are nevertheless a breakthrough, providing excellent approximations which are valid from the lowest energies through cross-over regimes. These approximations are far different from the standard, mean-field ones, for they contain all the crucial features of low dimensional, strong interactions. In particular the results presented here represent an improvement on previous approximate methods found in the literature. The quality of our approach can be gauged from the excellent reproduction (with no fitting parameter) of Costi et al.'s NRG finite temperature linear response curve. It is unlikely other analytical techniques could do the same.

Our work raises two kinds of questions. The first is whether higher order approximations can be devised in the present problem, akin to taking higher energy intermediate states into account in form-factors calculations of correlation functions. More precisely, is it possible to develop further the description of the fermions in terms of the integrable states

found in (2.52). The other, more practical question, is whether similar calculations can be performed in other models of interest, and so obtain excellent approximations of out-of-equilibrium transport properties based upon the exact solution of the thermodynamics and the proper identification of scattering states.

## 7. Acknowledgments

The authors would like to thank T. Costi for sharing his NRG data. R.K. would like to thank Y. Meir, N. Wingreen, L. Glazman, and T. Costi for useful discussions. H.S. thanks N. Andrei and A. Georges for many useful discussions. R.K. has been supported by NSERC, the NSF through grant number DMR-9802813 and through the Waterman Award under grant number DMR-9528578, and the University of Virginia Physics Department. H.S. has been supported by the Packard Foundation, the NYI Program, and the DOE (H.S.). H.S. also acknowledges hospitality and support from the LPTHE (Jussieu) and LPTMS (Orsay). A.W.W.L. has been supported by the NSF through grant DMR-00-75064. A.W.W.L. also acknowledges hospitality and partial support from NWO, University of Amsterdam (the Netherlands).

## Appendix A. Practical Computation of Density and Energy Functionals

Here we present equations for the energy and density functionals that are more amenable to numerical analysis. The original density equations are given by

$$\begin{aligned}\rho_p(k) + \rho_h(k) &= \frac{1}{2\pi} + \frac{\Delta(k)}{L} + g'(k) \int d\lambda a_1(g(k) - \lambda) \sigma_p(\lambda); \\ \sigma_p(\lambda) + \sigma_h(\lambda) &= -\frac{x'(\lambda)}{\pi} + \frac{\tilde{\Delta}(\lambda)}{L} - \int d\lambda' a_2(\lambda' - \lambda) \sigma_p(\lambda') - \int dk a_1(\lambda - g(k)) \rho_p(k).\end{aligned}\tag{A.1}$$

Expressing these equations in terms of the Fourier transform of  $\sigma(\lambda)$  gives us

$$\begin{aligned}\rho_p(k) + \rho_h(k) &= \frac{1}{2\pi} + \frac{\Delta(k)}{L} + g'(k) \int \frac{d\omega}{2\pi} e^{-i\omega g(k)} e^{-|\omega|/2} \sigma_p(\omega); \\ \sigma_p(\omega) + \sigma_h(\omega) &= -\frac{x'(\omega)}{\pi} + \frac{\tilde{\Delta}(\omega)}{L} - e^{-|\omega|} \sigma_p(\omega) - \int dk e^{i\omega g(k)} e^{-|\omega|/2} \rho_p(k).\end{aligned}\tag{A.2}$$

Solving for  $\sigma_p(\omega)$  and substituting into the r.h.s. of both of the above equations gives

$$\begin{aligned}
\rho_p(k) + \rho_h(k) &= \frac{1}{2\pi} + \frac{\Delta(k)}{L} - g'(k) \int d\lambda \sigma_h(\lambda) s(\lambda - g(k)) \\
&\quad - g'(k) \int \frac{d\omega}{2\pi} e^{-i\omega g(k)} \left( \frac{x'(\omega)}{\pi} - \frac{\tilde{\Delta}(\omega)}{L} \right) \frac{1}{2 \cosh(\omega/2)} \\
&\quad - g'(k) \int dk' \rho_p(k') R(g(k) - g(k')); \\
\sigma_p(\lambda) + \sigma_h(\lambda) &= -\frac{x'(\lambda)}{\pi} + \int d\lambda' R(\lambda' - \lambda) \frac{x'(\lambda')}{\pi} + \frac{\tilde{\Delta}(\lambda)}{L} - \int d\lambda' R(\lambda' - \lambda) \frac{\tilde{\Delta}(\lambda')}{L} \\
&\quad + \int d\lambda' \sigma_h(\lambda') R(\lambda' - \lambda) - \int dk \rho_p(k) s(\lambda - g(k)),
\end{aligned} \tag{A.3}$$

where  $R(\lambda)$  and  $s(\lambda)$  are given by

$$\begin{aligned}
R(\lambda) &= \frac{1}{2\pi} \int d\omega \frac{e^{-i\omega\lambda}}{1 + e^{|\omega|}}; \\
s(\lambda) &= \frac{1}{2 \cosh(\pi\lambda)} = \frac{1}{2\pi} \int d\omega \frac{e^{-i\omega\lambda}}{2 \cosh(\omega/2)}.
\end{aligned} \tag{A.4}$$

We can further simplify the first of the equations in (A.3) by using the relations

$$\begin{aligned}
-\frac{x'(\lambda)}{\pi} &= \int dk \frac{d\omega}{(2\pi)^2} e^{-i\omega(\lambda - g(k))} e^{-|\omega|/2}; \\
\tilde{\Delta}(\lambda) &= \int dk \frac{d\omega}{2\pi} \Delta(k) e^{-i\omega(\lambda - g(k))} e^{-|\omega|/2}.
\end{aligned} \tag{A.5}$$

Then

$$\begin{aligned}
\rho_p(k) + \rho_h(k) &= \left( \frac{1}{2\pi} + \frac{\Delta(k)}{L} + g'(k) \int dk' R(g(k) - g(k')) \left( \frac{1}{2\pi} + \frac{\Delta(k')}{L} \right) \right) \\
&\quad - g'(k) \int d\lambda \sigma_h(\lambda) s(\lambda - g(k)) - g'(k) \int dk' \rho_p(k') R(g(k) - g(k')); \\
\sigma_p(\lambda) + \sigma_h(\lambda) &= \int dk \left( \frac{\Delta(k)}{L} + \frac{1}{2\pi} \right) s(\lambda - g(k)) \\
&\quad + \int d\lambda' \sigma_h(\lambda') R(\lambda' - \lambda) - \int dk \rho_p(k) s(\lambda - g(k)).
\end{aligned} \tag{A.6}$$

These forms of the equations are better behaved numerically as

$$\int d\lambda R(\lambda) = \frac{1}{2}, \tag{A.7}$$

while

$$\int d\lambda a_n(\lambda) = 1. \quad (\text{A.8})$$

Hence when we go to solve these equations iteratively, successive iterations grow increasingly small as  $(1/2)^n$ , whereas before we would not expect convergence.

We can now derive new equations for the energy functional. As in (2.34) we find

$$\begin{aligned} \delta E &= L \int dk \{ \varepsilon^+(k) \delta \rho_p(k) - \varepsilon^-(k) \delta \rho_h(k) \} + L \int d\lambda \{ \varepsilon^+(\lambda) \delta \sigma_p(\lambda) - \varepsilon^-(\lambda) \delta \sigma_h(\lambda) \} \\ &= L \int dk \left( k - \frac{H}{2} \right) \delta \rho_p(k) + 2L \int d\lambda x(\lambda) \delta \sigma_p(\lambda). \end{aligned} \quad (\text{A.9})$$

But now from (A.6) we have

$$\begin{aligned} \delta \rho_p(k) + \delta \rho_h(k) &= -g'(k) \int d\lambda \delta \sigma_h(\lambda) s(\lambda - g(k)) - g'(k) \int dk' \delta \rho_p(k') R(g(k) - g(k')); \\ \delta \sigma_p(\lambda) + \delta \sigma_h(\lambda) &= \int d\lambda' \delta \sigma_h(\lambda') R(\lambda' - \lambda) - \int dk \delta \rho_p(k) s(\lambda - g(k)). \end{aligned} \quad (\text{A.10})$$

Solving for  $\delta \sigma_p / \delta \rho_h$  and substituting into (A.9) leaves us with

$$\begin{aligned} \varepsilon^+(k) + \varepsilon^-(k) &= k - \frac{H}{2} - 2 \int d\lambda x(\lambda) s(\lambda - g(k)) \\ &\quad + \int d\lambda \varepsilon^+(\lambda) s(\lambda - g(k)) - \int dk' g'(k') \varepsilon^-(k') R(g(k) - g(k')); \\ \varepsilon^+(\lambda) + \varepsilon^-(\lambda) &= 2x(\lambda) - 2 \int d\lambda' R(\lambda - \lambda') x(\lambda') \\ &\quad + \int d\lambda' \varepsilon^+(\lambda') R(\lambda - \lambda') + \int dk g'(k) \varepsilon^-(k) s(g(k) - \lambda). \end{aligned} \quad (\text{A.11})$$

## Appendix B. Computing Scattering via the Impurity Energy

In this appendix we compute the scattering phase of the electronic excitations through examining the impurity energy. To do so we will relate the impurity energy to the impurity momentum and then use the already established relations in Section 2. In doing so, we will bring out subtleties in defining the impurity energy for the purposes of deriving scattering phases.

To determine the impurity energy of the excitations, we play a game similar to that used previously in deriving  $\varepsilon(k)/\varepsilon(\lambda)$ . The total impurity energy has the form (from (2.10))

$$E_{\text{imp}} = - \int d\lambda \sigma_p(\lambda) (2\Gamma(\lambda)) - \int dk \rho_p(k) \delta(k), \quad (\text{B.1})$$

where  $\Gamma(\lambda) = \text{Re}\delta(x(\lambda) + iy(\lambda))$ . Hence the bulk energy is given by

$$\begin{aligned} E_{\text{bulk}} &= E - \frac{1}{L}E_{\text{imp}} \\ &= L \int d\lambda \sigma_p(\lambda)2(x(\lambda) + \frac{\Gamma(\lambda)}{L}) + L \int dk \rho_p(k)(k - \frac{H}{2} + \frac{\delta(k)}{L}). \end{aligned} \quad (\text{B.2})$$

We can thus derive equations for the bulk energy of the excitations:

$$\begin{aligned} \varepsilon_{\text{bulk}}^+(k) + \varepsilon_{\text{bulk}}^-(k) &= k - \frac{H}{2} + \frac{\delta(k)}{L} - \int d\lambda \varepsilon_{\text{bulk}}^-(\lambda)a_1(\lambda - g(k)); \\ \varepsilon_{\text{bulk}}^+(\lambda) + \varepsilon_{\text{bulk}}^-(\lambda) &= 2(x(\lambda) + \frac{\Gamma(\lambda)}{L}) \\ &\quad - \int d\lambda' \varepsilon_{\text{bulk}}^-(\lambda')a_2(\lambda' - \lambda) + \int dk g'(k)\varepsilon_{\text{bulk}}^-(k)a_1(g(k) - \lambda). \end{aligned} \quad (\text{B.3})$$

When we add particles to the system, we want to add them relative to the Fermi surface as determined by the host system (in other words we add them far from the impurity). In light of this, we have another constraint determining the locations,  $Q$  and  $B$ , of the two Fermi surfaces:

$$\varepsilon_{\text{bulk}}(k = B) = \varepsilon_{\text{bulk}}(\lambda = Q) = 0. \quad (\text{B.4})$$

Of course, any bulk quantity will not distinguish between a Fermi surface set as above or a Fermi surface determined by

$$\varepsilon(k = B) = \varepsilon(\lambda = Q) = 0. \quad (\text{B.5})$$

The difference between the two amounts to  $1/L$  corrections. However this difference is important if one is looking at impurity quantities. See in contrast [28] in the context of the Kondo problem.

We are now in a position to relate the impurity energy to the impurity density of states. Differentiating the above leads to

$$\begin{aligned} \partial_k \varepsilon_{\text{bulk}}^+(k) + \partial_k \varepsilon_{\text{bulk}}^-(k) &= 1 + \frac{\delta'(k)}{L} - g'(k) \int d\lambda \partial_\lambda \varepsilon_{\text{bulk}}^-(\lambda)a_1(\lambda - g(k)); \\ \partial_\lambda \varepsilon_{\text{bulk}}^+(\lambda) + \partial_\lambda \varepsilon_{\text{bulk}}^-(\lambda) &= 2(x'(\lambda) + \frac{\Gamma'(\lambda)}{L}) \\ &\quad - \int d\lambda' \partial_{\lambda'} \varepsilon_{\text{bulk}}^-(\lambda')a_2(\lambda' - \lambda) + \int dk \partial_k \varepsilon_{\text{bulk}}^-(k)a_1(g(k) - \lambda). \end{aligned} \quad (\text{B.6})$$

Writing

$$\partial \varepsilon_{\text{bulk}} = \partial \varepsilon - \frac{1}{L} \partial \varepsilon_{\text{imp}}, \quad (\text{B.7})$$

where  $\varepsilon_{\text{imp}}$  is the  $\frac{1}{L}$  contribution to the energy of the excitation, and comparing to (2.19) leads to the relations:

$$\begin{aligned}\partial_\lambda \varepsilon_{\text{imp}}(\lambda) &= -\partial_\lambda p_{\text{imp}}(\lambda) = 2\pi \sigma_{\text{imp}}(\lambda); \\ \partial_k \varepsilon_{\text{imp}}(k) &= -\partial_k p_{\text{imp}}(k) = -2\pi \rho_{\text{imp}}(k).\end{aligned}\tag{B.8}$$

Hence for spin  $\uparrow$  electrons, the scattering phase is given by

$$\delta_e^\uparrow = -\varepsilon_{\text{imp}}(k) - \varepsilon_{\text{imp}}(\lambda).\tag{B.9}$$

Moreover we have,

$$\begin{aligned}\varepsilon_{\text{imp}}(\lambda) &= -2\pi \int_\lambda^{\tilde{Q}} \sigma_{\text{imp}}(\lambda); \\ \varepsilon_{\text{imp}}(k) &= -2\pi \int_{-D}^k \rho_{\text{imp}}(k),\end{aligned}\tag{B.10}$$

allowing us to prove the Friedel sum rule. Note that these relationships only hold due to our choice in defining the Fermi surface as in (B.4).

## Appendix C. Direct Computation of the Scattering Phase

It is possible to provide another derivation of the Friedel sum rule that involves a direct computation of the scattering phase (as opposed to working through the mediating agent of the impurity densities). For (purely technical) simplicity we restrict ourselves to the case of a vanishing magnetic field where there are no real  $k$ 's in the ground state.

As we discussed in Section 2, the computation of an electron scattering phase involves the phases of a  $k$ -particle and a  $\lambda$ -hole. As we work in the zero field limit, the  $k$ -particle phase is zero and we can focus solely upon the phase of the  $\lambda$ -hole. To this end, we consider the bulk density of the  $\lambda_\alpha$ 's,  $\sigma_{\text{bulk}}(\lambda)$ . In the ground state,  $\sigma_{\text{bulk}}(\lambda)$  obeys the equation

$$\sigma_{\text{bulk}}(\lambda) + \int_Q^\infty d\lambda' a_2(\lambda - \lambda') \sigma_{\text{bulk}}(\lambda') = -\frac{1}{\pi} x'(\lambda). \quad (\text{C.1})$$

Following the discussion in [37], the key quantity in the following will be the shift of this distribution when a particle or a hole is created at rapidity  $\Lambda$ . To study this quantity, we go back to the discrete form of the Bethe ansatz equations, which read

$$2\pi J_\alpha + \sum_{\beta=1}^M \theta_2(\lambda_\alpha - \lambda_\beta) = -2Lx(\lambda_\alpha). \quad (\text{C.2})$$

If a hole is made at  $\Lambda$ , the rapidities shift  $\lambda_\alpha \rightarrow \lambda_\alpha^{(1)}$  and the above equation becomes

$$2\pi J_\alpha + \sum_{\beta=1}^M \theta_2(\lambda_\alpha^{(1)} - \lambda_\beta^{(1)}) - \theta_2(\lambda_\alpha^{(1)} - \Lambda) = -2Lx(\lambda_\alpha^{(1)}). \quad (\text{C.3})$$

Setting

$$\sigma_{\text{bulk}}(\lambda_\alpha) \left[ \lambda_\alpha^{(1)} - \lambda_\alpha \right] \equiv \frac{1}{L} F(\lambda_\alpha | \Lambda), \quad (\text{C.4})$$

it easily follows using the equation for  $\sigma_{\text{bulk}}(\lambda)$  in (C.1) that

$$F(\lambda | \Lambda) + \int_Q^\infty d\lambda' a_2(\lambda - \lambda') F(\lambda' | \Lambda) = -\frac{1}{2\pi} \theta_2(\lambda - \Lambda), \quad (\text{C.5})$$

where  $\theta_2(x) = 2 \tan^{-1}(x) - \pi$ . To proceed, it is convenient to introduce the integral operators  $\widehat{K}$  and  $\widehat{L}$  defined by

$$\widehat{K}(f(\lambda)) \equiv - \int_Q^\infty d\lambda' a_2(\lambda - \lambda') f(\lambda'), \quad (\text{C.6})$$



and

$$(\widehat{I} - \widehat{K})(\widehat{I} + \widehat{L}) = \widehat{I}. \quad (\text{C.7})$$

From (C.7), and the fact that  $a_2(\lambda) = \frac{1}{2\pi} \frac{d}{d\lambda} \theta_2(\lambda)$ , it follows that

$$F(\lambda|\Lambda) = \int_{\Lambda}^{\infty} d\lambda' L(\lambda, \lambda'). \quad (\text{C.8})$$

A similar formula with a minus sign would hold if a particle were created in lieu of a hole at  $\Lambda$ . One can represent  $\widehat{L}$  as a power series if one wishes:

$$L(\lambda, \lambda') = -a_2(\lambda - \lambda') + \int_Q^{\infty} d\lambda'' a_2(\lambda - \lambda'') a_2(\lambda'' - \lambda') + \dots \quad (\text{C.9})$$

Hence in particular,  $L(\lambda, \lambda') = L(\lambda', \lambda)$ .

Now consider the impurity density of states,  $\sigma_{imp}$ . It obeys

$$\sigma_{imp}(\lambda) + \int_Q^{\infty} d\lambda' a_2(\lambda - \lambda') \sigma_{imp}(\lambda') = \widetilde{\Delta}(\lambda), \quad (\text{C.10})$$

from which it follows,

$$\int_Q^{\infty} d\lambda \sigma_{imp}(\lambda) = -\frac{1}{2\pi} \phi(Q) + \int_Q^{\infty} d\lambda F(\lambda|Q) \widetilde{\Delta}(\lambda), \quad (\text{C.11})$$

having set  $\phi(\lambda) \equiv -2\text{Re} \delta [x(\lambda) + iy(\lambda)]$  and where we have used that  $\phi(\infty) = 0$ . As

$$n_d = 2 \int_Q^{\infty} d\lambda \widetilde{\sigma}_{imp}(\lambda), \quad (\text{C.12})$$

we find,

$$n_d = -\frac{1}{\pi} \phi(Q) + 2 \int_Q^{\infty} d\lambda \widetilde{\Delta}(\lambda) F(\lambda|Q), \quad (\text{C.13})$$

the key formula of this appendix. The r.h.s. of the above equation is highly suggestive: the first term is proportional to the bare scattering phase of the electron while the second term represents the dressing of the bare phase that results from the non-trivial ground state of the system.

To complete this section we now explicitly demonstrate the Friedel sum rule. To do so we first imagine scattering the unperturbed ground state through the impurity. The entire scattering phase is then

$$\sum_{\beta=1}^M \phi(\lambda_{\beta}). \quad (\text{C.14})$$

Now we imagine scattering the ground state plus hole through the impurity with a resultant total phase

$$-\phi(\Lambda) + \sum_{\beta=1}^M \phi(\lambda_{\beta}^1). \quad (\text{C.15})$$

The difference of the two defines the scattering phase of the electron:

$$\delta_{el} = -\phi(\Lambda) + 2\pi \int_Q^{\infty} d\lambda' F(\lambda'|\Lambda) \tilde{\Delta}(\lambda'). \quad (\text{C.16})$$

Comparing (C.13) with (C.16) shows that with  $\Lambda = Q$  we arrive at  $\delta_{el} = \pi n_d = 2\pi n_{d\uparrow/\downarrow}$ , the Friedel sum rule in the particular case when the magnetic field vanishes.

## Appendix D. Wiener-Hopf Analysis at the Symmetric Point

### D.1. An alternative equation for $\varepsilon^1(k)$

We first solve the equation governing  $\varepsilon^1(k)$ , the energy of excitations in lead 1 relative to the Fermi surface. To do so we cast it in a different form than found in (5.7). For simplicity we assume that  $\mu_1$  is zero. However finite  $\mu_1$  does not change the expression for  $\varepsilon^1$  provided  $\mu_1 \ll D$ .

Now  $\varepsilon^1(k)$  is the energy associated with adding or removing a  $k$ -excitation. Thus imagine removing a  $k_o < B$ . This induces a change in the densities  $\rho(k)$  and  $\sigma(\lambda)$ . At the symmetric point, the unperturbed densities have the form (see (A.6)):

$$\begin{aligned}\rho(k) &= \rho_o(k) - g'(k) \int_{-\infty}^B dk' \rho(k') R(g(k) - g(k')), \\ \sigma(\lambda) &= \sigma_o(\lambda) - \int_{-\infty}^B dk \rho(k) s(\lambda - g(k)),\end{aligned}\tag{D.1}$$

while the perturbed densities,  $\rho_1(k)$  and  $\sigma_1(\lambda)$ , due to the hole at  $k_o$ , are

$$\begin{aligned}\rho_1(k) &= \rho_o(k) - \frac{1}{L} \delta(k - k_o) - g'(k) \int_{-\infty}^B dk' \rho_1(k') R(g(k) - g(k')), \\ \sigma_1(\lambda) &= \sigma_o(\lambda) - \int_{-\infty}^B dk \rho_1(k) s(\lambda - g(k)),\end{aligned}\tag{D.2}$$

where  $L$  is the system size. Rewriting  $\rho_1$  by

$$\rho_1(k) \rightarrow \rho_1(k) - \frac{1}{L} \delta(k - k_o),$$

yields

$$\begin{aligned}\rho_1(k) &= \rho_o(k) + \frac{1}{L} g'(k) R(g(k_o) - g(k)) - g'(k) \int_{-\infty}^B dk' \rho_1(k') R(g(k) - g(k')); \\ \sigma_1(\lambda) &= \sigma_o(\lambda) + \frac{1}{L} s(\lambda - g(k_o)) - \int_{-\infty}^B dk \rho_1(k) s(\lambda - g(k)).\end{aligned}\tag{D.3}$$

And so changes in the density, apart from the  $\delta(k - k_o)/L$  term already scaled out, are governed by

$$\begin{aligned}\delta\rho(k) &\equiv L(\rho_1(k) - \rho(k)) = g'(k) R(g(k_o) - g(k)) - g'(k) \int_{-\infty}^B dk' \delta\rho(k') R(g(k) - g(k')); \\ \delta\sigma(\lambda) &\equiv L(\sigma_1(\lambda) - \sigma(\lambda)) = s(\lambda - g(k_o)) - \int_{-\infty}^B dk \delta\rho(k) s(\lambda - g(k)).\end{aligned}\tag{D.4}$$

The energy of the excitation can be expressed in terms of  $\delta\rho$  and  $\delta\sigma$ :

$$\begin{aligned}
-\varepsilon^1(k_o) &= -(k_o - \frac{H}{2}) + \int dk(k - H/2)\delta\rho(k) + 2 \int d\lambda x(\lambda)\delta\sigma(\lambda) \\
&= -[(k_o - H/2) - 2 \int d\lambda x(\lambda)s(\lambda - g(k_o))] \\
&\quad + \int dk \delta\rho(k) [k - \frac{H}{2} - 2 \int d\lambda x(\lambda)s(\lambda - g(k))].
\end{aligned} \tag{D.5}$$

We see that  $\varepsilon^1(k_o)$  depends now only upon  $\delta\rho$ . That this form for  $\varepsilon^1(k_o)$  is equivalent to the equations in Section 2 or Appendix A can be shown using the technology found in Appendix C.

Provided  $B < 0$ , we can introduce a change of variables that simplifies matters:

$$\rho(z) \equiv -\frac{\rho(k)}{g'(k)}, \quad z \equiv g(k), \quad k < 0. \tag{D.6}$$

At energies not far in excess of the Kondo temperature we have

$$(k - H/2) - 2 \int d\lambda x(\lambda)s(\lambda - g(k)) \approx \frac{\sqrt{2U\Gamma}}{\pi} e^{-\pi g(k)} - \frac{H}{2}. \tag{D.7}$$

The above then simplifies to

$$\begin{aligned}
\delta\rho(z) &= -R(z - g(k_o)) + \int_b^\infty dz' \delta\rho(z')R(z - z'), \quad b = \frac{B^2}{2U\Gamma}; \\
-\varepsilon^1(k_o) &= -\left[\frac{\sqrt{2U\Gamma}}{\pi} e^{-\pi g(k_o)} - \frac{H}{2}\right] + \int dz \delta\rho(z) \left[\frac{\sqrt{2U\Gamma}}{\pi} e^{-\pi z} - \frac{H}{2}\right], \\
&= -\frac{\sqrt{2U\Gamma}}{\pi} (e^{-\pi g(k_o)} - \delta\rho(\omega = i\pi)) + \frac{H}{2} (1 - \delta\rho(\omega = 0)),
\end{aligned} \tag{D.8}$$

where in the last line we have expressed  $\varepsilon^1(k)$  in terms of the Fourier transform of  $\delta\rho$ . It is to the equation for  $\delta\rho$  that we actually apply the Wiener-Hopf analysis.

The expression for  $\varepsilon^1(k)$  is valid provided we have removed a particle, i.e.  $g(k_o) > b$  or  $k < B$ . If we instead add a particle at  $k > B$  or  $g(k_o) < b$ , we obtain in a similar fashion the following description of  $\varepsilon^1(k)$ :

$$\begin{aligned}
\delta\rho(z) &= R(z - g(k_o)) + \int_b^\infty dz' \delta\rho(z')R(z - z'), \quad b = \frac{B^2}{2U\Gamma}; \\
\varepsilon^1(k_o) &= \frac{\sqrt{2U\Gamma}}{\pi} (e^{-\pi g(k_o)} + \delta\rho(\omega = i\pi)) - \frac{H}{2} (1 + \delta\rho(\omega = 0)).
\end{aligned} \tag{D.9}$$

### D.2. Review of the Wiener-Hopf Analysis

We so review the technique as presented in [28] on equations of the general form

$$f(z) = \int_A^\infty dz' f(z') h(z - z') + g(z). \quad (\text{D.10})$$

Writing  $f^\pm(z) = f(z)\theta(\pm z \mp A)$ , the Fourier transform of the above equation yields

$$f^+(\omega) + f^-(\omega) = f^+(\omega)h(\omega) + g(\omega), \quad (\text{D.11})$$

where Fourier transforms are defined by

$$a(\omega) = \int d\omega e^{i\omega z} a(z). \quad (\text{D.12})$$

The key step in the analysis is writing  $1 - h(\omega)$  as a product of functions,  $G^\pm$ , which are analytic in the upper/lower planes respectively:

$$1 - h(\omega) = \frac{1}{G^+(\omega)G^-(\omega)}. \quad (\text{D.13})$$

We can then write (D.11) as

$$e^{-i\omega A} \frac{f^+(\omega)}{G^+(\omega)} + e^{-i\omega A} f^-(\omega)G^-(\omega) = g(\omega)G^-(\omega)e^{-i\omega A}. \quad (\text{D.14})$$

Given  $e^{-i\omega A} f^\pm(\omega)$  is analytic in the upper/lower half plane, applying the operators

$$\pm \frac{1}{2\pi i} \int d\omega' \frac{1}{\omega' - (\omega \pm i\delta)}, \quad (\text{D.15})$$

to (D.14) yields solutions for both  $f^+$  and  $f^-$ :

$$\begin{aligned} f^+(\omega) &= G^+(\omega) \frac{e^{i\omega A}}{2\pi i} \int d\omega' \frac{1}{\omega' - (\omega + i\delta)} g(\omega') G^-(\omega') e^{-i\omega' A}; \\ f^-(\omega) &= -\frac{e^{i\omega A}}{G^-(\omega)} \frac{1}{2\pi i} \int d\omega' \frac{1}{\omega' - (\omega - i\delta)} g(\omega') G^-(\omega') e^{-i\omega' A}. \end{aligned} \quad (\text{D.16})$$

### D.3. Determination of $\delta\rho$

Applying the above analysis to (D.8), appropriate to the case of removing a particle,  $z > b$  ( $k < B$ ), we have

$$\begin{aligned} \delta\rho^+(\omega) &= -e^{i\omega b} \frac{G^+(\omega)}{2\pi i} \int d\omega' \frac{e^{i\omega'(z_0-b)}}{\omega' - (\omega + i\delta)} R(\omega') G^-(\omega'); \\ G^\pm(\omega) &= \sqrt{2\pi} \frac{(\mp i\omega + \delta) \mp \frac{i\omega}{2\pi}}{\Gamma(\frac{1}{2} \mp \frac{i\omega}{2\pi})}; \quad 1 - R(\omega) = \frac{1}{G_+(\omega)G_-(\omega)} \\ b &= \frac{1}{\pi} \log\left(\frac{2}{H} \sqrt{\frac{U\Gamma}{\pi e}}\right). \end{aligned} \quad (\text{D.17})$$

If  $\omega = 0$ , we can continue the  $\omega'$ -contour into the upper half plane about the branch cut of  $G^-(\omega)$  while picking up the pole at  $\omega' = 0$ :

$$\delta\rho(\omega = 0) = -1 + \frac{1}{\pi^{3/2}} \int_0^\infty d\omega' \frac{\sin(2\pi\omega')}{\omega'} \left(\frac{\omega'}{e}\right)^{-\omega'} \Gamma\left(\frac{1}{2} + \omega'\right) e^{-2\pi\omega'(g(k_o)-b)}. \quad (\text{D.18})$$

With  $\omega = i\pi$ , we find instead

$$\delta\rho(\omega = i\pi) = e^{-\pi g(k_o)} + e^{-\pi b} \frac{1}{\pi\sqrt{2e}} \int_0^\infty d\omega' \frac{\sin(2\pi\omega')}{\omega' - \frac{1}{2}} \left(\frac{\omega'}{e}\right)^{-\omega'} \Gamma\left(\frac{1}{2} + \omega'\right) e^{-2\pi\omega'(g(k_o)-b)}. \quad (\text{D.19})$$

If we now instead add a particle at  $k > B$  or  $g(k_o) < b$ , we obtain from the Wiener-Hopf analysis of (D.9) the following equations:

$$\begin{aligned} \delta\rho(\omega = 0) &= \frac{1}{\sqrt{\pi}} \int_0^\infty \frac{d\omega'}{\omega'} e^{2\pi\omega'(g(k_o)-b)} \frac{\tan(\pi\omega')}{\Gamma(\frac{1}{2} + \omega')} \left(\frac{\omega'}{e}\right)^{\omega'}, \\ \delta\rho(\omega = i\pi) &= \frac{e^{-\pi b}}{\sqrt{2e}} \int_0^\infty \frac{d\omega'}{\omega' + \frac{1}{2}} e^{2\pi\omega'(g(k_o)-b)} \frac{\tan(\pi\omega')}{\Gamma(\frac{1}{2} + \omega')} \left(\frac{\omega'}{e}\right)^{\omega'}. \end{aligned} \quad (\text{D.20})$$

#### D.4. Determination of $\delta(k) = 2\pi \int dk \rho_{\text{imp}}$

The impurity density of states,  $\rho_{\text{imp}}(k)$ , obeys an equation of the form

$$\begin{aligned} \rho_{\text{imp}}(z) &= \int_b^\infty dz' \rho_{\text{imp}}(z') R(z - z') + \frac{1}{2} \frac{1}{\cosh(\pi(z - I^{-1}))}; \\ \rho_{\text{imp}}(z) &\equiv -\frac{\rho_{\text{imp}}(k)}{g'(k)}, \quad z = g(k), \end{aligned} \quad (\text{D.21})$$

provided  $B < 0$ , i.e  $H \ll \sqrt{U\Gamma}$ . As we are interested in the scattering phase, we want to compute

$$\delta(k) = 2\pi \int_{-\infty}^k dk' \rho_{\text{imp}}(k'). \quad (\text{D.22})$$

If  $z > b$ , appropriate for when we are computing the phase of a hole,  $\delta(k)$  becomes

$$\delta(k) = 2\pi \int \frac{d\omega}{2\pi} \frac{-ie^{-i\omega g(k)}}{\omega - i\delta} \rho^+(\omega). \quad (\text{D.23})$$

In this case Wiener-Hopf gives the solution of  $\rho^+(\omega)$  as

$$\begin{aligned} \rho_{\text{imp}}^+(\omega) &= \frac{e^{i\omega b} G^+(\omega)}{2\pi i} \int d\omega' \frac{1}{\omega' - (\omega + i\delta)} \rho_o(\omega') G^-(\omega') e^{-i\omega' b}; \\ \rho_o(\omega) &= \frac{e^{i\omega I^{-1}}}{2 \cosh \frac{\omega}{2}}. \end{aligned} \quad (\text{D.24})$$

Provided we assume  $H > T_k$ , or roughly equivalently,  $I^{-1} > b$ , this simplifies to

$$\begin{aligned} \delta(k) &= 2 \tan^{-1}(2(I^{-1} - g(k))) + \pi \\ &\quad - \frac{1}{\pi^2} \int_0^\infty d\omega \frac{e^{-2\pi\omega(g(k)-b)}}{\omega} \sin(2\pi\omega) \left(\frac{\omega}{e}\right)^{-\omega} \Gamma\left(\frac{1}{2} + \omega\right) \\ &\quad \times \int_0^\infty d\omega' \frac{e^{-2\pi\omega'(I^{-1}-b)}}{\omega' + \omega} \sin(\pi\omega') \left(\frac{\omega'}{e}\right)^{-\omega'} \Gamma\left(\frac{1}{2} + \omega'\right). \end{aligned} \quad (\text{D.25})$$

If on the other hand we are interested in the phase of an added particle (i.e.  $z < b$ ), we compute  $\delta(k)$  via

$$\begin{aligned} \delta(k) &= 2\pi \int_{-\infty}^k dk' \rho_{\text{imp}}(k') \\ &= 2\pi - 2\pi \int_{-\infty}^{g(k)} dz \rho_{\text{imp}}(z) \\ &= 2\pi - 2\pi \int \frac{d\omega}{2\pi} \frac{e^{-i\omega g(k)}}{-i\omega + \delta} \rho^-(\omega). \end{aligned} \quad (\text{D.26})$$

The Wiener-Hopf analysis then yields for  $\rho^-(\omega)$

$$\rho_{\text{imp}}^-(\omega) = -\frac{e^{i\omega b}}{2\pi i G^-(\omega)} \int d\omega' \frac{1}{\omega' - (\omega - i\delta)} \rho_o(\omega') G^-(\omega') e^{-i\omega' b}. \quad (\text{D.27})$$

This gives the scattering phase as

$$\begin{aligned} \delta(k) &= \frac{3\pi}{2} - \sin^{-1}(\tanh(\pi(g(k) - I^{-1}))) \\ &\quad + \frac{1}{2\pi} \mathbf{P} \int d\omega \frac{e^{2\pi\omega(g(k)-b)}}{\omega} \frac{\tan(\pi\omega)}{\Gamma(\frac{1}{2} + \omega)} \left(\frac{\omega}{e}\right)^\omega \\ &\quad \times \mathbf{P} \int d\omega' \frac{e^{-2\pi\omega'(I^{-1}-b)}}{\omega' - \omega} \sin(\pi\omega') \left(\frac{\omega'}{e}\right)^{-\omega'} \Gamma\left(\frac{1}{2} + \omega'\right), \end{aligned} \quad (\text{D.28})$$

where  $\mathbf{P}$  indicates the principal value of the integral is to be taken.

## References

- [1] D. Goldhaber-Gordon, J. Göres, M. Kastner, H. Shtrikman, D. Mahalu, and U. Meirav, cond-mat/9807233.
- [2] S. Cronenwett, T. Oosterkamp, and L. Kouwenhoven, cond-mat/9804211.
- [3] D. Goldhaber-Gordon, H. Shtrikman, D. Mahalu, D. Abusch-Magder, U. Meirav, and M. Kastner, Nature 391 (1998) 156.
- [4] W.G. van der Wiel, S. De Franceschi, T. Fujisawa, J. Elzerman, S. Tarucha, and L. Kouwenhoven, Science 289 (2000) 2105.
- [5] J. Nygard, D. Cobden, and P. Lindelof, Nature 408 (2000) 342.
- [6] J. Appelbaum, Phys. Rev. Lett. 17 (1966) 91; P. Anderson, Phys. Rev. Lett. 17 (1966) 95.
- [7] T. Ng and P. Lee, Phys. Rev. Lett. 61 (1988) 1768.
- [8] M. Hettler, J. Kroha, and S. Hershfield, Phys. Rev. Lett. 73, 1967 (1994); *ibid*, Phys. Rev. B 58 (1998) 5649.
- [9] N. Wingreen and Y. Meir, Phys. Rev. B 49 (1994) 11040.
- [10] Y. Meir, N. Wingreen, and P. Lee, Phys. Rev. Lett. 70 (1993) 2601.
- [11] N. Sivan and N. Wingreen, Phys. Rev. B 54 (1996) 11622.
- [12] S. Hershfield, J. Davies, and J. Wilkins, Phys. Rev. B 46 (1992) 7046.
- [13] A. Kaminski, Y. Nazarov, and L. Glazman, cond-mat/0003353.
- [14] A. Schiller and S. Hershfield, Phys. Rev. B 51 (1995) 12 896; *ibid* 58 (1998) 14978.
- [15] N. Kawakami and A. Okiji, Phys. Lett. A 86 (1982) 483; *ibid*. J. Phys. Soc. Japan 51 (1982) 1143; *ibid* Solid St. Commun. 43 (1982) 365; Okiji, A. and Kawakami, N., J. Phys. Soc. Japan 51 (1982) 3192.
- [16] P. Wiegmann, V. Filyov, and A. Tsvelick, Soviet Phys. JETP Lett. 35 (1982) 77; P. Wiegmann and A. Tsvelick, Soviet Phys. JETP Lett. 35 (1982) 100; *ibid.*, J. Phys. C 16 (1982) 2281; A. Tsvelick and P. Wiegmann, Phys. Lett. A 89 (1982) 368; *ibid.*, J. Phys. C 16 (1983) 2281; V. Filyov, A. Tsvelick, and P. Wiegmann, Phys. Lett. A 89 (1982) 157.
- [17] J. Moore and X. Wen, cond-mat/9911068.
- [18] N. Andrei, Phys. Lett. A. 87 (1982) 299.
- [19] J. von Delft, U. Gerland, T. Costi, and Y. Oreg, cond-mat/9909401.
- [20] D. Meyer, T. Wegner, M. Potthoff, and W. Nolting, cond-mat/9905089.
- [21] T. Costi, A. Hewson, and V. Vlatič, Journal of Physics: Cond. Mat. 6 (1994) 2519; T. Costi, cond-mat/0004302
- [22] J. Cardy and G. Mussardo, Nucl. Phys. B 410 (1993) 451.; G. Delfino and G. Mussardo, Nucl. Phys B 455 (1995) 724.; G. Delfino and J. Cardy, hep-th/9712111.; J. Cardy and G. Mussardo, Nucl. Phys. B 410 (1993) 451.



- [23] F. Lesage, H. Saleur and S. Skorik, Phys. Rev. Lett. 76 (1996) 3388; Nucl. Phys. B474 (1996) 602.
- [24] P. Fendley, A.W.W. Ludwig, and H. Saleur, Phys. Rev. Lett. 74 (1995) 3005; *ibid.* 75 (1995) 2196; Phys. Rev. B52 (1995) 8934.
- [25] S. Skorik, cond-mat/9708163
- [26] P. Fendley, A. Ludwig, and H. Saleur, cond-mat/9710205.
- [27] R. M. Konik, H. Saleur, A. W. W. Ludwig, cond-mat/0010270.
- [28] A. Tsvetick and P. Wiegmann, Adv. in Phys. 32 (1983) 453.
- [29] N. Andrei, cond-mat/9408101.
- [30] D. Langreth, Phys. Rev. 150 (1966) 516.
- [31] D. Haldane, Phys. Rev. Lett. 40 (1978) 416.
- [32] H. Desgranges and K. Schotte, Phys. Lett. 91 (1982) 240.
- [33] J. Johnson and B. McCoy, Phys. Rev. A 6 (1972) 1613.
- [34] M. Gaudin, Saclay Note CEA-N-1559 (1), unpublished.
- [35] J. Nozières, J. Low Temp. Phys. 17 (1974) 31.
- [36] K. Yamada, Prog. Theo. Phys. 53 (1975) 970.
- [37] V. Korepin, N. Bogoliubov, and A. Izergin, **Quantum Inverse Scattering Method and Correlation Functions**, Cambridge, CUP (1993).